

Investigation into co-crystal formation with cyclophosphazenes

by
Helene Wahl



*Thesis presented in partial fulfilment of the requirements for
the degree Master of Science in Chemistry at the University
of Stellenbosch*

Supervisor: Dr Delia Ann Haynes
Co-supervisor: Dr Tanya le Roex
Faculty of Science
Department of Chemistry & Polymer Science

March 2012

Declaration

By submitting this thesis/dissertation electronically, I declare that the entirety of the work contained therein is my own, original work, that I am the sole author thereof (save to the extent explicitly otherwise stated), that reproduction and publication thereof by Stellenbosch University will not infringe any third party rights and that I have not previously in its entirety or in part submitted it for obtaining any qualification.

March 2012

Abstract

This study aimed to combine the principles of crystal engineering with the properties of cyclotriphosphazene derivatives to construct supramolecular assemblies in the solid state. The ease with which the chloro substituents on cyclotriphosphazenes can be replaced makes them ideal candidates for this study. The substituents were chosen for their ability to form either hydrogen bonding interactions or halogen bonding interactions in the solid state. The cyclotriphosphazene derivatives were co-crystallised with various small organic molecules with complementary functional groups, as well as with other cyclophosphazene derivatives. The aim was to form co-crystals or solvates with these cyclophosphazene derivatives as co-crystals contain a wealth of information regarding the forces governing the aggregation of molecules in the solid state. Cyclotriphosphazenes, with their array of substituents, could broaden the range of potential interactions governing crystalline assembly.

Fifteen cyclotriphosphazene derivatives were synthesised and characterised in this study. The novel crystal structures of two cyclotriphosphazene derivatives have been elucidated by single crystal X-ray diffraction. These are 2,2-bis(4-formylphenoxy)-4,4,6,6-bis[spiro(2',2''-dioxo-1',1''-biphenyl)]cyclotriphosphazene and hexakis(4-cyano-phenoxy)cyclotriphosphazene.

In the course of this study two novel polymorphs of hexakis(4-fluorophenoxy)cyclotriphosphazene were identified and studied. The novel triclinic form undergoes an irreversible transformation to the previously reported monoclinic phase at high temperatures. The reported monoclinic phase, however, transforms to a monoclinic *C* phase in a single-crystal to single-crystal fashion. It is also suspected that this phase transformation is in fact reversible on cooling of the crystal to temperatures below -45 °C.

One novel co-crystal structure of hexakis(4-pyridyloxy)cyclotriphosphazene with terephthalic acid was identified and characterised. However, analysis of the Cambridge Structural Database indicates that co-crystal formation with cyclophosphazenes is not a commonly occurring phenomenon. This leads to the conclusion that cyclotriphosphazenes can be used in crystal engineering as supramolecular building blocks, but their shape and size tend to inhibit the formation of co-crystals. Therefore co-crystal formers have to be chosen with great care.

Opsomming

Die doel van hierdie studie was om die beginsels van kristalingenieurswese te kombineer met die eienskappe van siklotrifosfaseen afgeleides om sodoende supramolekulêre versamelings in die vastetoestand te bou. Die gemak waarmee die chloor substituentte op die siklotrifosfaseenring vervang kan word, maak hierdie molekules ideaal vir hierdie studie. Die substituentte is gekies op grond van hul potensiaal om waterstofbindings of intermolekulêre halogeenbindings in die vastetoestand te vorm. Ko-kristallisatie eksperimente is met die siklotrifosfaseen afgeleides en verskeie klein organiese molekules met komplementêre funksionele groepe uitgevoer, asook tussen die verskeie siklotrifosfaseen afgeleides met mekaar. Die doel was om mede-kristalle of solvate met hierdie siklotrifosfaseen afgeleides te vorm aangesien mede-kristalle 'n magdom inligting bevat rakende die kragte wat die versameling van molekules in die vaste fase beheer. Die siklotrifosfaseen afgeleides wat 'n wye verskeidenheid substituentte kan dra, kan hierdeur die moontlike intermolekulêre interaksies wat die versameling in die kristallyne vaste fase beheer verbreed.

In hierdie studie is vyftien siklotrifosfaseen afgeleides gesintetiseer en gekarakteriseer. Die voorheen onbekende kristalstrukture van twee siklotrifosfaseen afgeleides is in hierdie studie geïdentifiseer, naamlik 2,2-bis(4-formielfenoksie)-4,4,6,6-bis[spiro(2',2''-dioksie-1',1''-bifeniliel)]siklotrifosfaseen en hekza(4-sianofenoksie)siklotrifosfaseen. Die strukture is bepaal deur enkelkristal X-straaldiffraksie.

In die loop van hierdie studie is twee voorheen onbekende polimorfs van hekza(4-fluorofenoksie)siklotrifosfaseen geïdentifiseer en bestudeer. Die nuwe trikliniese vorm ondergaan 'n onomkeerbare faseverandering na die monokliniese vorm by hoë temperature. Die bekende monokliniese *P* fase ondergaan egter 'n verdere faseverandering na 'n monokliniese *C* fase. Hierdie geskied as 'n enkel-kristal na 'n enkel-kristal faseverandering. Daar word ook gespekeer dat hierdie spesifieke faseverandering wel omkeerbaar is indien die kristal na -45 °C afgekoel word.

Een nuwe mede-kristal tussen hekza(4-pyridieloksie)siklotrifosfaseen en 1,3-dibensoësuur is in hierdie studie geïdentifiseer en gekarakteriseer. 'n Analise van die Cambridge Strukturele Databasis het egter aangedui dat die vorming van mede-kristalle nie 'n alledaagse verskynsel is in siklotrifosfaseen afgeleides nie. Dit lei tot die gevolgtrekking

dat sikotrifosfaseen molekules wel in kristalgenieurswese gebruik kan word as supramolekulêre boustene, maar dat die vorm en grootte van die molekules die kristallisering van mede-kristalle verhoed. Dus moet die molekules wat saam met die siklotrifosfaseen molekules gekristalliseer wil word, goed deurdink word.

Acknowledgements

First and foremost, I would like to thank my supervisors Drs Delia Haynes and Tanya le Roex for providing me with the opportunity to learn from them. You have given me endless support and encouragement throughout my degree. All this while raising twins and organising theatre productions. With your guidance I have grown as a researcher; able to think critically about many scientific issues. It has been an absolute pleasure working with you and I look forward to the next adventure!

Then, Vincent Smith, not only for his patience and willingness to help with hours of powder X-ray diffraction and hot stage analyses, but also for his advice, friendship and long discussions (and jokes...) about life in general.

The Supramolecular Materials Chemistry Group for their support and the laughter-filled working environment they inspire. Members of the group include Len Barbour, Catharine Esterhuysen, Tanya le Roex, Delia Haynes, Vincent Smith, Matteo Lusi, Prashant Bhatt, Storm Potts, Anneli Heynes, Charl Bezuidenhout, Ine Grobler, Marike du Plessis, Eustina Batisai, Ferdi Groenewald, Leigh Loots, Sean Robinson and Malcolm Applewhite.

I would like to give a special thanks to Leigh, Sean and Malcolm for making research a pleasant experience.

To my friends and family for all their support, especially Stuart von Berg who spent hours reading my work.

And of course, without funding there would be no research, therefore I would like to thank the University of Stellenbosch and the Wilhelm Frank Trust for financial support.

Conferences

SACI 2011 – 40th South African Chemical Institute Convention

University of the Witwatersrand, Johannesburg, 16 – 21 January 2011

Poster presentation – *Supramolecular assemblies formed by cyclophosphazenes*

ICCOSSXX – 20th International Conference on the Chemistry of the Organic Solid State

Indian Institute of Science (IISc), Bangalore, India, 26 – 30 June 2011

Poster presentation – *Supramolecular assemblies formed by cyclophosphazenes*

Publications

Not part of this work:

H. Wahl, D. A. Haynes and T. le Roex, *CrystEngComm*, 2011, **13**, 2227 - 2236.

H. Wahl, D. A. Haynes and T. le Roex, *Chem. Commun.*, 2012, **48**, 1775 - 1777

List of abbreviations

NMR	-	Nuclear magnetic resonance
FT	-	Fourier transform
d	-	doublet
dd	-	doublet of doublets
t	-	triplet
dt	-	doublet of triplets
TPP	-	Tris(<i>o</i> -phenylenedioxy)cyclotriphosphazene
TLC	-	Thin-layer chromatography
SCD	-	Single crystal X-ray diffraction
PXRD	-	Powder X-ray diffraction
VT PXRD	-	Variable temperature powder X-ray diffraction
DSC	-	Differential scanning calorimetry
CSD	-	Cambridge Structural Database
CIF	-	Crystallographic information file
mp	-	Melting point
Z	-	Number of formula units in the cell
Z'	-	Number of formula units in the asymmetric unit
α	-	angle between the <i>b</i> and <i>c</i> axes
β	-	angle between the <i>a</i> and <i>c</i> axes
γ	-	angle between the <i>a</i> and <i>b</i> axes
T _t	-	Transition temperature

Atomic colour key





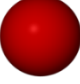




	Carbon
	Hydrogen
	Nitrogen
	Phosphorus
	Oxygen
	Chlorine
	Fluorine
	Bromine
	Iodine

Table of contents

Declaration	i
Abstract	ii
Opsomming	iii
Acknowledgements	v
List of conferences	vi
List of publications	vi
List of abbreviations	vii
Atomic colour key	viii
Table of contents	ix

Chapter 1 – Introduction

1.1. Cyclotriphosphazenes	2 1
1.1.1. Chemistry and reactivity	2 1
1.1.2. ³¹ P Nuclear magnetic resonance (NMR)	3 1
1.2. Supramolecular chemistry	4 1
1.3. Crystal engineering	4 1
1.4. Supramolecular synthons	5 1
1.5. Intermolecular interactions	7 1
1.5.1. The hydrogen bond	7 1
1.5.2. π - π Stacking interactions	8 1
1.5.3. Halogen bonding.....	8 1
1.5.4. Van der Waals forces and close packing	9 1
1.6. Co-crystals	9 1
1.7. Crystal engineering in cyclotriphosphazenes.....	10 1
1.7.1. Inclusion studies with tris(<i>o</i> -phenylenedioxy)- cyclotriphosphazene (TPP)	10 1
1.7.2. Hydrogen bonded supramolecular networks of cyclotriphosphazene hydrazides	11 1
1.7.3. Co-crystals with cyclotriphosphazenes.....	12 1
1.8. This study.....	13 1
References	14 1

Chapter 2 – Synthetic methods

2.1. General procedure for the synthesis of a cyclotriphosphazene derivative.....	1 2
2.2. Attempted synthesis of 2,2-bis(4-formylphenoxy oxime)- 4,4,6,6-bis- [spiro(2',2''-dioxo-1',1''-biphenyl)]cyclotriphosphazene	2 2
2.2.1. Attempted oxime synthesis <i>via</i> sonication.....	7 2
2.2.2. Attempted mechanochemical conversion of an aldehyde to an oxime	7 2
2.2.3. The crystal structure of 3	8 2
2.3. Synthesis of the hexakis(4-pyridyloxy)cyclotriphosphazene	10 2
2.4. Synthesis of a hexa(4-cyanophenyl)cyclotriphosphazene	13 2
2.5. Attempted synthesis of a cyclotriphosphazene with carboxylic acid functionality	16 2
2.6. Conclusions.....	24 2
2.7. Detailed synthetic procedures	26 2
2.7.1. Tris(1,3-diaminopropane)cyclotriphosphazene	26 2
2.7.2. 2,2-Bis(4-formylphenoxy)-4,4,6,6-bis[spiro(2',2''-dioxo- 1',1''-biphenyl)]-cyclotriphosphazene	27 2
2.7.3. Hexakis(4-hydroxyphenoxy)cyclotriphosphazene	29 2
2.7.4. Hexakis(4-formylphenoxy)cyclotriphosphazene.....	30 2
2.7.5. Hexakis(4-fluorophenyl)cyclotriphosphazene.....	31 2
2.7.6. Hexakis(4-iodophenyl)cyclotriphosphazene	31 2
2.7.7. Hexakis(4-bromophenyl)cyclotriphosphazene	32 2
2.7.8. Hexakis(4-chlorophenyl)cyclotriphosphazene	32 2
2.7.9. Tris(<i>o</i> -phenylenedioxy)cyclotriphosphazene.....	33 2
2.7.10. Hexakis(4-cyanophenoxy)cyclotriphosphazene	33 2
2.7.11. Hexakis(4-pyridyloxy)cyclotriphosphazene	34 2
References	35 2

Chapter 3 – Two novel polymorphs of hexakis(4-fluorophenoxy)cyclotriphosphazene

3.1. Polymorphism	1 3
3.2. Single crystal X-ray diffraction studies of the monoclinic phase of hexakis(4-fluorophenoxy)cyclotriphosphazene.....	3 3
3.3. The novel triclinic phase of 12.....	8 3
3.3.1. Crystallisation experiments	8 3
3.3.2. Single crystal X-ray diffraction studies of the triclinic phase, T	10 3
3.4. Differential scanning calorimetry (DSC) and PXRD studies of M and T	16 3
3.5. Hot stage microscopy.....	21 3
3.6. Investigation into the phase transformation of the monoclinic <i>P</i> polymorph.....	23 3
3.6.1. Variable temperature studies on the conversion from triclinic to monoclinic	23 3
3.6.2. Variable temperature studies of the transformations in the monoclinic phase, M.....	28 3
3.7. Conclusions and future work	36 3
References	38 3

Chapter 4 – Attempted co-crystal formation with cyclotriphosphazenes

4.1. Co-crystallisation experiments.....	2 4
4.1.1. The trispiro and monospiro diaminoalkane cyclotriphosphazenes.....	2 4
4.1.2. Crystallisation experiments with 2,2-bis(4-formylphenoxy)-4,4,6,6- bis[spiro(2',2''-dioxy-1',1''-biphenyl)]cyclotriphosphazene.....	6 4
4.1.3. Attempted co-crystallisation <i>via</i> halogen-halogen and halogen-nitrile interactions.....	10 4
4.1.4. Attempted mechanochemical synthesis of co-crystals	16 4
4.2. The co-crystal with hexakis(4-pyridyloxy)cyclotriphosphazene.....	20 4
4.3. A Cambridge Structural Database survey of co-crystal occurrence with cyclotriphosphazenes	24 4
4.4. Conclusions and future work	27 4
References	29 4

Chapter 5 – Summary and concluding remarks
.....1|5

Appendix – Experimental techniques
.....1|A

Chapter 1

Introduction

This study aims to use the principles of crystal engineering to organise cyclotriphosphazene derivatives into supramolecular architectures. This introduction will highlight certain aspects of the field of supramolecular chemistry to better understand the scope of this study. Key concepts used in this study will be explained, of which the first is the chemistry and reactivity of cyclotriphosphazenes. This relates to why cyclotriphosphazenes were chosen as the building blocks for this study. The term supramolecular chemistry will be introduced, with a specific focus on crystal engineering. In crystal engineering tailor-made molecules are used to study the effect on the packing in the solid state and to what extent it can be controlled and directed. This project serves as a further investigation into the potential use of cyclotriphosphazenes in this research niche.

1.1 Cyclotriphosphazenes

1.1.1 Chemistry and reactivity

Phosphazenes are formally unsaturated compounds containing alternating phosphorus-nitrogen bonds.¹ They can be classified as monophosphazenes, diphosphazenes, polyphosphazenes and cyclophosphazenes. This project focuses on the derivatives and supramolecular assemblies of the cyclotriphosphazenes – more specifically the phosphonitrilic chloride trimer (Figure 1.1).^{2, 3} The trimer comprises a planar six-membered ring of alternating phosphorus and nitrogen atoms.

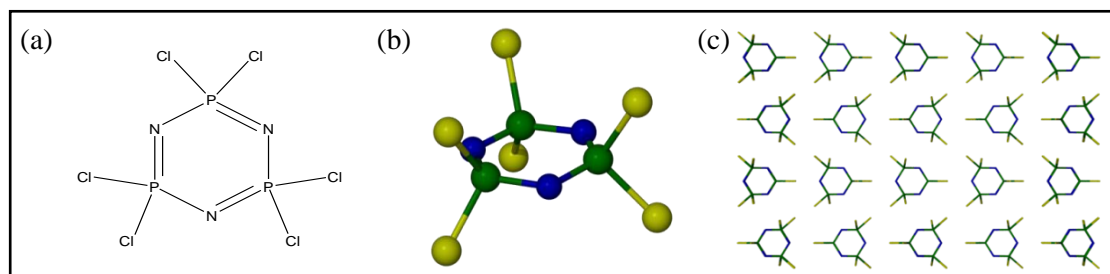


Figure 1.1 (a) and (b) Structure of the phosphonitrilic chloride trimer where the phosphorus atoms are green and the nitrogen atoms are blue. (c) Packing arrangement of phosphonitrilic chloride trimer in the solid state.

The nitrogen atoms in $N_3P_3Cl_6$ are sp^2 hybridised and the phosphorus atoms are approximately sp^3 hybridised.⁴ The bonding involved in the ring has been the cause of some debate in the past few years.⁵ In benzene there is extensive electron delocalisation due to p_π - p_π bonding,¹ but in the cyclotriphosphazene system there is the possibility of p_π - d_π interaction. The lone pair electrons on the nitrogen reside in a sp^2 orbital in the plane of the ring with the remaining electrons occupying the other two sp^2 orbitals and a p_z orbital (Figure 1.2a).¹ One theory is that the p_z orbital on the nitrogen atom can interact with the d_{xz} or d_{yz} orbital on the phosphorus atom.⁶ This out-of-plane interaction can lead to heteromorphic (N-P) p_π - d_π bonding (Figure 1.2b), or homomorphic (N-N) p_π - p_π bonding (Figure 1.2c).¹ This mismatch of the orbitals causes a node to form on every phosphorus atom, making the delocalised molecular orbital less stable.⁴ This could possibly explain why the cyclotriphosphazenes do not have true aromatic character.

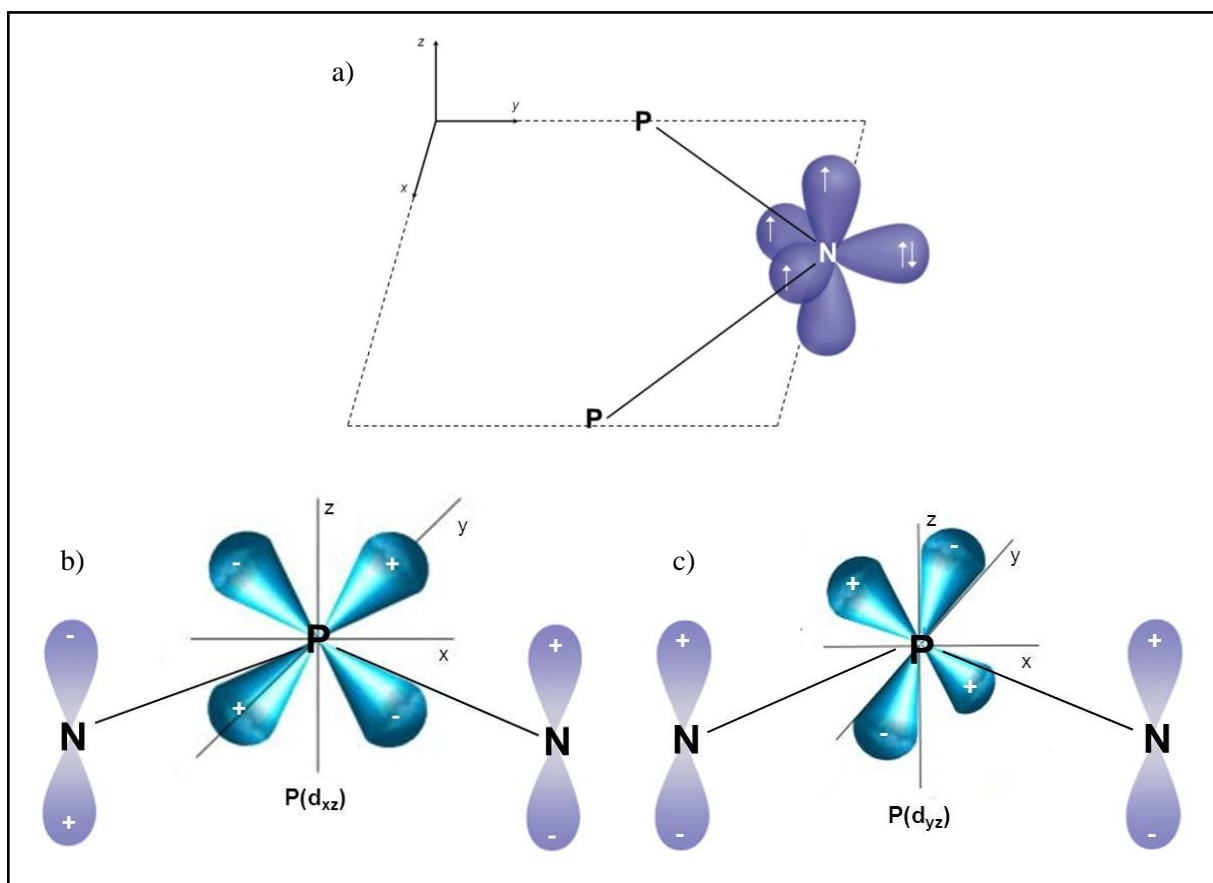


Figure 1.2 Adapted from reference 1, Greenwood & Earnshaw, *Chemistry of the elements*. Orbital diagrams representing the bonding in the cyclotriphosphazene ring.¹ (a) The lone pair electrons of the nitrogen reside in the sp^2 orbital in the plane of the ring. (b) Heteromorphic (N-P) p_π - d_π bonding. (c) Homomorphic (N-N) p_π - p_π bonding.

The chloro substituents on $N_3P_3Cl_6$ can be easily replaced by a wide range of functional groups. Substitution can take place *via* two pathways: either geminal or non-geminal substitution.⁵ Geminal substitution involves the replacement of two chlorine atoms *on the same* phosphorus, whereas with non-geminal substitution two chlorine atoms *on different* phosphorus atoms are replaced. The type of substitution is determined by the nature of the functional group. When the substituent is more electronegative, it polarizes the phosphorus-nitrogen bond, activating the phosphorus atom and causing the second substituent to bond to the same phosphorus atom. Generally small electronegative substituents favour geminal substitution. Non-geminal substitution is mostly favoured by larger electron-rich substituents. Non-geminal substitution can also give *cis* and *trans* isomers – the substituents point either up or down. These two pathways are however not exclusively followed and in some cases a mixture of products is obtained – containing products of both geminal and non-geminal substitution. This effect only becomes significant when products that are not fully substituted are desired.

1.1.2 ^{31}P nuclear magnetic resonance spectroscopy (^{31}P NMR)

Nuclear magnetic resonance (NMR) is a spectroscopic method that is invaluable in the characterisation of molecules. It is also a relatively easy and reliable method of analysing the products of a reaction and to ensure purity of the product. 1H and ^{13}C NMR is often used to elucidate the structure of a compound. The ^{31}P nucleus has numerous convenient NMR properties that make it ideal for Fourier transform (FT) NMR. Two of these properties are its spin quantum number of $\frac{1}{2}$ and the fact that it occurs in 100% natural abundance.^{7, 8} The ^{31}P solution NMR done in this study exclusively measured 1H decoupled spectra, as this simplifies the interpretation of the data. The phosphorus atoms of cyclotriphosphazenes couple to each other, resulting in characteristic peaks depending on the level of substitution of the phosphorus atoms, as well as the conformation of the ring.⁹ In the case of the phosphonitrilic chloride trimer used in this study, the ring is nearly planar. Therefore all the phosphorus atoms are equivalent and only one signal will be seen in the ^{31}P spectrum.⁹ When the chloro substituents are replaced with other substituents, the phosphorus atoms in the ring are no longer equivalent. This causes the appearance of doublets, doublets of doublets (dd) or triplets in the spectrum as the phosphorus atoms couple to each other. Once all the chloro substituents are replaced with the same

substituent, the phosphorus atoms are once again equivalent and only a singlet is seen in the spectrum. The level of substitution of the cyclotriphosphazene can therefore be closely monitored by ^{31}P NMR.

1.2 Supramolecular chemistry

It is very difficult to assign a definition to a field that has expanded so much in recent years. It is an ever-changing field of science where researchers tend to have their own understanding of the terminology used.¹⁰ In his Nobel lecture¹¹, Jean-Marie Lehn defined the field as follows:

“Supramolecular chemistry is the chemistry of the intermolecular bond, covering the structures and functions of the entities formed by association of two or more chemical species.”

This means that, broadly, supramolecules are combinations of molecules that come together either spontaneously or by design, to form a larger unit with properties resulting from the original components. Supramolecular chemistry is the umbrella term for describing the study of systems ‘beyond the molecule’.¹² Braga¹³ stated it so eloquently when he said that “...Supramolecular chemistry has dissolved all the traditional barriers between the subdivisions of chemistry...focusing attention on the *collective* properties...”. That is essentially what supramolecular chemists do: they use their knowledge from different areas of chemistry to design molecular assemblies in order to study the properties of these compounds for possible practical application. When these methods are specifically applied to crystalline solids, it leads to the area of crystal engineering.¹³

1.3 Crystal engineering

In crystal engineering the aim is to understand crystal packing with regard to intermolecular interactions, and then to use this information to design new materials with specific physical and chemical properties.¹⁴ Or, more simply put, it is the making of crystals by design.¹³

The phrase ‘crystal engineering’ was first coined by Pepinsky¹⁵ in 1955 and has been used ever since, as it is a rather accurate description of what it is that chemists do in this field.

The first step in crystal engineering is studying the packing arrangement of a crystal in order to understand the intermolecular interactions that are responsible for the specific arrangement of the molecules.¹⁶ This is needed to develop a design strategy. When these two concepts are understood, the physical and chemical properties can be studied as well as the effect that variation in the packing has on the properties of the material. Aakeröy described crystal engineering as being “*defined by nature and structural consequences of intermolecular forces, and the way in which such interactions are utilised for controlling the assembly of molecular building blocks into infinite architectures*”.¹⁷ The key focus of crystal engineering is to develop reliable methods with the aim to create molecular materials with specific properties that can be fine-tuned according to the crystal engineer’s desire. If for instance, the aim is to design a material with nonlinear optical properties,^{18, 19} the molecules must arrange in a noncentrosymmetric way with their dipole moments aligned.²⁰ If the goal is to design a porous material, the molecules must have a sufficiently awkward shape to prohibit efficient packing, resulting in solvent-filled voids or channels in the crystal structure. The crystal engineering of materials is therefore dependent on the interactions at play in the structures. Just as houses are made from brick and cement, crystal structures are made of building blocks where the molecules are the bricks and the intermolecular interactions serve as the cement holding the structure together and directing assembly.

1.4 Supramolecular synthons

In crystal engineering it is essential to identify patterns regarding the intermolecular interactions guiding the solid-state structure of crystals and therefore it is necessary to find reliable substructural units that regularly occur in crystal structures.²¹ Desiraju was the first to define the term supramolecular synthon as “*structural units within supermolecules which can be formed and/or assembled by known or conceivable synthetic operations involving intermolecular interactions*”.^{21, 22} A synthon is therefore derived from designed combinations of interactions.²¹ This is illustrated in Figure 1.3. The carboxylic acid moiety hydrogen bonds to the complementary carboxylic acid moiety of another molecule to form the well-known carboxylic acid dimer.²³ This spatial arrangement of an intermolecular interaction is termed a supramolecular synthon.²⁴ These supramolecular synthons are

dependent on the types of intermolecular interactions that occur in the solid state. Figure 1.4 illustrates a selection of other supramolecular synthons.

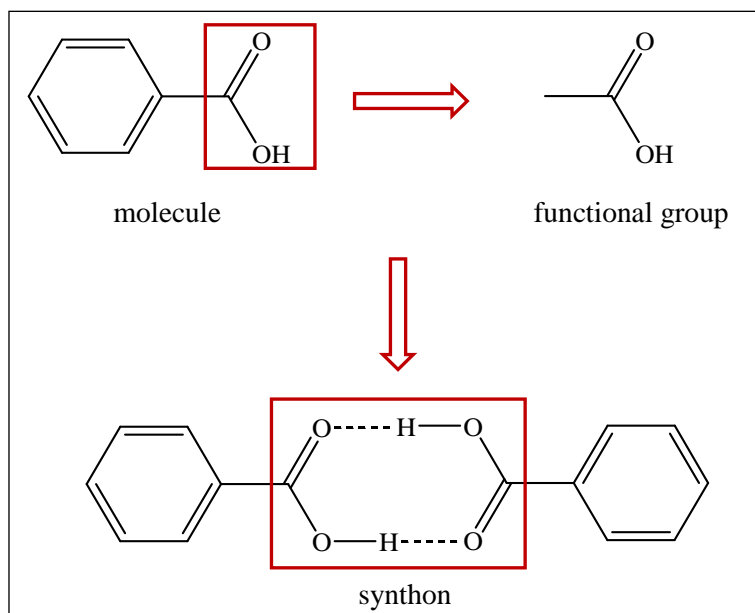


Figure 1.3 This figure illustrates the concept of a supramolecular synthon, adapted from Desiraju, *Crystal engineering, from molecules to materials*.²³ The functional groups hydrogen bond to form this carboxylic acid dimer, i.e. a synthon.

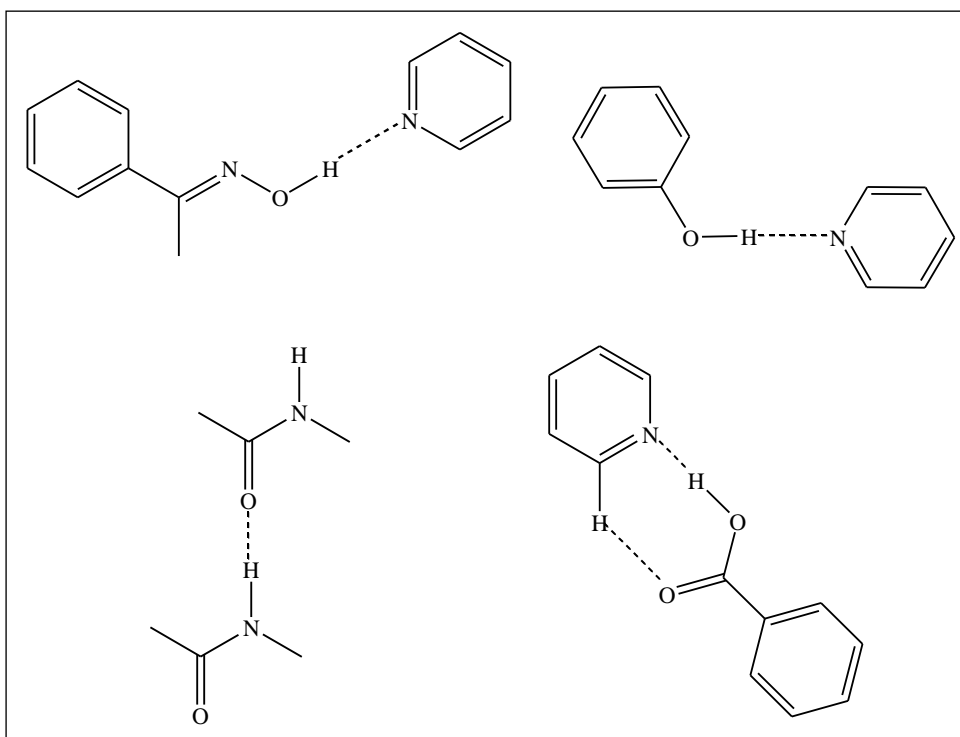


Figure 1.4 Selected supramolecular synthons, adapted from Aakeröy & Salmon, *CrystEngComm*³⁴ and Desiraju, *Angew. Chem.*²¹

1.5 Intermolecular interactions

As was previously stated, intermolecular interactions are essentially the cement holding the crystal structure together. These interactions are specifically defined as being between atoms that are not directly bonded.²⁵ Intermolecular interactions are classified according to their strength with respect to distance and their directionality.²⁵ Medium-range forces generally govern close-packing, and include interactions such as C \cdots H, C \cdots C and H \cdots H interactions.²¹ Long-range forces include heteroatom interactions, namely interactions among N, O, S, Cl, Br, I or any of these atoms and carbon or hydrogen.^{21, 25} These interactions generally lead to a minimisation of the free energy of the crystal lattice.²⁶ There is a wide variety of possible intermolecular interactions, but only the interactions pertinent to this study will be briefly discussed.

1.5.1 The hydrogen bond

The hydrogen bond is possibly the most well-known intermolecular interaction in crystal engineering and has been called the ‘master-key of molecular recognition’.¹⁴ In its simplest form, it can be written as X-H \cdots A with X being the donor and A the acceptor.²⁷ It is such a well-known interaction due to the fact that it is relatively strong and suitably directional.²⁷ If a molecule contains a functional group that has the ability to form a hydrogen bond, it will always do so, unless there are factors such as steric hindrance that prohibit this from happening.²⁷

These bonds can be classified as very strong, strong and weak.²⁸ This depends on how successfully the hydrogen bond in question can direct the aggregation of the molecules in any crystal structures obtained.²⁷ The strength of the hydrogen bond is also dependent on the atoms that are involved in the hydrogen bond.²⁹ For neutral molecules the typical values for a hydrogen bond are in the range of 10 – 65 kJ mol⁻¹. If one of the species that is taking part in the hydrogen bond is ionic (a charge assisted hydrogen bond) the strength of the interaction can increase to 80 – 120 kJ mol⁻¹.²⁹ Weak hydrogen bonds involve interactions between O-H \cdots Ph and C \equiv C-H \cdots O that are barely stronger than van der Waals interactions.²⁷ These weaker bonds can however still play an important role in directing the aggregation of molecules in the solid state.^{28, 29} To guide the crystal engineer

in designing molecular solids with the aid of hydrogen bonding, Etter and co-workers developed the following guidelines²⁸:

- (i) All good proton donors and acceptors are used in hydrogen bonding.
- (ii) The formation of six-membered ring intramolecular hydrogen bonds will take preference over the formation of intermolecular hydrogen bonds.
- (iii) After the formation of intramolecular hydrogen bonds, the remaining best proton donors and acceptors will form hydrogen bonds.

The hydrogen bond is clearly a well-researched and robust interaction that is often used in crystal engineering to direct supramolecular assemblies.

1.5.2 π - π Stacking interactions

This type of interaction occurs between aromatic rings and ranges in the value of 0 – 50 kJ mol⁻¹.¹² These stacking interactions can be divided into two types: face-to-face and edge-to-face.¹² It has been shown that this stacking interaction is due to the interaction between a positive σ -framework of one molecule and the negatively charged π -cloud of the other molecule.³⁰ It has been suggested that nondirectional van der Waals stabilisation also plays an important role in stabilising these interactions.³¹

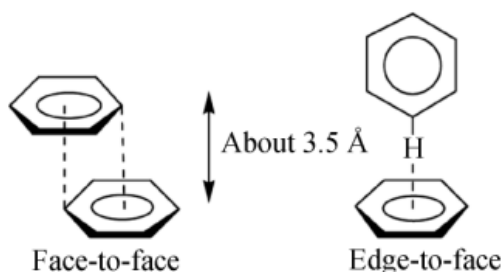


Figure 1.5 The two types of π - π stacking interactions.²¹

1.5.3 Halogen bonding

This term describes the attractive donor-acceptor interactions of halogen atoms that play the role of a Lewis acid.³² The halogens can either interact with other halogen atoms, or with carbon or nitrogen atoms. The angle of the intermolecular halogen bond can be found in the range 160° to 180°, even for weak interactions where the interaction distance is

greater than 3 Å.³² Figure 1.6 illustrates some of the elements normally involved in halogen bonding.

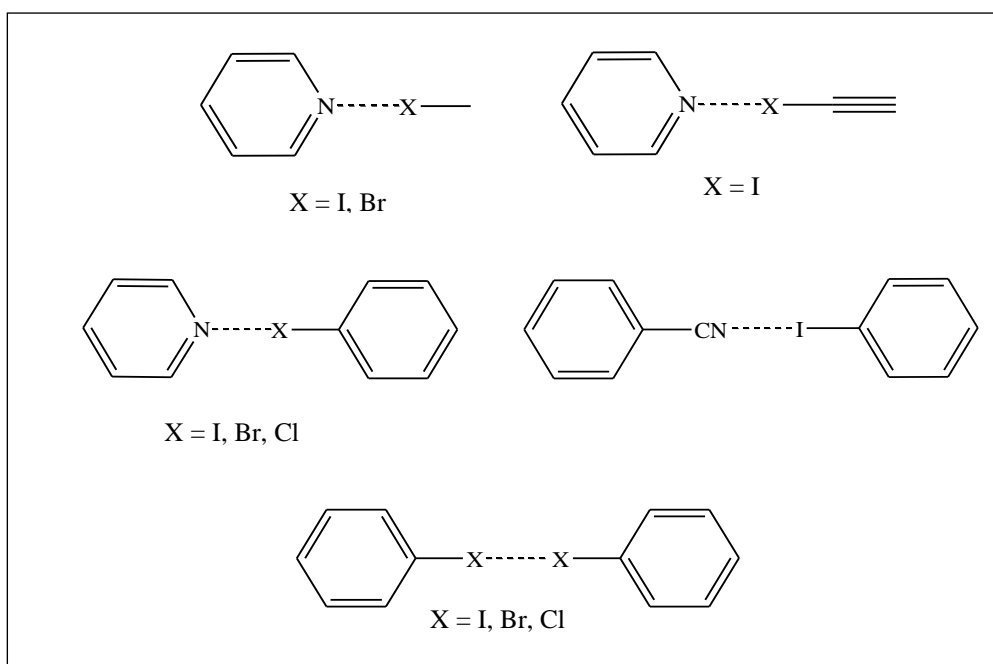


Figure 1.6 Some of the halogen-based supramolecular synthons used in crystal engineering. Adapted from Metrangola and Resnati in *Encyclopedia of supramolecular chemistry*³²

1.5.4 Van der Waals forces and close packing

Van der Waals interactions occur because of the polarization of the electron cloud of a molecule by the close proximity of a nearby nucleus. This results in weak electrostatic interactions.¹² The value for this type of interaction is variable, but generally less than 5 kJ/mol. These types of interactions include the induced dipole to induced dipole, or London forces.¹⁴ Van der Waals interactions provide a general attractive interaction for assembly of molecules in the solid state, but they are unfortunately not strongly directing interactions.^{12, 33} The interplay between attractive and repulsive forces allows molecules to orientate themselves in such a way as to utilise all available space and pack efficiently.¹⁴

1.6 Co-crystals

There has been much debate about how to define this seemingly innocent term.³⁴ Dunitz described the co- in co-crystal as indicating “togetherness”,³⁵ i.e. two or more components crystallising together in the same crystal structure.

For the purpose of this study, the term ‘co-crystal’ will be defined as a multicomponent molecular crystal as described by Bond.³⁶ Furthermore, some of the restrictions placed on the term by Aakeröy and Salmon³⁷ will also be used in this study. Only multicomponent crystals that contain neutral chemical species will be accepted as co-crystals and the different chemical entities comprising the crystal have to be present in stoichiometric amounts.³⁷ Aakeröy and Salmon placed a further restriction on co-crystals, stipulating that the components of the co-crystal have to be solids at ambient conditions. This restriction therefore excludes solvates as co-crystals. In this study solvates will be considered as a subclass of co-crystals, meaning the components of the co-crystal do not have to specifically be solids at ambient conditions.

It is unfortunately not a trivial exercise to prepare co-crystals. It appears to be thermodynamically more favourable for similar molecules to assemble in a solid, rather than heteromeric molecules.¹⁷ The interactions between the heteromeric molecules must therefore be much more favourable than the interactions between homomeric molecules for co-crystallisation to occur. In order to design co-crystals an understanding of the intermolecular interactions between functional groups is essential. This understanding will guide the choice of co-crystal formers used in co-crystallisation experiments.³⁸

1.7 Crystal engineering in cyclotriphosphazenes

1.7.1 Inclusion studies with tris(*o*-phenylenedioxy)cyclotriphosphazene (TPP)

It is nearly impossible to study cyclotriphosphazenes without being guided to studies done with TPP (Figure 1.7).³⁹ TPP is made by the reaction between catechol and phosphonitrilic chloride trimer in the presence of a base. The product of this reaction (once crystallised) is a highly robust inclusion complex that includes a variety of solvents, whether it is exposed to the solvent or only the vapour.⁴⁰⁻⁴² The high density, nonporous structure of TPP (Figure 1.7) has also been characterised and it has been shown that under CO₂ pressure the high density structure can be transformed to the low density, porous structure.⁴³ Not only does this particular organic host include a wide variety of small organic molecules, but it has also been shown to include various polymers.^{44, 45} The sorption properties of TPP are however not what prompted this study. It was speculated that if TPP has the ability to form a broad range of inclusion compounds, the possibility exists that other

cyclotriphosphazene derivatives could also form a range of interesting supramolecular assemblies – be they inclusion compounds or co-crystals.

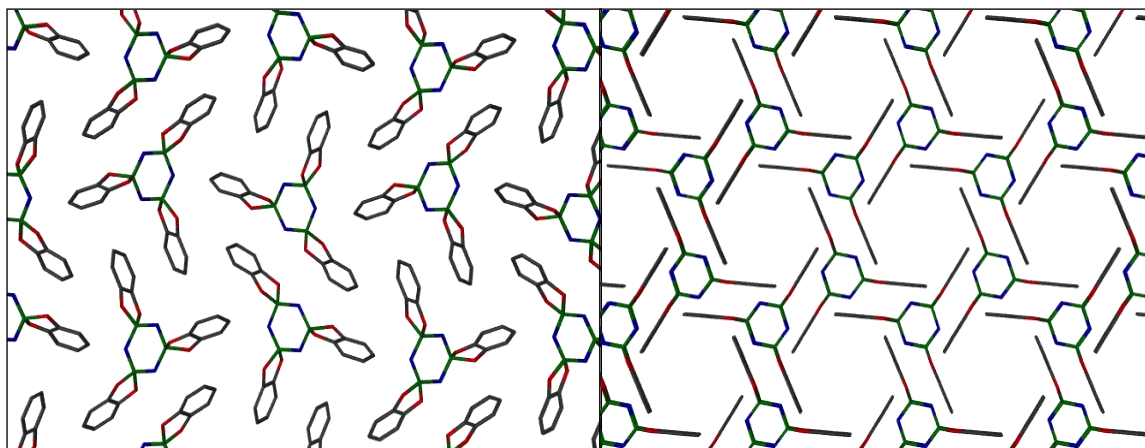


Figure 1.7 A packing diagram of TPP showing the high density structure with no channels (left) and the low density, porous phase (right).

1.7.2 Hydrogen bonded supramolecular networks of cyclotriphosphazene hydrazides

The specific design of organic molecules into assemblies that are guided by hydrogen bonding has been extensively studied.^{21, 23} Benzene serves as the basis to which a wide range of modifications can be made in order to create the potential for hydrogen bonding interactions to guide the assembly of the organic molecules in the solid state. In the area of inorganic chemistry the molecules with the closest resemblance to benzene are the cyclotriphosphazenes. Chandrasekhar and co-workers⁴⁶ used cyclotriphosphazenes and the principles of directional hydrogen bonding to design supramolecular assemblies in the solid state. They specifically selected hydrazide derivatives with the intent of using the terminal -NH_2 groups as proton donors and the ring nitrogen atoms as proton acceptors. This interaction results in the formation of a hexagonal close-packed sheet in the case of $\text{N}_3\text{P}_3[\text{N}(\text{Me})\text{NH}_2]_6$ (Figure 1.8a). When one of the phosphorus atoms is substituted with a 2,2'-biphenol group - *spiro*- $\text{N}_3\text{P}_3[\text{O}_2\text{C}_{12}\text{H}_8][\text{N}(\text{Me})\text{NH}_2]_4$ - it results in the formation of a double chain through hydrogen bonding of a ring nitrogen atom to a $\text{N}(\text{Me})\text{NH}_2$ substituent (Figure 1.8b). This is one of the few examples of using tailored intermolecular interactions to direct the aggregation of cyclotriphosphazenes.

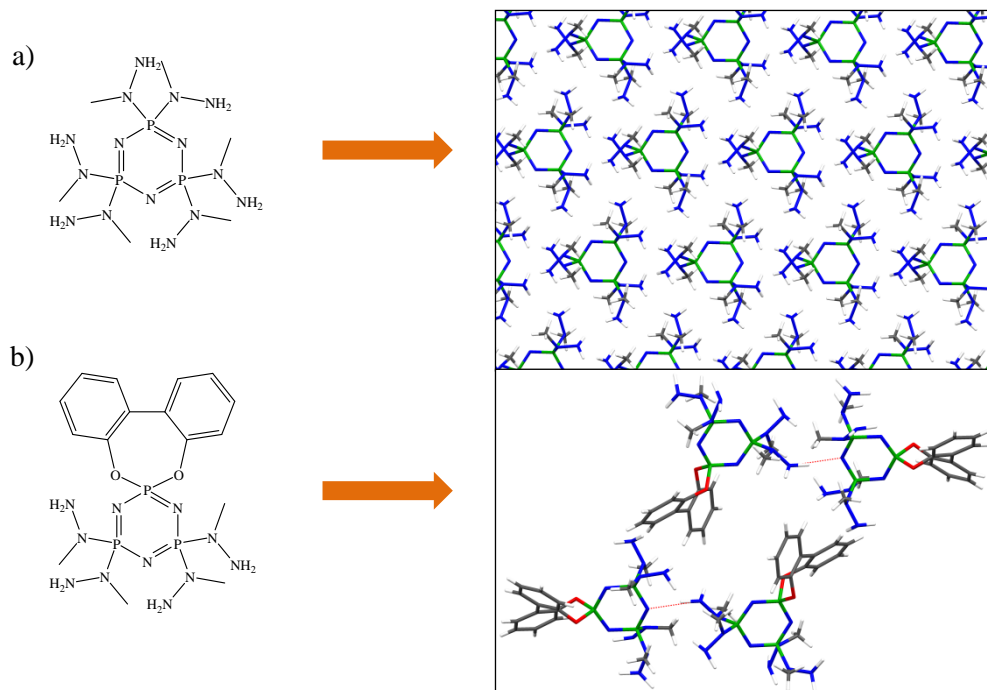


Figure 1.8 (a) The hexagonal close-packed sheets of $N_3P_3[N(Me)NH_2]_6$. (b) The double chains of $spiro-N_3P_3[O_2C_{12}H_8][N(Me)NH_2]_4$ where a $N(Me)NH_2$ substituent hydrogen bonds to a ring nitrogen.

1.7.3 Co-crystals with cyclotriphosphazenes

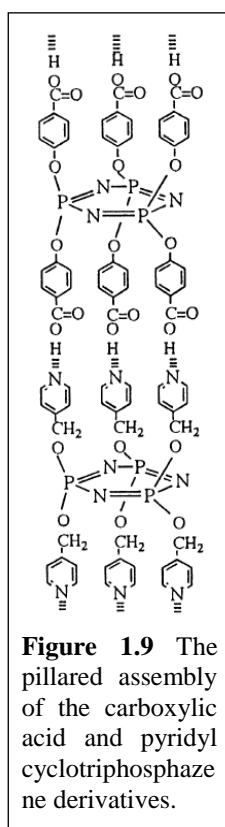


Figure 1.9 The pillared assembly of the carboxylic acid and pyridyl cyclotriphosphazene derivatives.

There are a number of known co-crystals containing a cyclotriphosphazene derivative.⁴⁷⁻⁴⁹ One of the most interesting co-crystals is that of hexakis(4-carboxyphenoxy)cyclotriphosphazene and hexakis(4-pyridylcarboxy)cyclotriphosphazene (Figure 1.9).⁵⁰ Hydrogen bonds are formed between the carboxylic acid and pyridyl groups on the cyclotriphosphazenes. Due to the three-up and three-down arrangement of the substituents on each cyclotriphosphazene, they assemble to form columns in the crystal structure. There are however no 3D-coordinates for this structure in the Cambridge structural database. It was decided to attempt to grow crystals of this particular co-crystal to be able to study the interactions in the structure. This co-crystal therefore served as the inspiration to design similar pillared assemblies with other cyclotriphosphazene derivatives.

1.8 This study

True to the field of supramolecular chemistry, this project is a multi-disciplinary approach to design supramolecular assemblies of cyclotriphosphazenes. This research was not pursued for its potential practical applications, but rather for the contribution to the fundamental knowledge of crystal engineering. The more we understand, the better we can apply our knowledge with the eventual goal of real-life, practical applications.

This study aimed to synthesise various known cyclotriphosphazene derivatives, using synthetic skills from both organic and inorganic chemistry. The aim was to synthesise cyclotriphosphazene derivatives with functional groups that have the potential to form strong supramolecular synthons with suitable small molecules in the solid state, i.e. to form co-crystals of cyclotriphosphazenes. Intensive research has been conducted into the synthesis of cyclotriphosphazenes, but few studies have been done on the potential to form co-crystals with cyclotriphosphazenes. An initial survey of the Cambridge Structural Database (CSD) also indicated that there are very few known co-crystals with cyclotriphosphazenes, therefore this study aimed to fill this apparent gap in the literature regarding the supramolecular chemistry of cyclotriphosphazenes.

This study used various crystal growth techniques to investigate the occurrence of co-crystal formation with cyclotriphosphazenes. This investigation will aid in the understanding of intermolecular interactions and which factors play a role in the assembly of these molecules in crystals. The results from this study will help to determine whether the intermolecular interactions controlling the assembly of cyclotriphosphazenes in the solid state are a reliable and robust way of designing supramolecular architectures with predictable packing arrangements.

References

1. N. N. Greenwood and A. Earnshaw, *Chemistry of the elements*, 2 edn., Pergamon Press, Great Britain, 1997.
2. G. J. Bullen, *J. Chem. Soc. A*, 1971, 1450 - 1453.
3. S. W. Bartlett, S. J. Coles, D. B. Davies, M. B. Hursthouse, I. Hanife, A. Kiliç, R. A. Shaw and I. Un, *Acta Crystallogr., Sect. B: Struct. Sci.*, 2006, **B62**, 321 - 329.
4. J. E. Huheey, *Inorganic chemistry: principles of structure and reactivity*, 3 edn., Harper & Row Publishers, New York, 1983.
5. H. R. Allcock, *Chem. Rev.*, 1972, **72**, 315 - 356.
6. M. J. S. Dewar, E. A. C. Lucken and M. A. Whitehead, *J. Chem. Soc. (resumed)*, 1960, 2423 - 2429.
7. G. David G, *Prog. Nucl. Magn. Reson. Spectrosc.*, 1984, **16**, 1 - 98.
8. D. L. Pavia, G. M. Lampman, G. S. Kriz and J. R. Vyvyan, *Introduction to spectroscopy*, Fourth edn., Brooks/Cole, Cengage Learning, Belmont, 2009.
9. R. Keat, R. A. Shaw and M. Woods, *J. Chem. Soc., Dalton Trans.*, 1976, 1582 - 1589.
10. J. W. Steed, in *Encyclopedia of supramolecular chemistry*, eds. J. L. Atwood and J. W. Steed, Marcel Dekker, Inc., New York, 2004, vol. 2, pp. 1401 - 1419.
11. J.-M. Lehn, *Angew. Chem., Int. Ed. Engl.*, 1988, **27**, 89 - 112.
12. J. W. Steed and J. L. Atwood, *Supramolecular chemistry*, John Wiley & Sons, Ltd., West Sussex, 2000.
13. D. Braga, *Chem. Commun.*, 2003, 2751 - 2754.
14. G. Desiraju, J. J. Vittal and A. Ramanan, *Crystal engineering: a textbook*, World Scientific Publishing Co. Pte. Ltd., Singapore, 2011.
15. R. Pepinsky, *Physical Reviews*, 1955, **100**, 971.
16. G. R. Desiraju, *Angew. Chem., Int. Ed.*, 2007, **46**, 8342 - 8356.
17. C. B. Aakeröy, *Acta Crystallogr., Sect. B: Struct. Sci.*, 1997, **B53**, 569 - 586.
18. M. Muthuraman, R. Masse, J.-F. Nicoud and G. R. Desiraju, *Chem. Mater.*, 2001, **13**, 1473 - 1479.
19. O. Konig, H.-B. Burgi, T. Armbruster, J. Hulliger and T. Weber, *J. Am. Chem. Soc.*, 1997, **119**, 10632 - 10640.

20. C. B. Aakeröy and N. Schultheiss, in *Making crystal by design*, eds. D. Braga and F. Grepioni, Wiley-VCH Verlag GmbH & Co. KGaA, Weinheim, 2007, pp. 209 - 240.
21. G. R. Desiraju, *Angew. Chem., Int. Ed. Engl.*, 1995, **34**, 2311 - 2327.
22. V. R. Thalladi, B. S. Goud, V. J. Hoy, F. H. Allen, J. A. K. Howard and G. R. Desiraju, *Chem. Commun.*, 1996, 401 - 402.
23. G. Desiraju, *J. Mol. Struct.*, 2003, **656**, 5 - 15.
24. A. Nangia and G. Desiraju, in *Design of Organic Solids*, eds. E. Weber, Y. Aoyama, M. Caira, G. Desiraju, J. Glusker, A. Hamilton, R. Meléndez and A. Nangia, Springer Berlin / Heidelberg, 1998, vol. 198, pp. 57 - 95.
25. G. Desiraju, in *Solid-state supramolecular chemistry: crystal engineering*, eds. D. D. MacNicol, F. Toda and R. Bishop, Pergamon, Oxford, 1996, vol. 6, p. 1.
26. J. Glusker, in *Design of organic solids*, ed. E. Weber, Springer-Verlag Berlin Heidelberg, Germany, 1998, vol. 198, pp. 3 - 56.
27. G. R. Desiraju, in *Encyclopedia of supramolecular chemistry*, eds. J. L. Atwood and J. W. Steed, Marcel Dekker, Inc., New York, 2004, vol. 1, pp. 658 - 672.
28. M. C. Etter, *J. Phys. Chem.*, 1991, **95**, 4601 - 4610.
29. C. B. Aakeröy and D. S. Leinen, in *Crystal engineering: from molecules and crystals to materials*, eds. D. Braga, F. Grepioni and A. G. Orpen, Kluwer Academic Publishers, Netherlands, 1999, vol. 538, pp. 89 - 106.
30. C. A. Hunter and J. K. M. Sanders, *J. Am. Chem. Soc.*, 1990, **112**, 5525 - 5534.
31. I. Dance, in *Encyclopedia of supramolecular chemistry*, eds. J. L. Atwood and J. W. Steed, Marcel Dekker, Inc., New York, 2004, vol. 2, pp. 1076 - 1092.
32. P. Metrangolo and G. Resnati, in *Encyclopedia of supramolecular chemistry*, eds. J. L. Atwood and J. W. Steed, Marcel Dekker, Inc., New York, 2004, vol. 1, pp. 626 - 635.
33. C. N. R. Rao, *Curr. Sci.*, 2001, **81**, 1030 - 1037.
34. G. R. Desiraju, *CrystEngComm*, 2003, **5**, 466 - 467.
35. J. D. Dunitz, *CrystEngComm*, 2003, **5**, 506 - 506.
36. A. Bond, *CrystEngComm*, 2007, **9**, 833 - 834.
37. C. B. Aakeröy and D. J. Salmon, *CrystEngComm*, 2005, **7**, 439 - 448.

38. P. Vishweshwar, J. A. McMahon and M. J. Zaworotko, in *Frontiers in crystal engineering*, eds. E. R. T. Tiekink and J. J. Vittal, John Wiley & Sons, Ltd., West Sussex, 2006.
39. H. R. Allcock, *J. Am. Chem. Soc.*, 1964, **86**, 2591 - 2595.
40. H. R. Allcock, R. W. Allen, E. C. Bissell, L. A. Smeltz and M. Teeter, *J. Am. Chem. Soc.*, 1976, **98**, 5120 - 5125.
41. H. R. Allcock, M. L. Levin and R. R. Whittle, *Inorg. Chem.*, 1986, **25**, 41 - 47.
42. G. Couderc and J. Hulliger, *Chem. Soc. Rev.*, 2010, **39**, 1545 - 1554.
43. J. Tian, P. Thallapally, J. Liu, G. J. Exarhos and J. L. Atwood, *Chem. Commun.*, 2011, **47**, 701 - 703.
44. H. R. Allcock, A. P. Primrose, N. J. Sunderland, A. L. Rheingold, I. A. Guzei and M. Parvez, *Chem. Mater.*, 1999, **11**, 1243 - 1252.
45. S. Bracco, A. Comotti, P. Valsesia, M. Beretta and P. Sozzani, *CrystEngComm*, 2010, **12**, 2318 - 2321.
46. V. Chandrasekhar, V. Krishnan, G. Thangavelu Senthil Andavan, A. Steiner and S. Zacchini, *CrystEngComm*, 2003, **5**, 245 - 247.
47. R. Bertani, E. Ghedini, M. Gleria, R. Liantonio, G. Marras, P. Metrangolo, F. Meyer, T. Pilati and G. Resnati, *CrystEngComm*, 2005, **7**, 511 - 513.
48. R. Bertani, F. Chaux, M. Gleria, P. Metrangolo, R. Milani, T. Pilati, G. Resnati, M. Sansotera and A. Venzo, *Inorg. Chim. Acta*, 2007, **360**, 1191 - 1199.
49. T. Itaya, N. Azuma and K. Inoue, *Bull. Chem. Soc. Jpn.*, 2002, **75**, 2275 - 2281.
50. K. Inoue and T. Itaya, *Supramol. Sci.*, 1998, **5**, 163 - 166.

Chapter 2

Synthetic methods

Cyclotriphosphazenes were chosen as the building blocks for this study because of the relative ease with which the chloro substituents can be replaced. The synthesis of a great variety of cyclotriphosphazene derivatives has been reported,¹⁻⁴ but only the cyclotriphosphazenes that contained functional groups with either the potential for hydrogen or halogen bonding were selected for this study. The synthetic procedures that proved to be more challenging than initially expected will be discussed in this chapter, as well as the alternative and novel methods that were developed. Because the aim of this study was to generate co-crystals, any syntheses that did not yield immediate positive results were abandoned without making attempts to characterise by-products or optimise reaction conditions. The detailed experimental procedures for all successfully synthesised cyclotriphosphazene derivatives are listed at the end of this chapter.

All reactions were carried out under dry nitrogen using standard inert atmosphere techniques, in this case Schlenk techniques, unless otherwise stated.

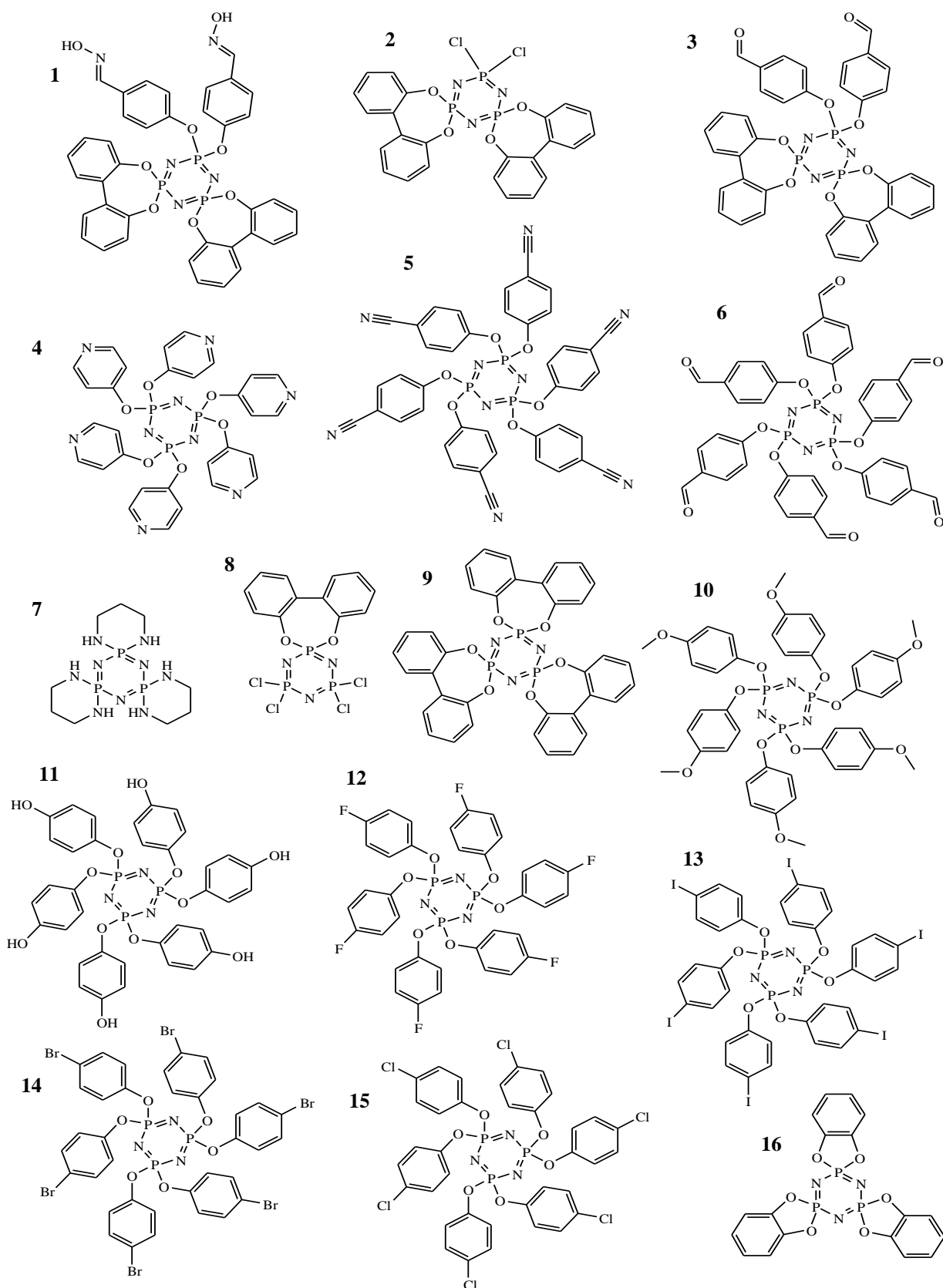
2.1 General procedure for the synthesis of a cyclotriphosphazene derivative

The procedure for preparing most cyclotriphosphazene derivatives is essentially the same: the desired substituent is deprotonated by a suitable base and allowed to react with the phosphonitrilic chloride trimer under reflux conditions. The work-up differs depending on the solubility and air sensitive nature of the product. The reactions are normally carried out in THF, acetone or DCM with reflux. These are however not the only solvents that are used, but this largely depends on the reactivity of the reagents. If more energy is required to activate the reaction, then a solvent with a higher boiling point should be used.

For the reaction to take place, the desired substituent (normally a phenol derivative) needs to be deprotonated. This is done by adding a base such as potassium carbonate (K_2CO_3) or triethylamine. The base has to be added either in slight excess or in an amount equivalent to the substituent. In the case of triethylamine, two equivalents of base have to be added: one equivalent to deprotonate the reagent and another equivalent to trap the HCl that is

formed during the reaction.⁵ The reaction mixture is then refluxed for two to twelve hours, depending on the reactivity of the reagents. The work-up involves removing the solvent *in vacuo*, either before or after filtering, and washing the residue with an appropriate solvent, which in some cases is water. A variety of solvents can be used for recrystallisation and purification of the crude product.

Scheme 2.1 lists all the derivatives that were synthesised (or attempted) during this project. Each derivative has been numbered for ease of reference. The syntheses of **1 – 6** will be described in detail. The syntheses for **7 – 16** can be found at the end of this chapter in section 2.7.



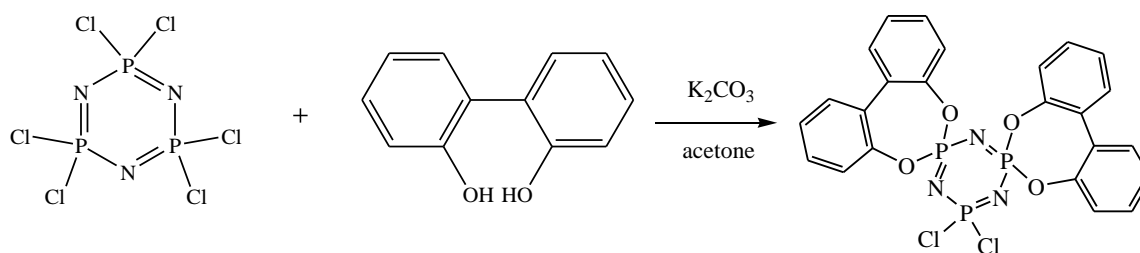
Scheme 2.1 A list of all the cyclotriphosphazene derivatives that were synthesised (or attempted, in the case of **1**) in this study.

2.2 Attempted synthesis of 2,2-bis(4-formylphenoxy oxime)- 4,4,6,6-bis[spiro(2',2''-dioxo-1',1''-biphenyl)]cyclotriphosphazene (**1**)⁶

Various attempts were made at synthesising the oxime derivative of the cyclotriphosphazene depicted in Scheme 2.1. The reason why this specific molecule was chosen for synthesis is because of the oxime group, which has a high propensity to form hydrogen bonds in the solid state.⁷⁻⁹ The motive behind incorporating bulky biphenyl groups in the molecule is the hope that these groups would prohibit the molecule from packing efficiently in the solid state, therefore allowing voids to form that could potentially be filled with solvent.

The synthesis of **1** is a three-step process where the bulky groups are first attached to the cyclotriphosphazene ring. This product (**2**) is allowed to react with 4-hydroxybenzaldehyde and then lastly the aldehyde is converted to the oxime. The last step proved to be more problematic than anticipated, and various methods were used to attempt to convert the aldehyde to the oxime.

The first step in the synthesis of **1** is to produce the dioxobiphenyl derivative **2** via the reaction depicted in Scheme 2.2. Two equivalents of biphenyl-2,2'-diol were added to four equivalents of potassium carbonate. In this case only two equivalents of the reagent are needed as one biphenyl-2,2'-diol is capable of bonding to one phosphorus atom through the two deprotonated oxygen molecules. Two phosphorus atoms are then substituted with this bulky group.



Scheme 2.2 First step in the synthesis of **1**.

This reaction was performed in acetone as the reaction has been proven to occur faster in acetone than in THF.¹⁰ It was also not necessary to reflux the first step in this reaction as this bifunctional nucleophile promotes the replacement of the chlorine atoms. In fact, the trimer and biphenol were added to acetone that was cooled in an ice bath. This is

presumably done to prevent the reaction from taking place too fast and forming trimer that is triply substituted with biphenyl-2,2'-diol.¹⁰ When the first nucleophilic oxygen reacts with the phosphorus atom, it activates the phosphorus atom for further substitution (geminal substitution).¹¹ The neighbouring oxygen is the next-closest nucleophile and substitution of the second chlorine atom occurs. Crosslinking of trimer molecules does not occur because the closest reactive site is on the same molecule.¹⁰ The reaction mixture was stirred at room temperature for 24 hours under an atmosphere of dry nitrogen because the biphenyl-2,2'-diol is air sensitive. The solvent was then removed under vacuum and the product extracted with DCM. More than one product can potentially form during the reaction, but the main product is isolated *via* extraction and recrystallisation as the solubility of the doubly and triply substituted derivatives differs in different solvents. Characterisation was done by ¹H and ³¹P NMR spectroscopy. The ¹H NMR spectrum indicated the presence of the protons of the biphenyl-2,2'-diol and ³¹P NMR showed two signals, a doublet and doublet of doublets (dd) that overlap (Figure 2.1). The doublet can be assigned to the phosphorus atoms that have been substituted with the biphenyl-2,2'-diol due to coupling to the phosphorus atom with the chloro groups. This will give the phosphorus atoms a multiplicity of two (multiplicity = n+1).¹² The dd is therefore the phosphorus atom with the chlorine atoms as substituents, which couples to the other two phosphorus atoms that are not exactly chemically equivalent. The coupling is however close enough to cause the doublets to overlap to some extent. The peak at 26.34 ppm is due to the presence of a small amount of the triply substituted derivative.

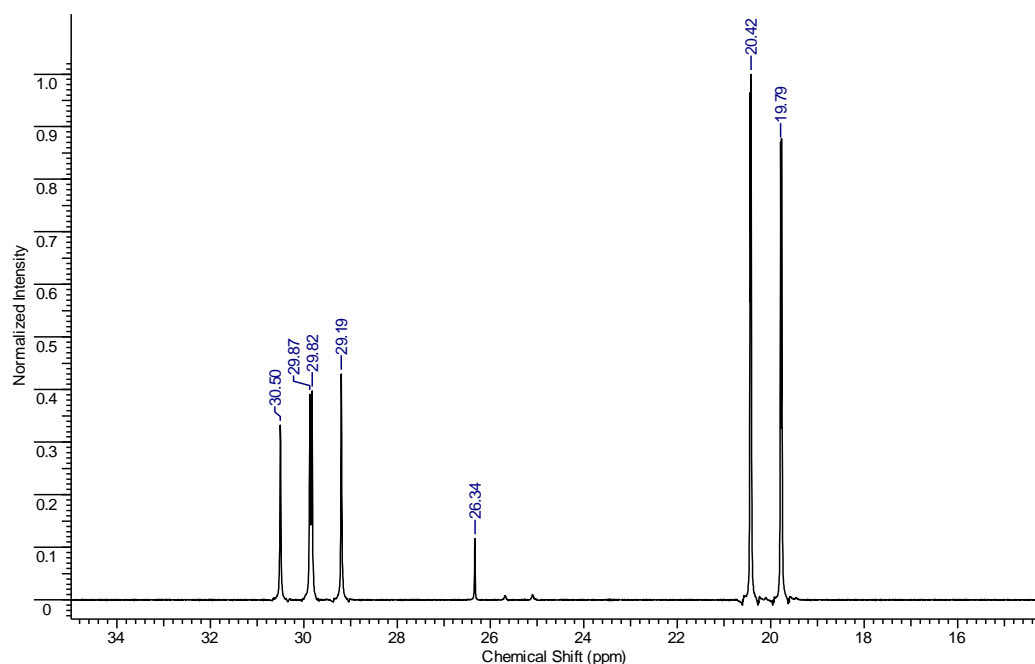
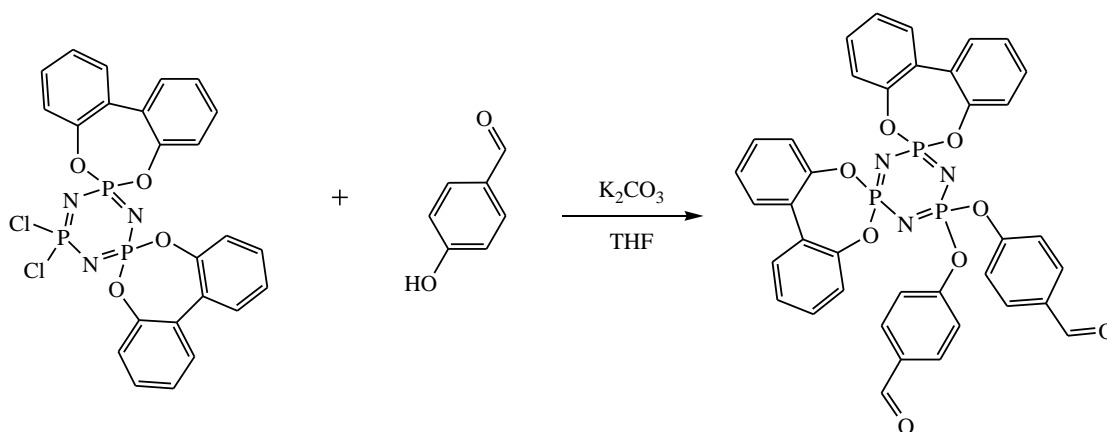
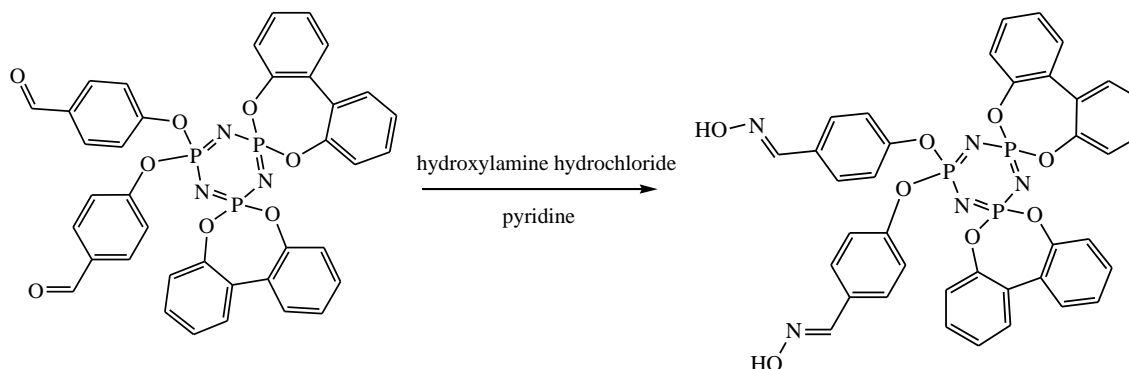


Figure 2.1 ^{31}P NMR of **2**. The phosphorus atom substituted with the chloro groups is the overlapping doublet of doublets at 29.87 ppm. The doublet at 19.79 ppm is the two phosphorus atoms substituted with the biphenyl-2,2'-diol.

The reaction depicted in Scheme 2.3 was carried out by refluxing in THF for eight hours to produce **3**.⁶ It is necessary to reflux in this step as the groups on the cyclotriphosphazene ring are quite bulky, causing steric hindrance which would mean that the reaction will need more energy to take place. It was not necessary to do this reaction under inert conditions. The work-up for the second step is similar to the first step. The solvent was removed under vacuum and the product extracted with DCM. The DCM was then removed *in vacuo*. ^1H and ^{31}P NMR spectroscopy confirmed the synthesis of the aldehyde.



Scheme 2.3 Step two in the synthetic procedure for the biphenyl aldehyde derivative.



Scheme 2.4 This synthetic step involves the conversion of the aldehyde to the oxime by a condensation reaction of **3** with hydroxylamine hydrochloride.

The oxime can be produced by condensation of the aldehyde with hydroxylamine hydrochloride in the presence of a polar, aprotic solvent such as pyridine.⁶ This mixture was allowed to reflux for 3.5 to 4 hours and on cooling, poured slowly into water. This resulted in the formation of a dark, gel-like substance that could not be filtered off. Repeated attempts to precipitate the product from water did not yield any positive results. Efforts were made to dissolve the gel-like substance in an organic solvent, effectively extracting the product. A saturated sodium chloride solution was then added to the organic layer in order to induce the precipitation of **1**. This was unfortunately also unsuccessful. The synthesis was reattempted, but alternative methods were tried to convert the aldehyde to the oxime, as pyridine is a highly unpleasant and toxic substance to handle.

2.2.1 Attempted oxime synthesis *via* sonication^{13, 14}

According to an article by Li and co-workers in *Ultrasonics Sonochemistry*,¹³ it is possible to convert an aldehyde to an oxime by a condensation reaction of the aldehyde with hydroxylamine hydrochloride in ethanol with sonication. However, **3** is not soluble in ethanol, therefore THF was used. Two equivalents of hydroxylamine hydrochloride and a small amount of sodium sulfate were added and the reaction mixture was sonicated for 30 minutes. The mixture was then filtrated and the solvent was removed under reduced pressure. The residue was dissolved in DCM and washed with water. The organic layer was then dried on anhydrous magnesium sulfate, filtered and the solvent removed. Unfortunately the small amount of product that was isolated was shown to be starting material, as analysed by thin layer chromatography (TLC), ¹H and ³¹P NMR. Sonication time was varied from 10 minutes to an hour, although this was also not successful.

2.2.2 Attempted mechanochemical conversion of an aldehyde to an oxime⁷

Mechanochemical synthesis involves the grinding together of two compounds in the solid state, either with or without solvent. Grinding for a certain amount of time can supply the energy needed for a reaction to take place.^{7, 15}

Two equivalents of sodium hydroxide and hydroxylamine hydrochloride were ground together with derivative **3** while adding four to five drops of a 1:1 mixture of DCM and ethanol. The mixture was ground for approximately five minutes until the sample was dry. This mixture was then washed with water to remove any excess sodium hydroxide and inorganic salts formed during the reaction and dried in air. ¹H NMR analysis unfortunately indicated that no reaction had taken place (Figure 2.2). In the case of successful conversion, the signal for the aldehyde proton at 10.03 ppm would no longer be observed. The signal for the proton on that carbon would have shifted further downfield if the aldehyde was converted to the oxime. There would also have been two signals representing the different isomers of the oxime.⁶

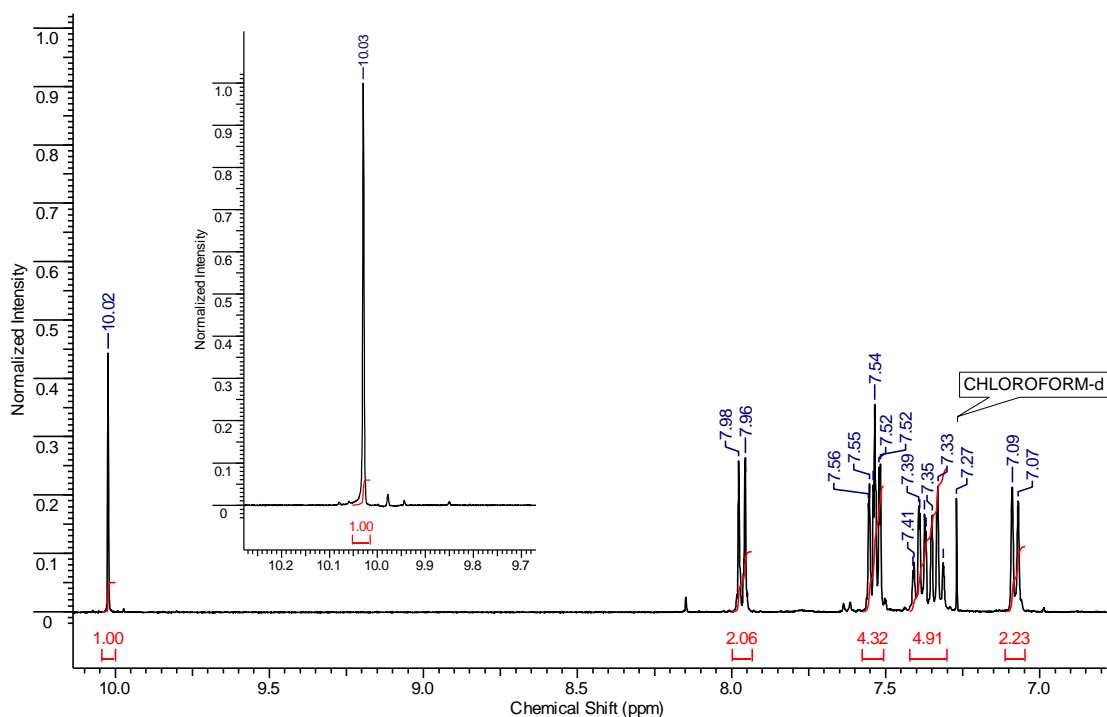


Figure 2.2 ¹H NMR results for the attempted conversion of **3** to **1**. The signal at 10.02 ppm unfortunately corresponds to the signal for the aldehyde proton. The insert is taken from the ¹H spectrum of **3**.

2.2.3 The crystal structure of **3**

As we were not able to synthesise the oxime derivative **1**, it was decided to conduct co-crystallisation experiments with **3** to attempt to form co-crystals. These experiments will be described in greater detail in Chapter 4. Even though the aldehyde moiety is not a very strong hydrogen bond acceptor, co-crystallisation experiments were carried out with hydrogen bond donor molecules such as acids, alcohols and amines. A crystal of **3** was isolated from a co-crystallisation experiment with 1,6-dihydroxynaphthalene in THF. Data was collected at 100 K and the structure of this derivative was determined (Figure 2.3).

The biphenyl-2,2'-diol substituents on the cyclotriphosphazene ring were expected to disrupt efficient packing of the molecule and subsequently create voids in the solid state structure. This is however not the case as the molecule still packs efficiently, leaving no cavities (Figure 2.4). It packs in the monoclinic crystal system in the space group $P2_1/n$.

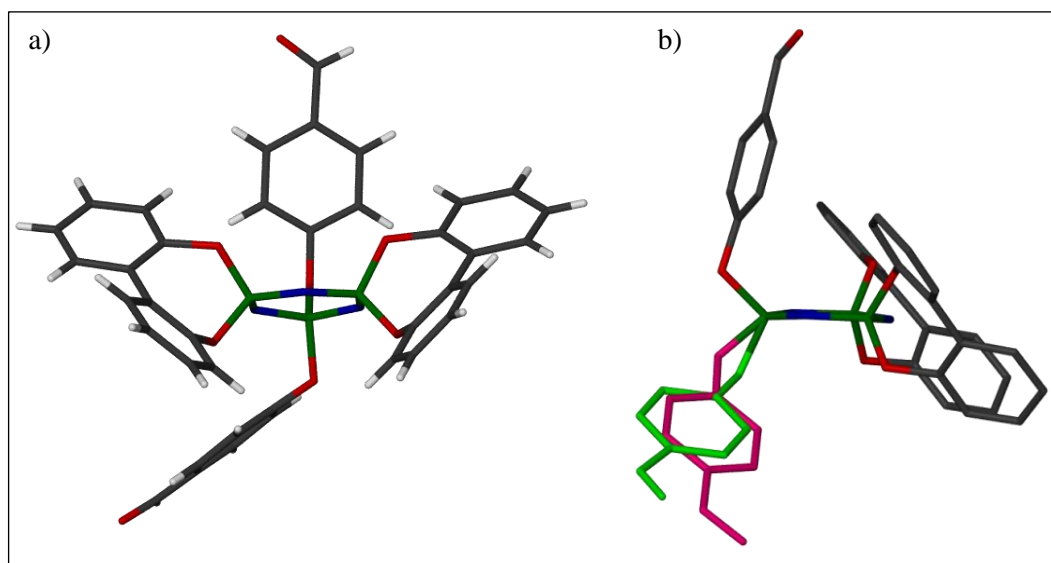
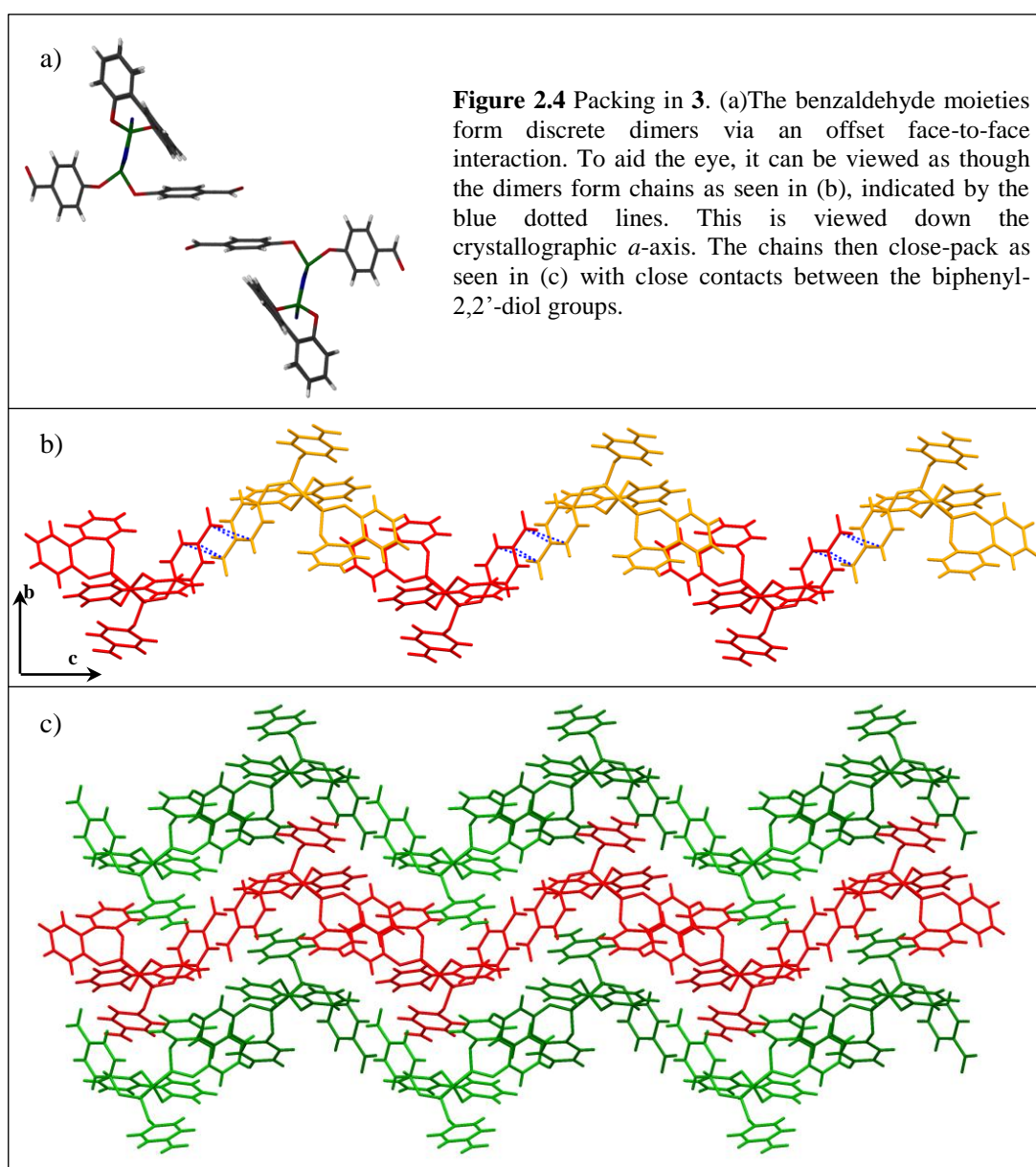


Figure 2.3 A capped stick representation of **3**. (a) This image illustrates the conformation of the biphenyl-2,2'-diol substituents. (b) One of the benzaldehyde substituents is disordered over two positions (pink and green). Hydrogens have been omitted for clarity.

One of the benzaldehyde groups is disordered over two positions, shown in green (53%) and pink (47%) in Figure 2.3b. Occupancy is therefore nearly equal for the two positions. There are no hydrogen bonds evident in the structure, confirming that the aldehyde moiety is not a strong hydrogen bond acceptor. The molecules form discrete dimers *via* an offset face-to-face interaction between benzaldehyde groups (Figure 2.4a). These dimers form chains through π -stacking interactions of the biphenyl groups (Figure 2.4b). The chains then close-pack with close contacts between the biphenyl-2,2'-diol groups (Figure 2.4c).



2.3 Synthesis of the hexakis(4-pyridyloxy)cyclotriphosphazene (**4**)

The pyridyloxy cyclotriphosphazene derivative has previously been synthesised and characterised by single crystal X-ray diffraction analysis.¹⁶ It has been shown that this compound undergoes coordination to transition metals.^{16, 17}

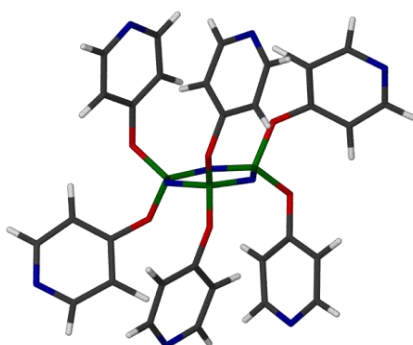
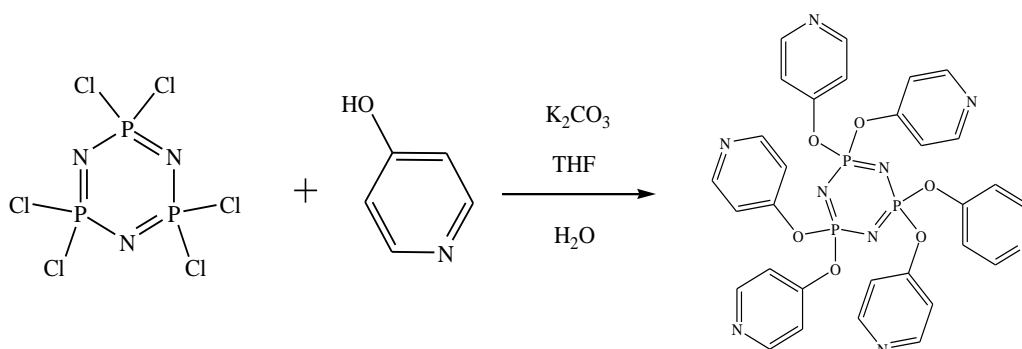


Figure 2.5 Capped stick representation of the structure of the hexakis(4-pyridyloxy)-cyclotriphosphazene (**4**).

The first synthetic procedure that was followed was the one set out by Carriedo and co-workers.¹⁶ The phosphonitrilic chloride trimer, six equivalents of 4-hydroxypyridine and six equivalents of potassium carbonate were refluxed in acetone for five hours under strict inert conditions. The solvent was removed under vacuum and the residue extracted with acetone. While extracting the residue by cannula filtration, dark green and black particles appeared in the solution. This is possible evidence that the product or reagents had begun to degrade due to contact with moisture. This solution was then stirred with ammonium chloride for 30 minutes, after which the solvent was evaporated and the residue extracted with toluene. The final product, after removal of toluene under vacuum, was recrystallised from DCM/petroleum ether. The yield for this reaction was very low (only 8 %) and no suitable crystals could be grown from the solvent system. It was not possible to do any analysis or carry out any co-crystallisation experiments with such a small amount of product. It was decided to search for better synthetic methods or modify **4** to make it more stable.

The modification of **4** was first attempted by trying to incorporate one biphenyl-2,2'-diol group into the structure^{17, 18} This was done by refluxing in THF as was previously described in this chapter, but only one equivalent of biphenyl-2,2'-diol was added. The second part of the procedure was again carried out in refluxing acetone under inert conditions.¹⁷ The first attempt yielded a yellow solution, whereas the second attempt yielded a red solution, and on removal of the solvent, a dark red solid. ¹H and ³¹P NMR analysis of the dark red solid did not give any conclusive evidence that it was the desired product. Attempts to recrystallise the product from various solvents were also not successful as crystals only appeared to be that of various starting materials. Other attempts were also made to synthesise **4**, such as forming the sodium 4-pyridinolate before reacting it with the phosphonitrilic chloride trimer, but they were also unsuccessful.^{19, 20}



Scheme 2.5 The successful synthetic procedure for the hexakis(4-pyridyloxy)cyclotriphosphazene. The final product is precipitated from water.

A final attempt adapted from work done by Carriedo and co-workers²¹ was made where the reaction mixture containing phosphonitrilic trimer, 4-hydroxypyridine and potassium carbonate in THF was stirred for two and a half days at room temperature, after which the mixture was refluxed for approximately six hours (Scheme 2.5). The solvent was removed and the residue was dispersed in 100 ml water. The white precipitate was isolated by filtration and dried. NMR analysis (Figure 2.6) was performed on the crude product (before further purification) and very clean spectra were obtained, indicating successful synthesis of the pyridyloxy derivative. Simpler is evidently better! One novel co-crystal with **4** has been isolated and will be discussed in detail in chapter 4.

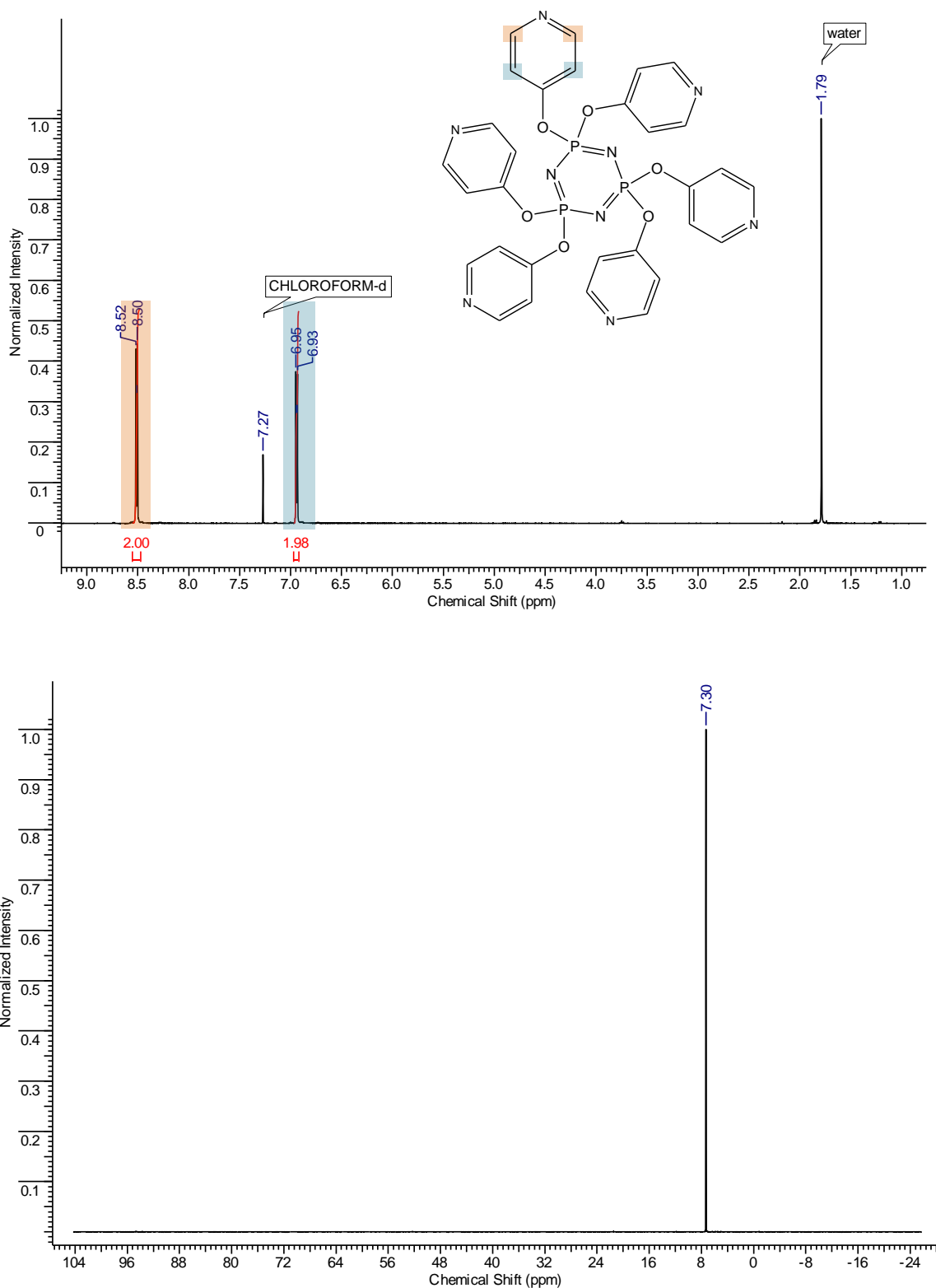


Figure 2.6 The ^1H (top) and ^{31}P (bottom) analysis of the pyridyloxy derivative. Each of the signals at 8.50 and 6.95 ppm integrate for two protons of one ring. There is only one signal in the ^{31}P spectrum, indicating complete substitution of the cyclotriphosphazene ring as all of the phosphorus atoms are chemically equivalent.

2.4 Synthesis of a hexa(4-cyanophenyl)cyclotriphosphazene (5)

Allcock^{22, 23} was one of the first to obtain a crystal structure of a cyclotriphosphazene containing the cyano functionality (Figure 2.7). These groups are quite sought after in supramolecular chemistry as they can coordinate to transition metals²³ and halogens. For this reason it was decided to attempt to synthesise a cyano derivative.

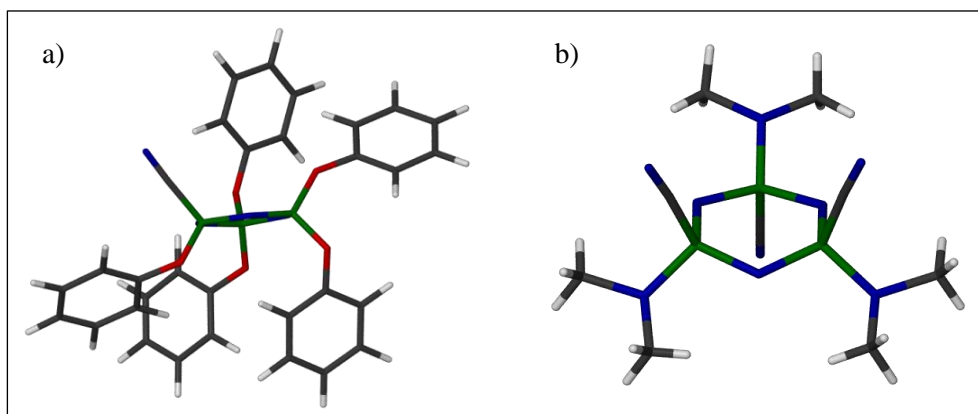
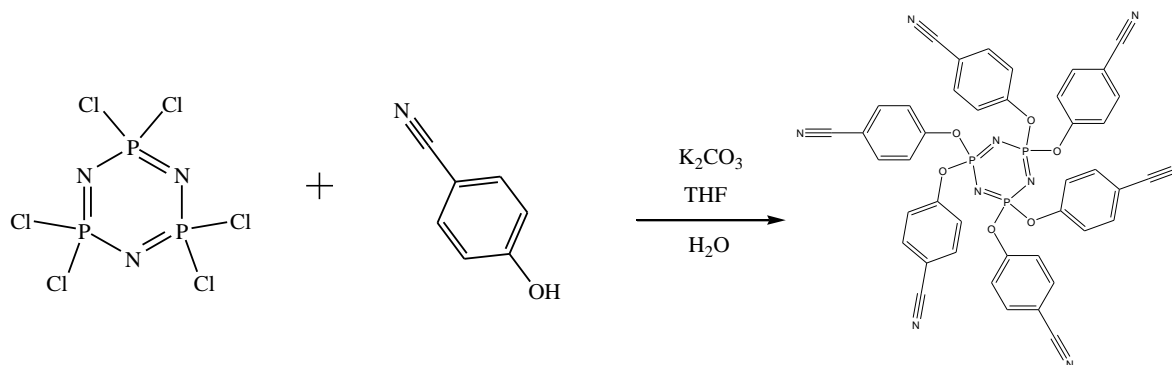


Figure 2.7 Cyclotriphosphazenes containing cyano substituents are shown in this figure.²³ These compounds are stable in air and do not decompose when heated to moderate temperatures. The molecule in (b) has two cyano groups that point in the same direction, while the other points in the opposite direction.

The compound in Figure 2.7a was isolated in very low yield in the literature (5 %).²³ It did therefore not seem to be a feasible idea to synthesise a product in such low yield if a large number of crystallisation experiments needed to be conducted. A cyclotriphosphazene with the cyanophenyl functionality has also been reported in the literature, although not characterised by single crystal X-ray diffraction (SCD).²⁴ The synthetic route is very simple and identical to the procedure followed for the pyridyloxy derivative described earlier and therefore it was decided to attempt the synthesis of this molecule (Scheme 2.6). It was surmised that the cyanophenyl groups would allow the molecules to pack in columns in the crystal structure, or allow for halogen-nitrile interaction.



Scheme 2.6 The synthetic procedure for the cyanophenyl derivative. The procedure is identical to that of the pyridyloxy derivative.

In this case the reaction mixture was not stirred at room temperature for two to three days because the cyano group is a highly electron-withdrawing group that activates the phosphorus atom for substitution.²⁴ The phosphonitric chloride trimer, 4-cyanophenol and potassium carbonate were refluxed for six hours in THF and after completion of the reaction the solvent was removed under vacuum. The residue was washed with water and the product isolated by filtration. 1H and ^{31}P analysis revealed that the white product was pure (Figure 2.8) and that substitution of the chlorine atoms of the phosphonitric chloride trimer had occurred completely because a singlet was present in the ^{31}P spectrum (Figure 2.9).

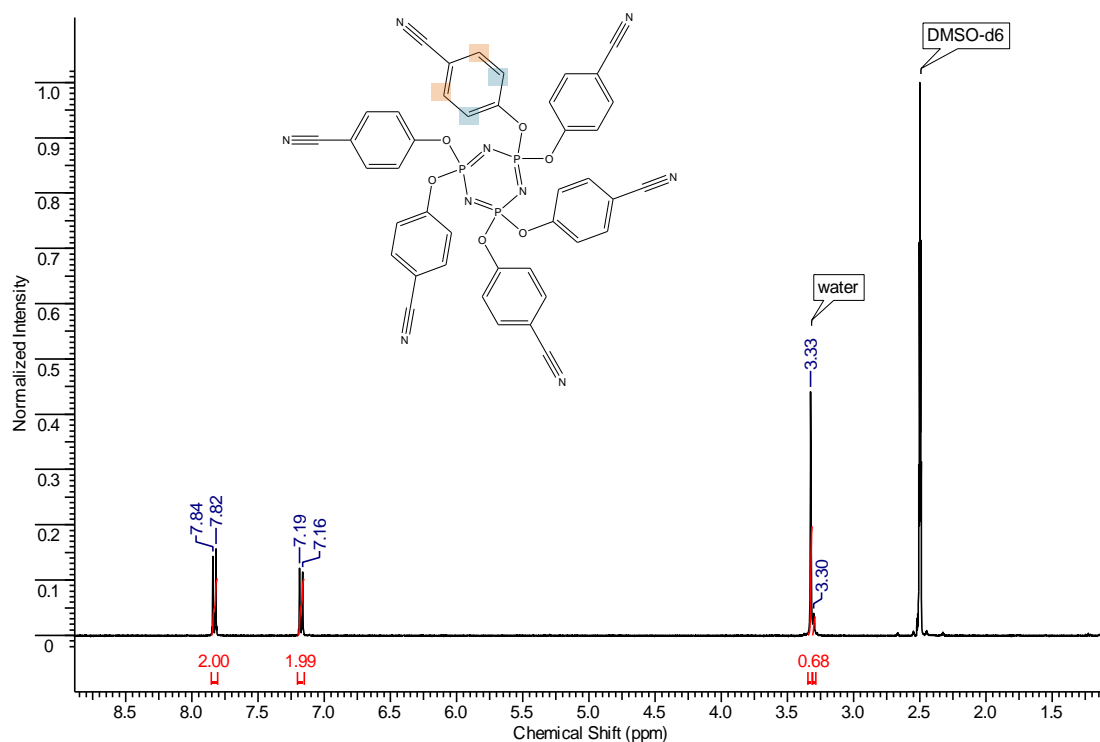


Figure 2.8 The 1H analysis of the cyanophenyl derivative. The two signals in the 1H spectrum correspond with the aromatic protons of the cyanophenyl group.

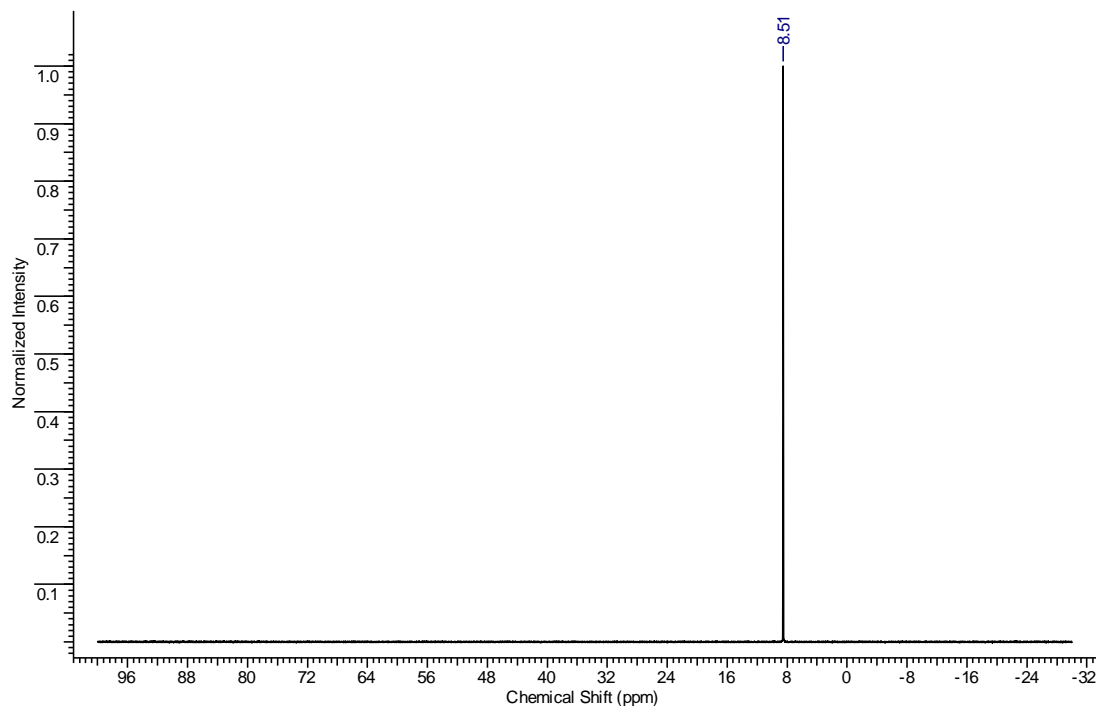


Figure 2.9 ^{31}P analysis of the cyanophenyl derivative. The ^{31}P spectrum shows only one signal, indicating that complete substitution occurred as all phosphorus atoms are chemically equivalent.

Solid state infrared analysis also confirmed the presence of the nitrile functionality (Figure 2.10). The peak at 2225 cm^{-1} is caused by the $\text{C}\equiv\text{N}$ stretch.

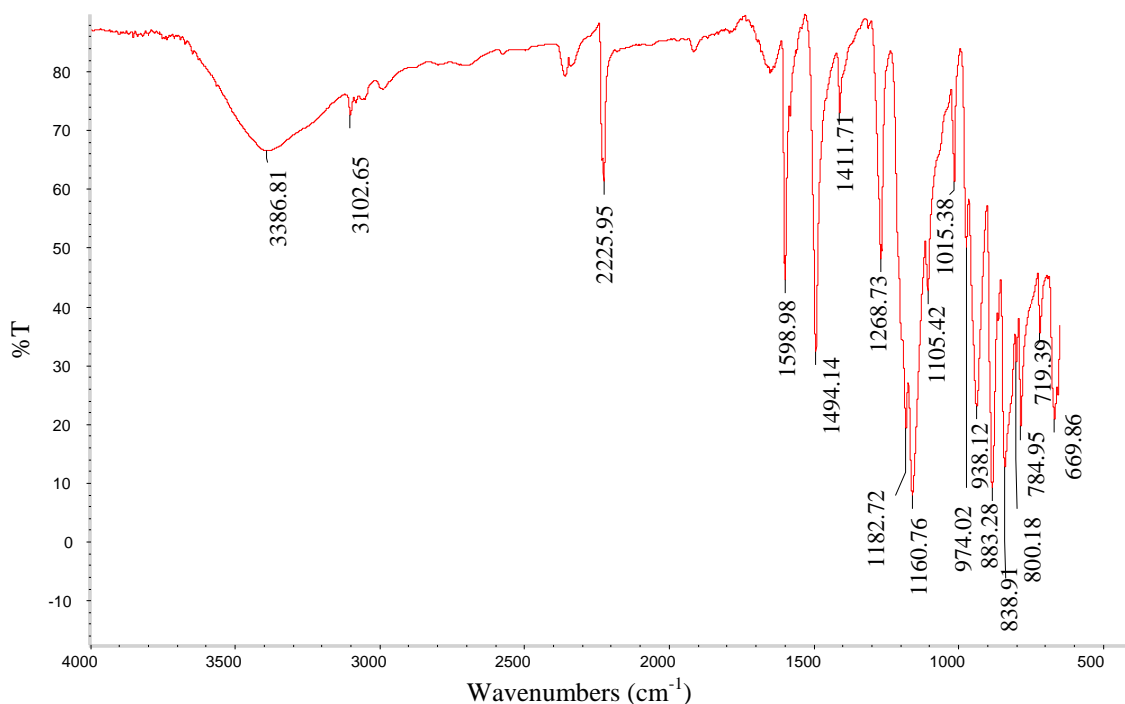


Figure 2.10 The infrared spectrum of hexakis(4-cyanophenoxy)cyclotriphosphazene. The peak at 2225 cm^{-1} is due to the $\text{C}\equiv\text{N}$ stretch.

The product is sparingly soluble in most solvents, except for DMSO and DMF in which it readily dissolves. Rod-shaped crystals of **5** were grown from a co-crystallisation experiment with bromopentafluorobenzene in DMSO. Data was collected at 100 K and the structure was determined (Figure 2.11). Two cyanophenyl rings are twisted towards each other, forming pairs in the molecule above and below the plane of the cyclotriphosphazene ring. One cyanophenyl ring forms a short contact with a molecule beneath it in the chain, allowing for propagation of the chain (Figure 2.12).

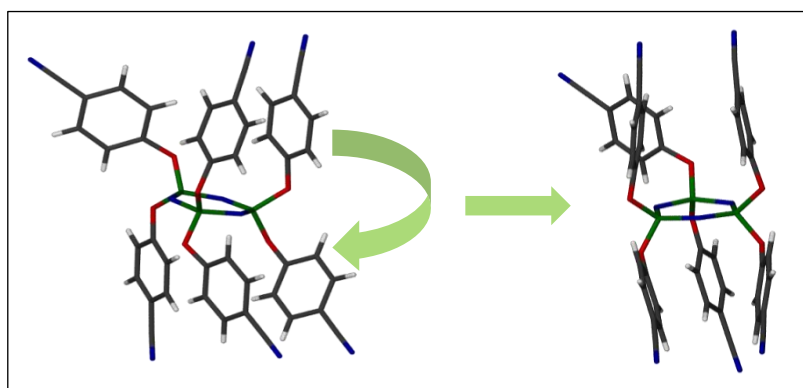


Figure 2.11 This figure illustrates the conformation of the cyanophenyl rings. Two of these rings are twisted towards each other, one pair on each side of the phosphorus-nitrogen ring.

The remaining cyanophenyl ring faces away from the molecule, allowing for interaction between the chains. The chains interact *via* offset face-to-face π -interactions, shown in red in Figure 2.12a as well as edge-to-face π -interactions shown in green in Figure 2.12b.

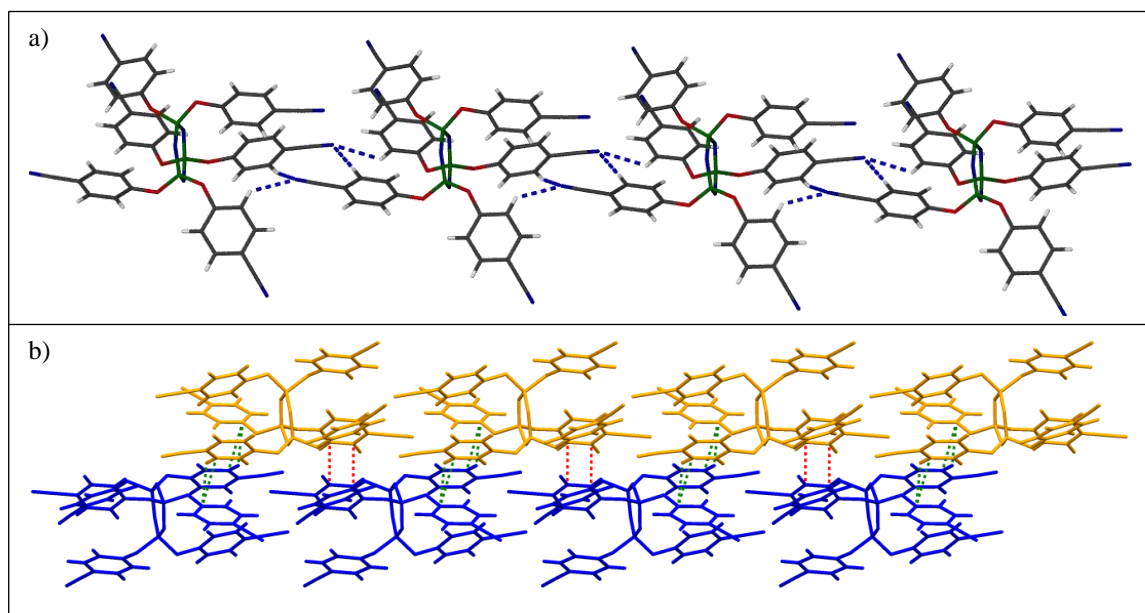
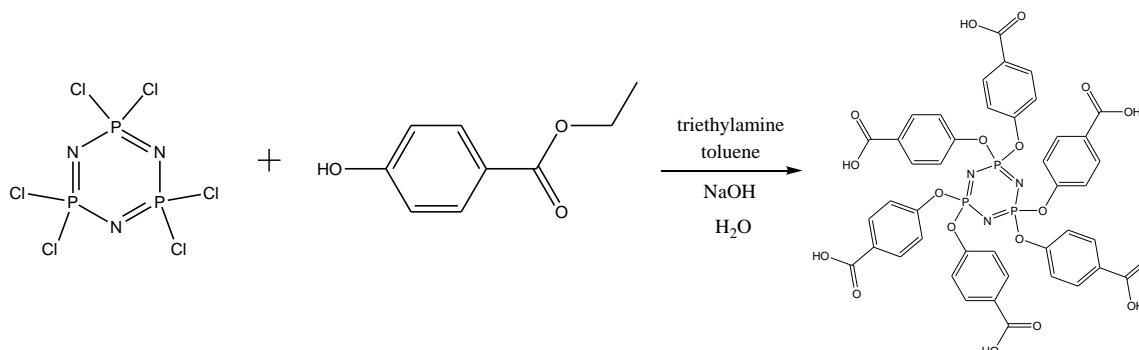


Figure 2.12 (a) Close contacts between the nitrile groups and hydrogens allow the molecules to form a chain. (b) These chains close pack via edge-to-face (green dotted lines) and offset face-to-face π -interactions (red dotted lines).

2.5 Attempted synthesis of a cyclotriphosphazene with carboxylic acid functionality

The carboxylic acid group is a functional group that readily forms hydrogen bonds – a feature that is essential in crystal engineering. The crystal structure of the carboxylic acid derivative seen in Scheme 2.7 has also not yet been elucidated, therefore various attempts were made to synthesise this derivative. The first method used involved the hydrolysis of an ester in basic medium²⁵ (Scheme 2.7).



Scheme 2.7 The first method used in the attempt to synthesise the carboxylic acid derivative. This involves the basic hydrolysis of an ester to yield the carboxylic acid.

A mixture of phosphonitrilic chloride, ethyl-4-hydroxybenzoate and triethylamine was stirred in dry toluene at room temperature for 25 hours.²⁶ Triethylamine serves as the base that deprotonates the ethyl-4-hydroxybenzoate. Smaller bases like sodium hydride or sodium hydroxide were not used for the first step because they can react with the ester at the carbonyl carbon, rather than deprotonating only the hydroxyl group.²⁵ This then leads to the premature formation of the acid. It is also possible that if the ester is first hydrolysed to the carboxylic acid and is then allowed to react with the phosphonitrilic chloride trimer, coordination to the phosphorus atom can occur through one of the carboxylate oxygen ions, rather than the hydroxyl oxygen. The amine hydrochloride was filtered off and a large proportion of the solvent was removed, although the product could not be purified or dried. ³¹P NMR analysis indicated that a variety of phosphorus-containing by-products had formed during the reaction (Figure 2.13). This could either imply that the phosphonitrilic ring system had opened up and polymerised,²⁷ or that products of various degrees of substitution had formed. The product was used as is for the rest of the synthetic procedure. It was dissolved in aqueous methanol and hydrolysed with sodium hydroxide.²⁸ This mixture was then poured into an excess of water and acidified with 2 M hydrochloric acid. A small amount of white solid was collected and washed with water. NMR analysis was performed on the sample (Figure 2.14) and the ¹H spectra showed that the ester had not been hydrolysed. If it had been hydrolysed, the signal for the ethyl group would no longer be visible. This is however not the case as the signals for the methylene and methyl protons are still visible in the spectrum, integrating for two and three protons respectively. There is even a weak signal present for the proton of the hydroxyl group, indicating that substitution had also not taken place. The ³¹P spectrum only shows one weak signal at a chemical shift too far downfield for the expected product.^{27, 29} This NMR spectrum also corresponds with the NMR spectrum of the starting material, ethyl-4-hydroxybenzoate.

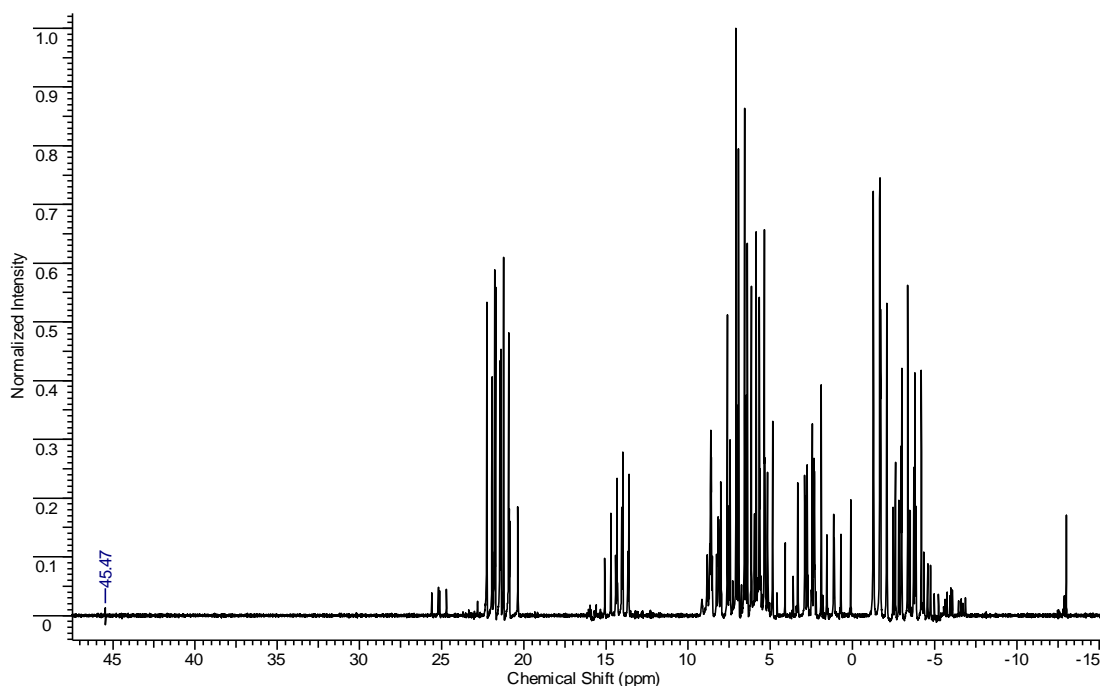


Figure 2.13 This ^{31}P spectrum shows that many phosphorus-containing side-products formed during the reaction. This could however also indicate the polymerisation of the cyclotriphosphazene.

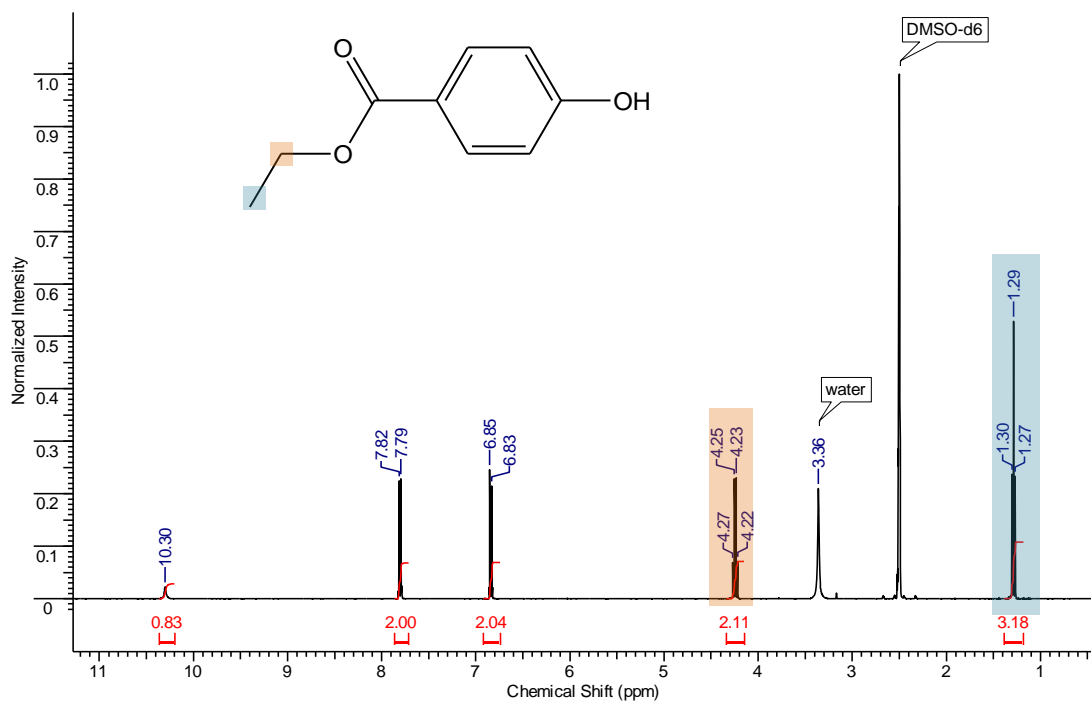
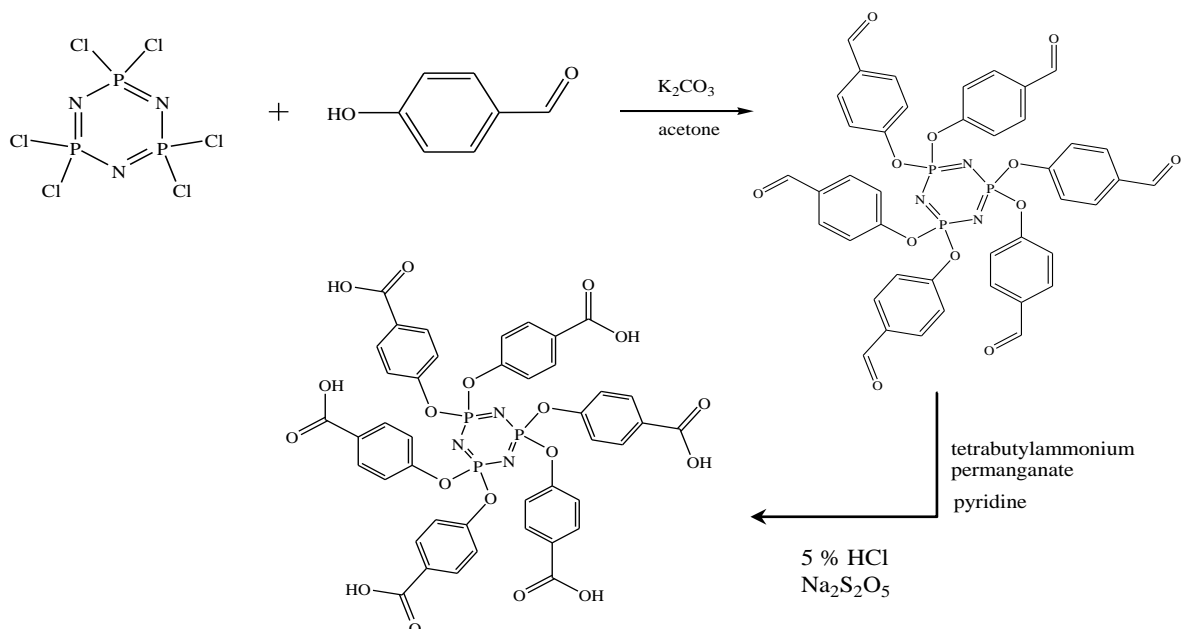


Figure 2.14 ^1H analysis shows the presence of ethyl-4-hydroxybenzoate and not the carboxylic acid. The signals for the methylene and methyl protons are still present, integrating for two and three protons respectively. The peak at 10.30 ppm is that of the hydroxyl group, indicating that substitution onto the cyclotriphosphazene ring did not occur.

The second method that was used to try to synthesise the carboxylic acid was the oxidation of an aldehyde to a carboxylic acid, illustrated in (Scheme 2.8).³⁰⁻³²



Scheme 2.8 The synthetic procedure for oxidising the fully substituted benzaldehyde to a cyclotriphosphazene containing the carboxylic acid functionality.

The first step seen in Scheme 2.8 involves the substitution of the chlorine atoms on the cyclotriphosphazene ring by 4-hydroxybenzaldehyde. The potassium carbonate again acts as a base to deprotonate the hydroxyl group of the 4-hydroxybenzaldehyde. The reagents were dissolved in acetone as it has been shown that the combination of potassium carbonate and acetone allow the reaction to occur faster. This is due to the high polarity of the acetone which promotes a higher reaction rate.^{24, 33} The reaction mixture was refluxed for twelve hours and the solution filtered, yielding a yellow product. ³¹P NMR analysis of the yellow product indicated that all the phosphorus atoms had been fully substituted, with a single peak at 9.68 ppm. The chemical shift value reported in the literature is at 6.90 ppm.³⁰ The shift in the signal could be due to the different solvents used for NMR analysis – the analysis by Ye and co-workers was done in CDCl₃ or benzene, whereas the NMR analysis in this study was done in DMSO.

For the second step, tetrabutylammonium permanganate was needed. This was prepared by mixing aqueous solutions of KMnO₄ and tetrabutylammonium bromide (N-*n*-Bu₄Br) and collecting the purple precipitate.³² This is a potentially explosive substance, therefore

care must be taken to store it at a low temperature to slow down decomposition.³² Tetrabutylammonium permanganate was added over a period of five hours to the hexakis(4-formylphenoxy)cyclotriphosphazene in pyridine. The reaction mixture was stirred for another hour and subsequently cooled in an ice bath. 5 % HCl and Na₂S₂O₅ was used to quench the reaction and remove MnO₂. The next step was to separate the acid by filtration, however no precipitate formed during this reaction. Extended cooling in the ice bath also did not yield any product. Attempts to extract any product from the reaction mixture were unsuccessful and analysis of the reaction mixture did not lead to any conclusive results; therefore it was decided to search for an alternative, preferably pyridine-free, synthetic route.

First, substituting the chlorine atoms with *p*-aminobenzoic acid (PABA) was considered. This involved preparing a mixture of phosphonitrilic chloride trimer, PABA and triethylamine and refluxing for 24 hours in THF. The precipitate, aminehydrochloride, was filtered off and the filtrate acidified. The solvent was removed and the product was analysed by ¹H and ³¹P NMR (Figure 2.15). From the ³¹P spectrum it is apparent that full substitution had not occurred, because rather than the expected singlet of a fully substituted ring, various doublets and triplets were observed.

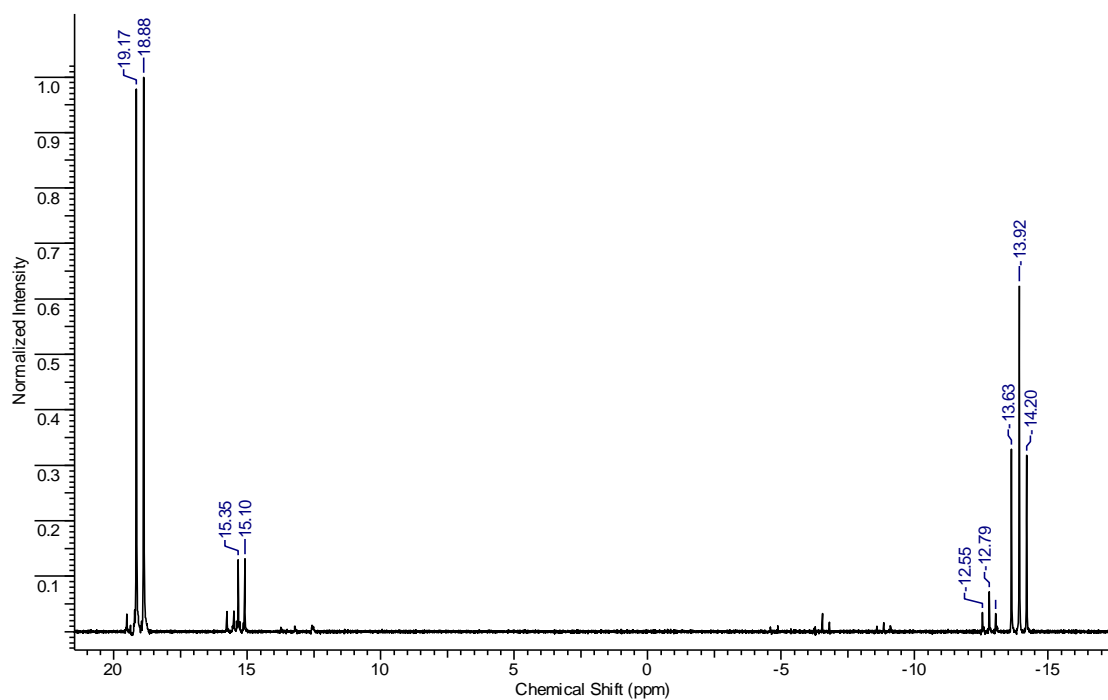


Figure 2.15 The ³¹P spectrum of the product of the reaction between phosphonitrilic chloride trimer and PABA. Peaks are observed much further upfield than is usual for substituents with a nitrogen linker.

Attempts were made to change the reaction conditions. These included changing the solvent to a higher boiling solvent like acetonitrile and refluxing for longer periods of time. However, these reactions were still not successful. It was decided to try mechanochemical synthesis in an attempt to provide the reagents with the necessary energy for the reaction to take place. This involves grinding the different components together for 5, 10 or 30 minutes, with or without base. No solvent was used during these grinding experiments. Powder X-ray diffraction data was collected on each of the grinding experiments and the results compared. The results are shown in Figure 2.16. The diffractograms show that the products from the grinding experiments without any base present only appear to be a mixture of the starting materials. If a new compound had formed, the patterns would not correspond with the simulated patterns of PABA and phosphonitrilic chloride trimer.

Figure 2.17 shows the results from grinding PABA and phosphonitrilic chloride trimer together in the presence of base. Upon grinding with the base, the powder becomes a thick brown paste after only a few minutes of grinding. Grinding without the base produced only powder samples creamy in colour. It is evident from Figure 2.16 that the patterns of the reagents and the products do not match. NMR analysis (Figure 2.18) did not yield any conclusive results as ^{31}P NMR indicated the presence of phosphorus, but not at the chemical shift expected for the phosphonitrilic chloride trimer. It is possible that the ring degraded to some extent due to a reaction with the base. This method of synthesis was therefore also not successful.

The last attempt at synthesising the carboxylic acid derivative consisted of reacting the hexakis(4-bromophenyl)cyclotriphosphazene (**4**) with *n*BuLi (*n*-butyl lithium). Hexakis(4-bromophenyl)cyclotriphosphazene was dissolved in THF and the solution cooled in a slurry of dry ice and acetone to $-78\text{ }^{\circ}\text{C}$. *n*BuLi was added to this solution, warmed up to room temperature and allowed to stir for 10 minutes. Excess dry ice was added to this solution and then the solution was washed with water. This is done to precipitate the product, however, no precipitate formed even on evaporation of the water. This synthetic procedure was also not successful.

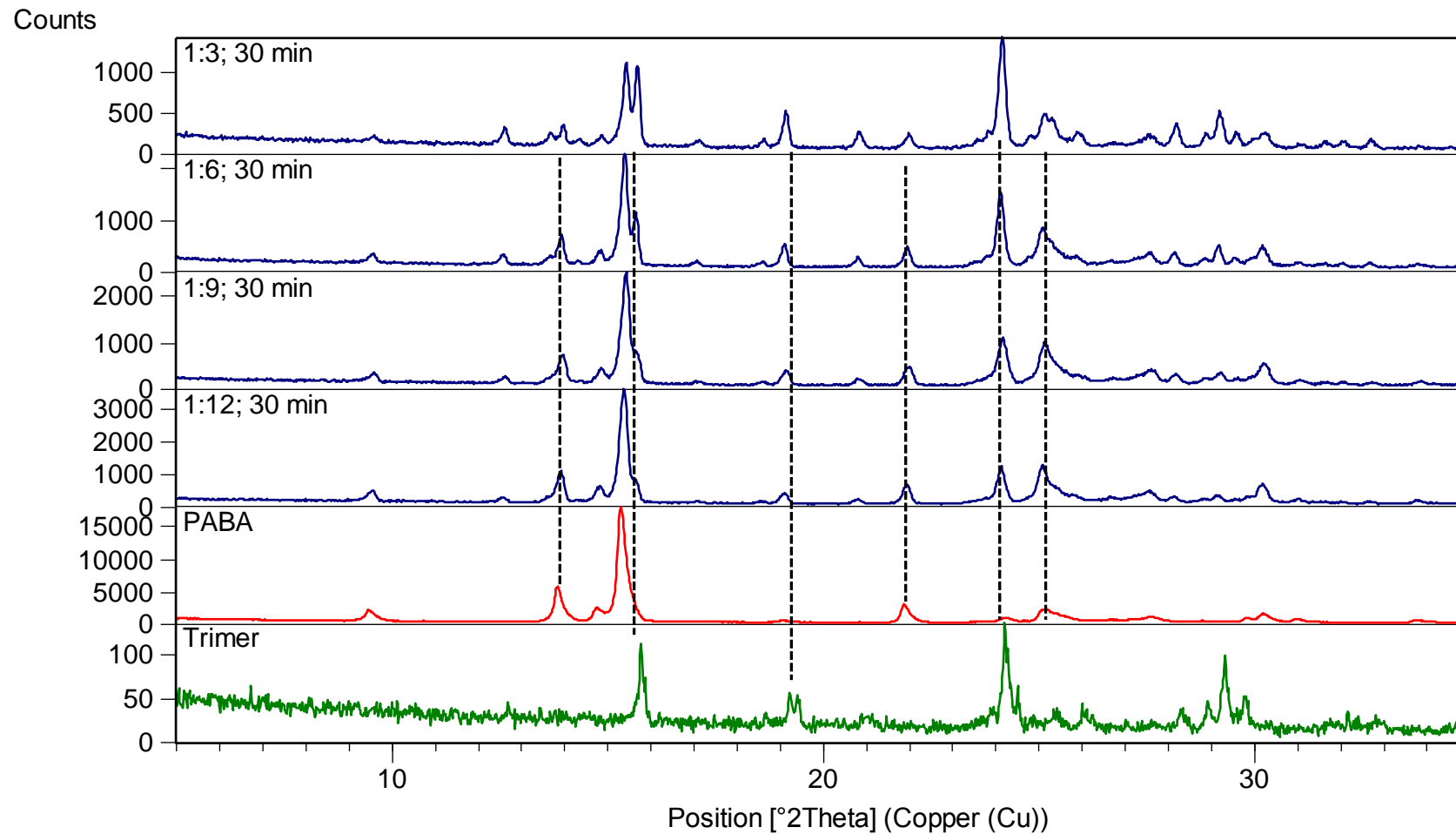


Figure 2.16 Powder X-ray diffraction results from the grinding experiments. The ratio of phosphonitric chloride trimer:PABA is indicated in each case. Peaks from the two simulated patterns appear in the product of the grinding experiments. This indicates that the product is simply a mixture of the two starting materials.

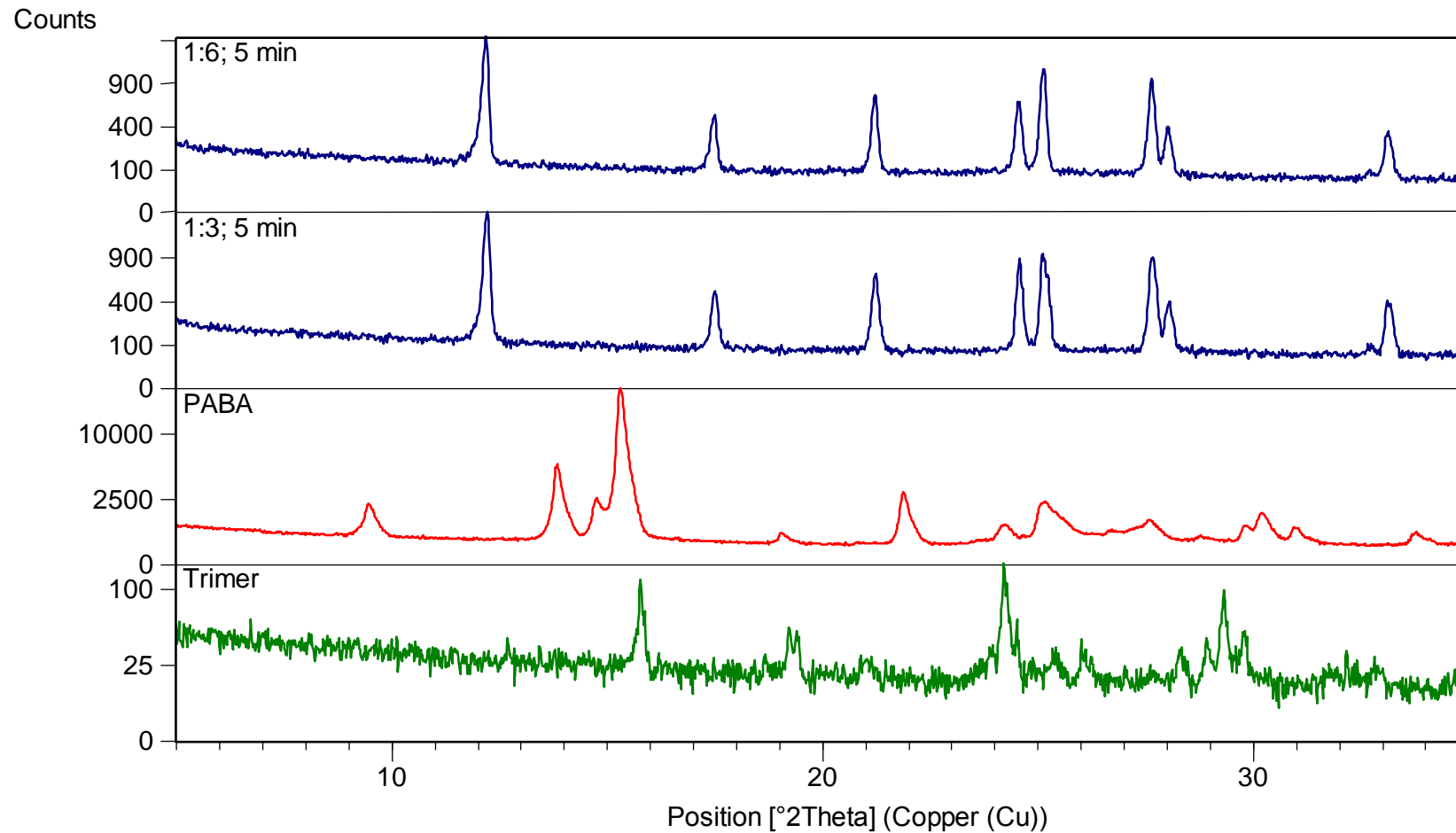


Figure 2.17 Powder X-ray diffraction results of the grinding experiments with triethylamine as base. The ratio of $N_3P_3Cl_6$:PABA is indicated. Only the results from 5 minutes of grinding are shown as grinding for longer periods of time became increasingly difficult with the formation of the paste.

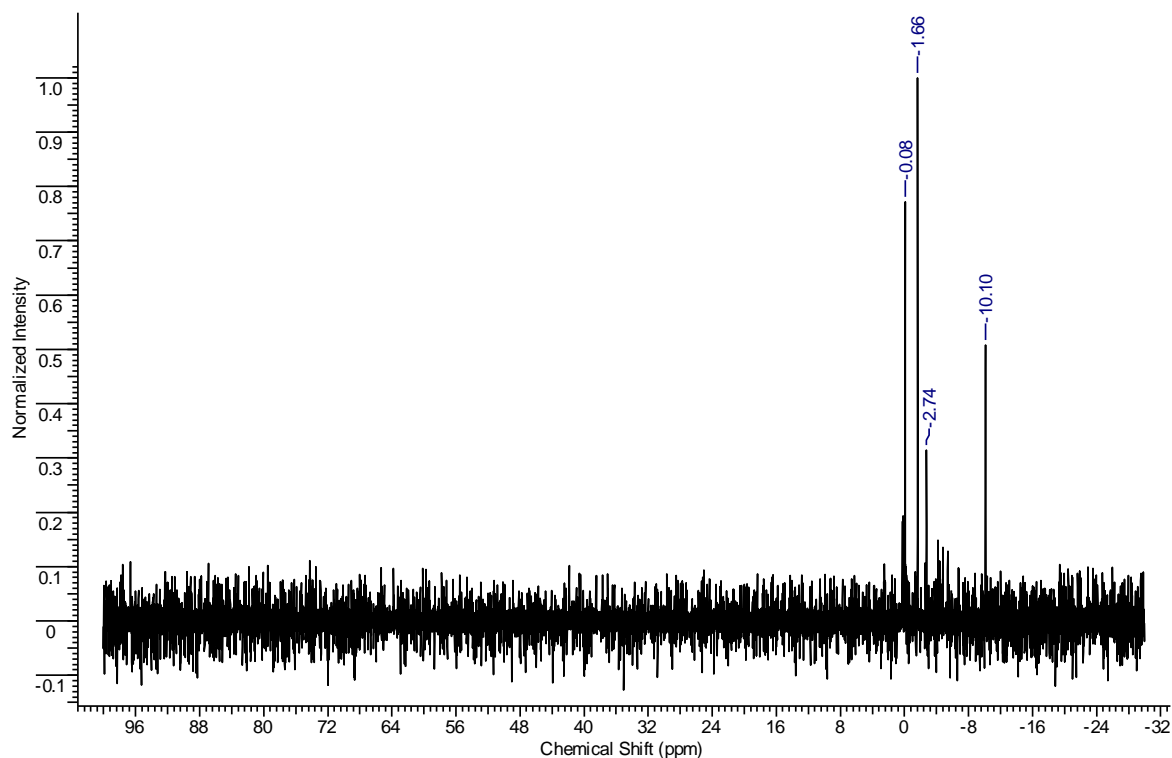


Figure 2.18 ³¹P NMR analysis of the grinding product between PABA and phosphonitrilic chloride trimer in the presence of base. The spectrum indicates the presence of phosphorus, but signals for the phosphonitrilic chloride trimer usually occur at 19 ppm.

2.6 Conclusions

In this study, out of the sixteen target molecules, fifteen cyclotriphosphazene derivatives were successfully synthesised. Most of these derivatives were synthesised using standard Schlenk techniques in order to perform the reactions under inert conditions.

Two novel crystal structures of the cyclotriphosphazene derivatives have been identified and characterised using single crystal X-ray diffraction. These are hexakis(4-cyanophenyl)cyclotriphosphazene (**5**) and 2,2-bis(4-formylphenoxy)-4,4,6,6-bis[spiro-(2',2''-dioxy-1',1''-biphenyl)]cyclotriphosphazene (**3**). The crystal structures of both have been described in this chapter.

Some synthetic procedures proved to be more challenging than expected and a variety of methods were employed in order to make the desired cyclotriphosphazenes. In some cases, the alternative method was successful, e.g. hexakis(4-pyridyloxy)-

cyclotriphosphazene. The original synthetic method that was used required working under strict inert conditions,¹⁶ whereas the alternative method precipitated the derivative from water.²¹ It is possible that impurities in the cannula filter used for the first synthesis might have caused the degradation of the starting materials. This could explain why, during the second attempt at the synthesis of **4**, less strict inert conditions still led to the formation of the correct product.

A variety of methods were used to attempt to synthesise the hexakis(4-carboxyphenoxy)cyclotriphosphazene. The procedure of exchanging the bromo groups of **14** for lithium, and then using dry ice to convert it to the carboxylic acid has never before been attempted on cyclotriphosphazenes. However, this particular procedure did not prove to be immediately successful. Future work could include optimising the conditions for this reaction, as it has been proven successful in many organic synthetic procedures. Excess *n*BuLi could be added to ensure the reaction occurs to completion. The reaction mixture could also be left to react for longer, as in this particular experiment it was only left to stir for approximately 5 minutes. It is strongly recommended that further studies be done into the synthesis of the hexakis(4-carboxyphenoxy)cyclotriphosphazene as the carboxylic acid moiety forms part of a robust synthon often used in crystal engineering for its structure-directing potential. A possible synthetic route could involve the use of 1,4-biphenol or 6-hydroxy-naphthalene-4-carboxylic acid as reagents. If the molecule is conformationally restricted, it would significantly decrease the ability of the molecule to coordinate to the phosphorus atom through both oxygen atoms.

Although the results of the attempted mechanochemical synthesis of the *p*-aminobenzoic acid derivative were inconclusive, it is definitely worthwhile to further analyse the products formed during the reaction. It is recommended that triethylamine be replaced with potassium carbonate which can be easily removed by washing the product with water. It is also possible to obtain a powder pattern of potassium carbonate to compare to the powder pattern of the product in order to investigate whether a reaction had taken place.

2.7 Detailed synthetic procedures

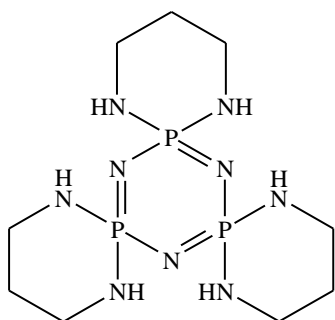
Detailed procedures and reagent quantities for all cyclotriphosphazenes prepared in this study can be found in this section. All chemicals were purchased from Sigma-Aldrich and used without further purification. THF, diethylether and toluene were distilled over sodium sand or wire with benzophenone as indicator, under an atmosphere of dry nitrogen. DCM and acetonitrile were distilled over dried calcium hydride under an atmosphere of dry nitrogen. Acetone and *n*-hexane were distilled over dried calcium chloride under nitrogen.

^1H and ^{31}P NMR spectra were obtained using a 300 MHz Varian VNMRS or a 400 MHz Varian Unity Inova. Chemical shift values are in ppm and were referenced to either chloroform-*d* or DMSO-*d*₆. Data for ^1H spectra are reported as chemical shift (δ ppm) (integration, multiplicity, coupling constant (Hz)). H_3PO_4 was used as an external standard for ^{31}P NMR.

Melting points for **2**, **8**, **3**, **6**, **12**, **13**, **14**, **15** and **5** were determined by differential scanning calorimetry using a TA Instruments Q100 system under a N_2 gas purge, with a flow rate of 50.0 ml/min and heating rate of 10 °C/min. The samples (ranging from 1.5 to 3 mg) were placed in aluminium pans that were non-hermetically sealed with vented aluminium lids. Melting points for **10** and **4** were determined by a Stuart SMP3 melting point apparatus in K10 glass capillary tubes.

All reactions were performed under an atmosphere of dry nitrogen unless otherwise stated.

2.7.1 Tris(1,3-diaminopropane)cyclotriphosphazene (**7**)^{34,35}



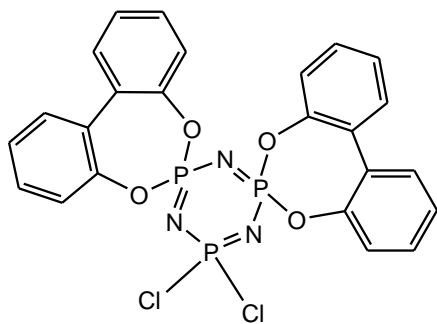
$\text{N}_3\text{P}_3\text{Cl}_6$ (0.5 g, 1.44 mmol) was dissolved in 50 ml of a 7:3 mixture of *n*-hexane: DCM. 1,3-diaminopropane (0.8 ml, 8.64 mmol) was added to this mixture,. The reaction mixture was refluxed for 4 hours after which the solution was cooled and filtered and the solvent removed under reduced pressure. The white powder was further purified by recrystallisation from methanol. Yield: 62% (0.313 g, 0.89 mmol).

^1H NMR (DMSO-*d*₆, 400 MHz): δ ppm 1.53 (2H, m), 3.04 (4H, m), 3.48 (2H, s), ^{31}P NMR (DMSO-*d*₆, 400 MHz, H_3PO_4): δ ppm 13.86 (d), 20.45 (t).

Crystals of **7** were also grown from a THF/hexane solution. This proved to be the known hydrate.³⁴

2.7.2 2,2-Bis(4-formylphenoxy)-4,4,6,6-bis[spiro(2',2''-dioxy-1',1''-biphenyl)]-cyclotriphosphazene⁶ (**3**)

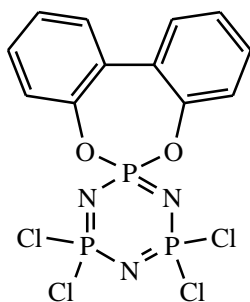
a. 2,2-Dichloro-4,4,6,6-bis[spiro(2',2''-dioxy-1',1''-biphenyl)]cyclotriphosphazene (**2**)



$\text{N}_3\text{P}_3\text{Cl}_6$ (2 g, 5.75 mmol), biphenyl-2,2'-diol (2.14 g, 11.51 mmol) and K_2CO_3 (3.98 g, 28.77 mmol) were mixed in 20 ml acetone at 0 °C. The reaction mixture was stirred at room temperature for 24 hours and when the reaction was complete the solvent was removed *in vacuo*. The product was extracted by washing with 15 ml of DCM four times, filtering each time with a

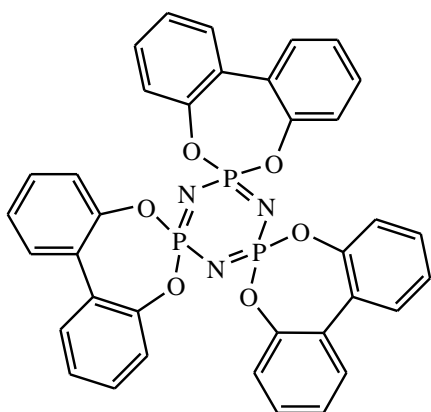
cannula filter. The solvent was then removed under vacuum to produce a white powder. Yield: 86 % (2.847 g, 4.96 mmol). Mp.: 268 – 275 °C.

^1H NMR (CDCl_3 , 300 MHz): δ ppm 7.55 (4H, d, $J = 7.63$ Hz), 7.46 (4H, d, $J = 7.63$ Hz), 7.36 (8H, m), ^{31}P NMR (CDCl_3 , 300 MHz, H_3PO_4): δ ppm 19.79 (d, $\text{C}_{12}\text{O}_2\text{H}_8$), 29.19 (dd, Cl_2).

b. 4,4,6,6-Tetrachloro-2,2-(biphenyl-2,2'-dioxy)cyclotriphosphazene (**8**)³⁶

A mixture of $\text{N}_3\text{P}_3\text{Cl}_6$ (1.018 g, 2.88 mmol), 2,2'-biphenol (0.543 g, 2.88 mmol) and K_2CO_3 (2.013 g, 14.4 mmol) were stirred together in 40 ml acetone at room temperature for 30 minutes. The volatiles were evaporated *in vacuo* and the residue extracted with 4 x 15 ml DCM. The solvent was evaporated to give a white solid. The product was recrystallised from DCM/petroleum ether. Yield: 80% (1.071 g, 2.32 mmol). Mp.: 181 – 189 °C.

^1H NMR (CDCl_3 , 400 MHz): δ ppm 7.57 (2H, d, $J = 7.62$ Hz), 7.49 (2H, t, $J = 7.42$ Hz), 7.41 (2H, t, $J = 7.62$ Hz), 7.33 (2H, d, 8.01 Hz), ^{31}P NMR (CDCl_3 , 400 MHz, H_3PO_4): δ ppm 21.87 (d, Cl_2), 9.74 (t, $\text{C}_{12}\text{O}_2\text{H}_8$).

c. Tris(2,2'-dioxybiphenyl)cyclotriphosphazene (**17**)^{10,37}

$\text{N}_3\text{P}_3\text{Cl}_6$ (1.003 g, 2.88 mmol), 2,2'-biphenol (1.815 g, 9.66 mmol) and K_2CO_3 (3.010 g, 21.8 mmol) were refluxed for 7 hours in 140 ml acetone. The solvent was evaporated *in vacuo* and the residue was washed with 100 ml water, 100 ml aqueous NaOH (0.5 M), 2 x 50 ml water, 50 ml ethanol and 50 ml ether. The white product was dried under vacuum. Yield: 75% (1.278 g, 1.86 mmol). Mp.: >350 °C.

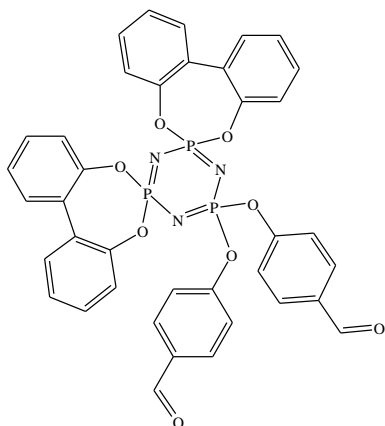
^1H NMR (CDCl_3 , 400 MHz): δ ppm 7.52 (2H, d, $J = 7.62$ Hz), 7.41 (4H, m), 7.33 (2H, t, $J = 7.642$ Hz), ^{31}P NMR (CDCl_3 , 400 MHz, H_3PO_4): δ ppm 26.27 (s).

The synthesis of all three derivatives was confirmed by single crystal X-ray diffraction analysis.

Table 2.1 The unit cell parameters of **2**, **8** and **17**. This data served as further confirmation that the synthetic procedures were successful.

Unit cell parameters	2	8	17
Crystal system	monoclinic <i>C</i>	monoclinic <i>P</i>	monoclinic <i>C</i>
<i>a</i> (Å)	10.99	11.09	15.30
<i>b</i> (Å)	26.34	12.17	10.85
<i>c</i> (Å)	17.09	13.71	20.15
α (°)	90	90	90
β (°)	101.13	100.92	108.23
γ (°)	90	90	90

d. 2,2-Bis(4-formylphenoxy)-4,4,6,6-bis[spiro(2',2''-dioxo-1',1''-biphenyl)]cyclotri-phosphazene (**3**)

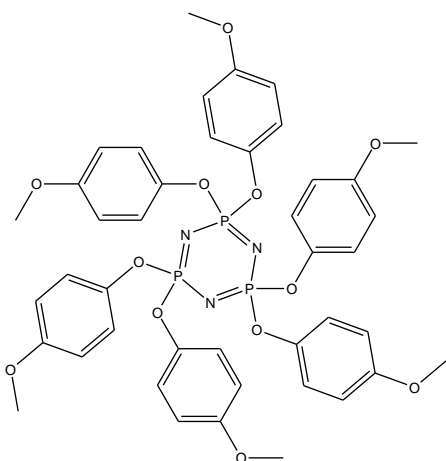


2 (2 g, 3.48 mmol), 4-hydroxybenzaldehyde (0.854 g, 6.96 mmol) and K_2CO_3 (2.663 g, 19.28 mmol) were added to 20 ml THF at 0 °C. The mixture was refluxed for 5 hours and the solvent removed under vacuum after the reaction was complete. The product was then extracted with 4 x 10 ml DCM and the solvent subsequently removed under vacuum yielding a white powder. The product was recrystallised from acetone. Yield: 72% (1.881 g, 2.52 mmol). Mp.: 220 – 224 °C.

1H NMR ($CDCl_3$, 300 MHz): δ ppm 7.07 (2H, d, $J = 7.80$ Hz), 7.31 – 7.41 (4H, m), 7.54 (4H, t, $J = 8.58$ Hz), 7.96 (2H, d, 8.19 Hz), 10.01 (1H, s) ^{31}P NMR ($CDCl_3$, 300 MHz, H_3PO_4): δ ppm 9.62 – 11.69 (tt), 25.59 – 26.71 (dt).

2.7.3 Hexakis(4-hydroxyphenoxy)cyclotriphosphazene³⁸ (11)

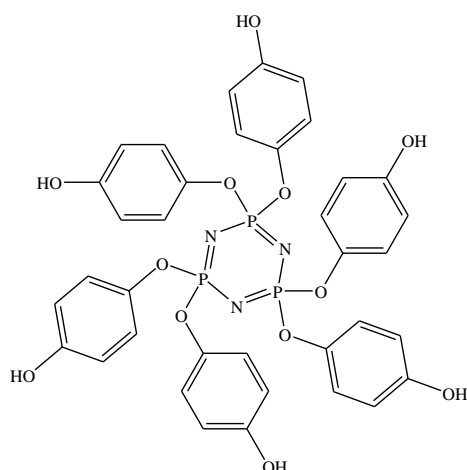
1. Hexakis(4-methoxyphenoxy)cyclotriphosphazene (10)



A suspension of sodium 4-methoxyphenoxide was prepared in 20 ml dry THF by allowing 4-methoxyphenol (4.274 g, 34.5 mmol) to react with 1.385 g NaH as a 60 % dispersion in mineral oil. This is equivalent to 0.828 g (34.5 mmol) pure NaH. The NaH was washed with dry petroleum ether to remove the mineral oil. A solution of $N_3P_3Cl_6$ (2 g, 5.75 mmol) in 20 ml THF was added dropwise to this suspension. On complete addition of the phosphonitrilic chloride trimer, the reaction mixture was refluxed for 24 hours with stirring. The reaction mixture was cooled and washed with 100 ml water in order to precipitate the product as a white powder. Yield: 82% (4.136 g, 4.733 mmol). Mp.: 105 – 106 °C.

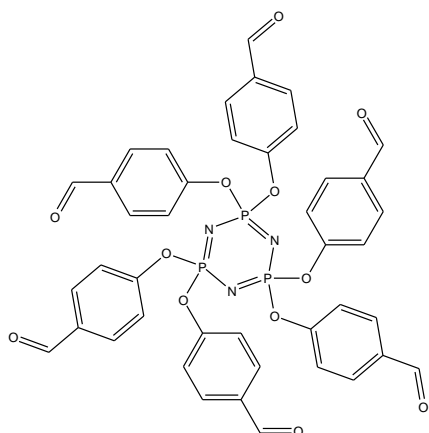
1H NMR ($CDCl_3$, 400 MHz): δ ppm 3.72 (3H, s), 6.77 (4H, s)

2. Hexakis(4-hydroxyphenoxy)cyclotriphosphazene (11)



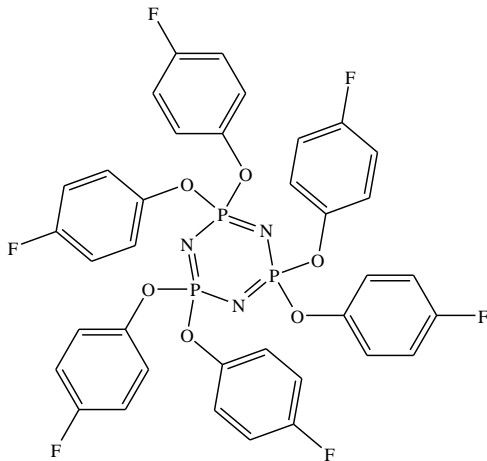
Hexakis(4-methoxyphenoxy)cyclotriphosphazene (3 g, 3.43 mmol) was dissolved in 30 ml DCM. A solution of BBr_3 (2 ml, 20.6 mmol) in 30 ml DCM was added dropwise to the solution of the cyclotriphosphazene. It was then left to stir for 3 hours, after which it was poured carefully into 100 ml of water to precipitate the product. The white precipitate was filtered off, washed with water and dried. Yield: 85% (2.303 g, 2.92 mmol).

1H NMR ($DMSO-d_6$, 400 MHz): δ ppm 6.59 (2H, s), 6.61 (2H, s), ^{31}P NMR ($DMSO-d_6$, 400 MHz, H_3PO_4): δ ppm 22.32 (s).

2.7.4 Hexakis(4-formylphenoxy)cyclotriphosphazene^{30,39} (6)

4-hydroxybenzaldehyde (2.128 g, 17.28 mmol), K_2CO_3 (4.788, 34.56 mmol) and $N_3P_3Cl_6$ (1.026 g, 2.88 mmol) were added to 40 ml acetone and refluxed for 12 hours. The solution was then filtered and the solvent removed under reduced pressure to produce a yellow powder. Yield: 57% (1.414 g, 1.64 mmol). Mp.: 215 – 220 °C.

1H NMR (DMSO- d_6 , 400 MHz): δ ppm 6.84 (2H, m), 7.25 (2H, m), 8.31 (1H, s), ^{31}P NMR (DMSO- d_6 , 400 MHz, H_3PO_4): δ ppm 9.68 (s).

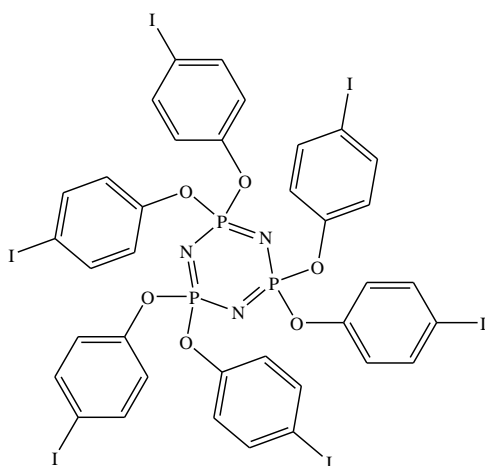
2.7.5 Hexakis(4-fluorophenyl)cyclotriphosphazene^{20,30} (12)

This synthetic procedure was not performed under inert conditions. 4-fluorophenol (1.94 g, 17.28 mmol) and $N_3P_3Cl_6$ (0.998 g, 2.88 mmol) were dissolved in 60 ml acetone. K_2CO_3 (4.797 g, 120.96 mmol) was added to this mixture and the reaction mixture was refluxed for 12 hours. The precipitate was filtered off, washed with DCM and combined with the filtrate. The solvent was then removed *in vacuo*. The white powder was recrystallised from methanol. Yield: 65% (3.131 g, 3.91 mmol). Mp.: 129 °C.

1H NMR ($CDCl_3$, 400 MHz): δ ppm 6.88 (2H, s), 6.9 (2H, s), ^{31}P NMR ($CDCl_3$, 400 MHz, H_3PO_4): δ ppm 9.86 (s).

Two novel polymorphs of this compound have been isolated in this study. These polymorphs will be discussed in detail in chapter 3.

2.7.6 Hexakis(4-iodophenyl)cyclotriphosphazene^{20,30} (13)

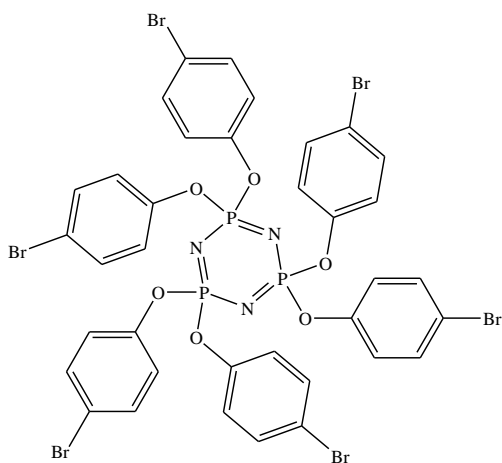


4-iodophenol (3.844 g, 17.28 mmol) and $\text{N}_3\text{P}_3\text{Cl}_6$ (1.007 g, 2.88 mmol) were dissolved in 75 ml acetone. K_2CO_3 (4.821 g, 34.56 mmol) was added to this mixture. The mixture was refluxed for 2 days. The solvent was evaporated under vacuum and the product was extracted with 3 x 20 ml DCM. The product was further purified by recrystallisation from acetonitrile to yield a white crystalline powder. Yield: 65% (2.702g, 1.86

mmol). Mp.: 187.6 °C.

^1H NMR (CDCl_3 , 400 MHz): δ ppm 6.62 (2H, d, $J = 8.79$ Hz), 7.52 (2H, d, 8.79 Hz), ^{31}P NMR (CDCl_3 , 400 MHz, H_3PO_4): δ ppm 9.27 (s).

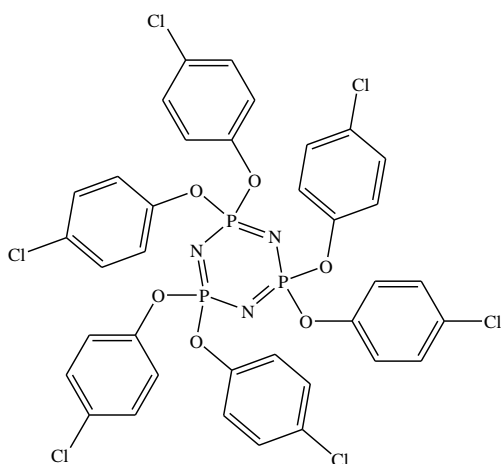
2.7.7 Hexakis(4-bromophenyl)cyclotriphosphazene^{20,30} (14)



4-bromophenol (3.030 g, 17.28 mmol) and K_2CO_3 (4.779 g, 34.56 mmol) were added to 50 ml acetone. $\text{N}_3\text{P}_3\text{Cl}_6$ (1.011 g, 2.88 mmol) in 10 ml acetone was added to this mixture. The reaction mixture was refluxed for 2 days. The solvent was removed under vacuum and the product purified by recrystallisation from acetonitrile to yield a white crystalline powder. Yield: 79 % (2.684 g, 2.3 mmol). Mp.: 176.8 °C.

^1H NMR (CDCl_3 , 400 MHz): δ ppm 6.75 (2H, d, 8.79 Hz), 7.33 (2H, d, 8.89 Hz), ^{31}P NMR (CDCl_3 , 400 MHz, H_3PO_4): δ ppm 9.29 (s).

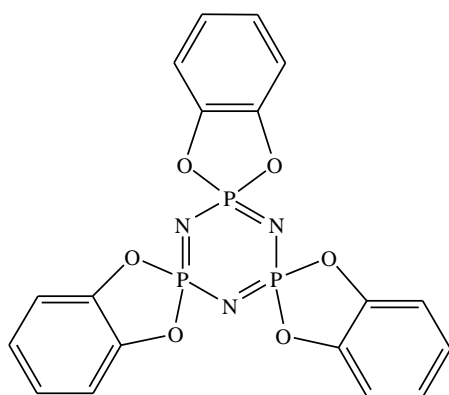
2.7.8 Hexakis(4-chlorophenyl)cyclotriphosphazene^{20,30} (15)



4-chlorophenol (2.240 g, 17.28 mmol) and K_2CO_3 (4.793 g, 34.56 mmol) were stirred together in 50 ml acetone. $N_3P_3Cl_6$ (1.004 g, 2.88 mmol), dissolved in 10 ml acetone, was added to the mixture and refluxed for 1 day. The solvent was removed under vacuum and the product extracted with DCM. The product was further purified by recrystallisation from acetonitrile. Yield: 76 % (1.982 g, 2.2 mmol). Mp.: 152 °C

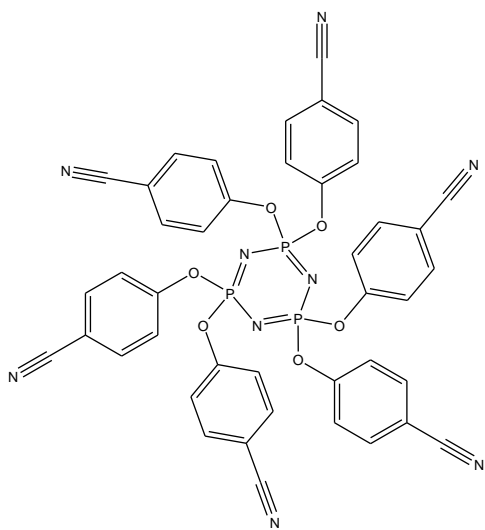
1H NMR ($CDCl_3$, 400 MHz): δ ppm 6.68 (2H, d, 8.20 Hz), 7.17 (2H, d, 8.40 Hz), ^{31}P NMR ($CDCl_3$, 400 MHz, H_3PO_4): δ ppm 9.59 (s).

2.7.9 Tris(*o*-phenylenedioxy)cyclotriphosphazene^{5,40} (16)



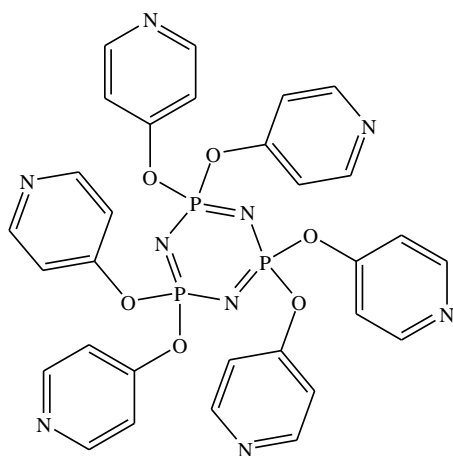
Catechol (0.982 g, 8.63 mmol) was dissolved in 80 ml dry THF. K_2CO_3 (2.400 g, 17.26 mmol) was added to this solution and the solution was then allowed to stir. $N_3P_3Cl_6$ (1.015 g, 2.88 mmol) was dissolved in 20 ml THF and added dropwise to the catechol/ K_2CO_3 suspension. The reaction mixture was refluxed overnight and the solvent then removed under reduced pressure. The residue was washed with 2 x 20 ml water and methanol, yielding a white powder. Yield: 44% (0.577 g, 1.26 mmol).

1H NMR ($CDCl_3$, 400 MHz): δ ppm 7.02 – 7.06 (2H, m), 7.08 – 7.12 (2H, m), ^{31}P NMR ($CDCl_3$, 400 MHz, H_3PO_4): δ ppm 33.83 (s).

2.7.10 Hexakis(4-cyanophenoxy)cyclotriphosphazene²⁴ (5)

A mixture of 4-cyanophenol (2.071 g, 17.28 mmol) and K_2CO_3 (4.804 g, 34.56 mmol) was prepared in 80 ml THF. $N_3P_3Cl_6$ (1.030 g, 2.88 mmol) in 15 ml THF was added dropwise to this mixture. The reaction mixture was refluxed for 6 hours with vigorous stirring. The solvent was removed *in vacuo* and the residue dispersed in 100 ml water. The white product was separated by filtration and allowed to dry. Yield: 94 % (2.284 g, 2.707 mmol). Mp.: 263 – 265 °C.

1H NMR (DMSO- d_6 , 400 MHz): δ ppm 7.16 (2H, d, 8.79 Hz), 7.82 (2H, d, 8.79 Hz), ^{31}P NMR (DMSO- d_6 , 400 MHz, H_3PO_4): δ ppm 8.51 (s).

2.7.11 Hexakis(4-pyridyloxy)cyclotriphosphazene²¹ (4)

4-hydroxypyridine (0.826 g, 8.64 mmol) and K_2CO_3 (1.818 g, 12.96 mmol) were added to 50 ml THF. $N_3P_3Cl_6$ (0.503 g, 1.44 mmol) was added to this mixture. The mixture was stirred for two and a half days at room temperature, after which it was refluxed for approximately 6 hours. The solvent was removed under vacuum and the residue washed with 100 ml water. The product was isolated by filtration and dried to yield a light yellow product. Yield: 89%

(0.897 g, 1.28 mmol). Mp.: 163 – 165 °C.

1H NMR ($CDCl_3$, 400 MHz): δ ppm 6.93 (2H, d, 6.44 Hz), 8.50 (2H, d, 6.25 Hz), ^{31}P NMR ($CDCl_3$, 400 MHz, H_3PO_4): δ ppm 7.30 (s).

References

1. V. Chandrasekhar, P. Thilagar and B. Murugesu Pandian, *Coord. Chem. Rev.*, 2007, **251**, 1045 - 1074.
2. A. Steiner, in *Polyphosphazenes for Biomedical Applications*, John Wiley & Sons, Inc., 2008, pp. 411 - 453.
3. G. Couderc and J. Hulliger, *Chem. Soc. Rev.*, 2010, **39**, 1545 - 1554.
4. M. Gleria and R. De Jaeger, *J. Inorg. Organomet. Polym.*, 2001, **11**, 1 - 45.
5. H. R. Allcock, *J. Am. Chem. Soc.*, 1964, **86**, 2591 - 2595.
6. E. Çil and M. Arslan, *Inorg. Chim. Acta*, 2009, **362**, 1421 - 1427.
7. C. B. Aakeröy and P. D. Chopade, *Org. Lett.*, 2010, **13**, 1 - 3.
8. E. A. Bruton, L. Brammer, F. C. Pigge, C. B. Aakeröy and D. S. Leinen, *New J. Chem.*, 2003, **27**, 1084 - 1094.
9. J. Maurin, *Acta Crystallogr., Sect. B: Struct. Sci.*, 1998, **B54**, 866 - 871.
10. G. A. Carriedo, L. Fernández-Catuxo, F. J. García Alonso, P. Gómez-Elipse and P. A. González, *Macromolecules*, 1996, **29**, 5320 - 5325.
11. N. N. Greenwood and A. Earnshaw, *Chemistry of the Elements*, 2 edn., Elsevier, Great Britain, 1998.
12. D. L. Pavia, G. M. Lampman, G. S. Kriz and J. R. Vyvyan, *Introduction to spectroscopy*, Fourth edn., Brooks/Cole, Cengage Learning, Belmont, 2009.
13. J.-T. Li, X.-L. Li and T.-S. Li, *Ultrason. Sonochem.*, 2006, **13**, 200 - 202.
14. B. Touaux, F. Texier-Boullet and J. Hamelin, *Heteroat. Chem.*, 1998, **9**, 351 - 354.
15. T. Friščić, *J. Mater. Chem.*, 2010, **20**, 7599 - 7605.
16. G. A. Carriedo, P. Gómez Elipse, F. J. García Alonso, L. Fernández-Catuxo, M. R. Díaz and S. García Granda, *J. Organomet. Chem.*, 1995, **498**, 207 - 212.
17. V. Chandrasekhar, B. Murugesu Pandian and R. Azhakar, *Polyhedron*, 2008, **27**, 255 - 262.
18. R. Bertani, E. Ghedini, M. Gleria, R. Liantonio, G. Marras, P. Metrangolo, F. Meyer, T. Pilati and G. Resnati, *CrystEngComm*, 2005, **7**, 511 - 513.
19. Y. Cho, H. Baek and Y. S. Sohn, *Macromolecules*, 1999, **32**, 2167 - 2172.

20. H. R. Allcock, D. C. Ngo, M. Parvez and K. B. Visscher, *Inorg. Chem.*, 1994, **33**, 2090 - 2102.
21. G. A. Carriedo, F. J. G. Alonso, J. L. García, R. J. Carbajo and F. L. Ortiz, *Eur. J. Inorg. Chem.*, 1999, **1999**, 1015 - 1020.
22. H. R. Allcock, J. S. Rutt, M. F. Welker and M. Parvez, *Inorg. Chem.*, 1993, **32**, 2315 - 2321.
23. J. S. Rutt, M. Parvez and H. R. Allcock, *J. Am. Chem. Soc.*, 1986, **108**, 6089 - 6090.
24. Y.-T. Xu, S.-Z. Liu, D. Li, S.-C. Tian, J.-J. Qiu and C.-M. Liu, *Synth. Commun.*, 2011, **41**, 1370 - 1375.
25. J. McMurry, *Organic chemistry*, Sixth edn., Thomson-Brooks/Cole, Belmont, 2004.
26. K. Miyata, Y. Watanabe, T. Itaya, T. Tanigaki and K. Inoue, *Macromolecules*, 1996, **29**, 3694 - 3700.
27. H. R. Allcock and S. Kwon, *Macromolecules*, 1989, **22**, 75 - 79.
28. V. Theodorou, K. Skobridis, A. G. Tzakos and V. Ragoussis, *Tetrahedron Lett.*, 2007, **48**, 8230 - 8233.
29. R. Keat, R. A. Shaw and M. Woods, *J. Chem. Soc., Dalton Trans.*, 1976, 1582 - 1589.
30. C. Ye, Z. Zhang and W. Liu, *Synth. Commun.*, 2002, **32**, 203 - 209.
31. G. Fantin, M. Fogagnolo, M. Gleria, A. Medici, F. Minto and P. Pedrini, *Tetrahedron*, 1996, **52**, 9535 - 9540.
32. J. B. Vincent, H. R. Chang, K. Folting, J. C. Huffman, G. Christou and D. N. Hendrickson, *J. Am. Chem. Soc.*, 1987, **109**, 5703 - 5711.
33. G. A. Carriedo, L. Fernández-Catuxo, F. J. G. Alonso, P. G. Elipe, P. A. González and G. Sánchez, *J. Appl. Polym. Sci.*, 1996, **59**, 1879 - 1885.
34. N. El Murr, R. Lahana, J.-F. Labarre and J.-P. Declercq, *J. Mol. Struct.*, 1984, **117**, 73 - 85.
35. S. S. Krishnamurthy, K. Ramachandran, A. R. V. Murthy, R. A. Shaw and M. Woods, *J. Chem. Soc., Dalton Trans.*, 1980, 840 - 844.
36. G. A. Carriedo, F. J. García-Alonso, J. L. García-Alvarez, G. C. Pappalardo, F. Punzo and P. Rossi, *Eur. J. Inorg. Chem.*, 2003, 2413 - 2418.

37. H. R. Allcock, M. T. Stein and J. A. Stanko, *J. Am. Chem. Soc.*, 1971, **93**, 3173 - 3178.
38. Y. W. Chen-Yang, C. Y. Yuan, C. H. Li and H. C. Yang, *J. Appl. Polym. Sci.*, 2003, **90**, 1357 - 1364.
39. H. R. Allcock and P. E. Austin, *Macromolecules*, 1981, **14**, 1616 - 1622.
40. M. Reynes, O. J. Dautel, D. Virieux, D. Flot and J. J. E. Moreau, *CrystEngComm*, 2011, **13**, 6050 - 6056.

Chapter 3

Two novel polymorphs of hexakis(4-fluorophenoxy)cyclotriphosphazene

Polymorphism in cyclotriphosphazenes is not an unheard of phenomenon as it has been observed before, among others, in the case of 2,2-dichloro-4,4:6,6-bis(2,2'-dimethylpropane-1,3-dioxy)-cyclotriphosphazene.^{1, 2} During the investigation into co-crystal formation with cyclotriphosphazenes, two novel polymorphs of the known hexakis(4-fluorophenoxy)cyclotriphosphazene (**12**) were isolated. First, a novel triclinic phase of the fluorophenoxy derivative was identified. Upon further investigation during variable temperature studies, another phase was discovered. In this case, the known monoclinic *P* phase converts to a monoclinic *C* phase at high temperatures. The known crystal structure of **12** will be discussed first.³ Crystal data for this structure was previously collected at room temperature. The structure will be compared to the crystal structure that was collected at 100 K to study the effect temperature has on the conformation of the molecule. The structure of the novel triclinic phase will then be discussed in detail and compared to that of the monoclinic phase. Differential scanning calorimetry (DSC) and powder X-ray diffraction (PXRD) studies were also performed on these polymorphs to explore the phase transition that occurs and to determine whether these are monotropic or enantiotropic polymorphs. Interesting results obtained from these experiments prompted further analysis by variable temperature single crystal X-ray diffraction (SCD). Analysis by hot stage microscopy investigated the phase transformation from the triclinic to monoclinic phase and determined that it did not occur in a single crystal to single crystal fashion. Variable temperature SCD and PXRD studies investigated the transformation from the monoclinic *P* to monoclinic *C* form.

3.1. Polymorphism

McCrone⁴ defined polymorphism as the capability of the same chemical compound to crystallise “as more than one distinct crystal species”. This implies that the same compound can pack in different ways in the solid state. This phenomenon has been of interest for many years, especially in the pharmaceutical industry. The properties of a

certain compound are greatly affected by its packing arrangement in the solid state, therefore a change in the structure can give the same chemical compound new properties.⁵ This has major implications for patents on drugs where a new polymorph might, for example, have better solubility properties.^{4, 5} The polymorph is considered to be a new compound; therefore a rival company can attain a patent for it subsequently costing other companies millions.^{6, 7}

Desiraju⁸ posed an excellent question regarding the abundance of polymorphism:

“Why should any molecule crystallise in more than one form especially when it appears that molecular recognition is such a subtle and specific event that demands an exact matching in geometrical and chemical terms of the various interacting molecules?”

Therefore, studying this phenomenon is of utmost importance. Studying these systems allow crystal engineers to fundamentally understand what controls molecular assembly and, in turn, use these principles to engineer specific compounds with specific properties. Crystallisation is a process that is dependent on the formation of nucleation sites within the crystallisation vessel. This process is dependent on the temperature, solvent system and the rate at which crystallisation is allowed to occur.⁹ Changing these experimental conditions can lead to the formation of polymorphs.

Molecular structure is determined by bond lengths, bond angles and torsion angles.⁶ These torsion angles allow some molecules a large degree of freedom of movement,⁹ which allows them to adopt different conformations in the solid state.¹⁰ This is termed *conformational polymorphism*. These types of polymorphs contain a large amount of information regarding the range and values of a torsion angle.⁶ However, the more important contribution is that they provide the opportunity to study the relationship between intra- and intermolecular energies.⁶ This leads to insight into when the lowest energy conformation of the single molecule will be sacrificed for the greater good: more efficient packing in the solid state that could lead to a lower energy state. Molecules that display a large variation in the torsion angles stand a greater chance to exhibit polymorphism.⁷ This is because the different conformations that the molecule adopts can lead to different hydrogen-bonding and close-packing styles.⁷

In some cases two or more polymorphs may appear under the same conditions, often crystallising in the same vessel.⁶ This is defined as *concomitant polymorphism*. This phenomenon has also been of great interest to the supramolecular community.¹¹ Not only does it give crystal engineers an indication of the role of kinetics in the crystallisation process, but it provides excellent computational models in the quest to predict crystal structures.^{6, 12} This is due to the fact that concomitant polymorphs are almost energetically equivalent. Since there appear to be conditions that both polymorphic forms favour, studying concomitant polymorphs and fine-tuning the conditions that favour one above the other, leads to a wealth of information regarding the control of polymorphic crystallisation.⁶

The relationship between two polymorphs can be classified into two systems: enantiotropic or monotropic. This classification is related to the Gibbs free energy (G) of the system. G will be at a minimum for the thermodynamically stable phase, whereas for the metastable phase G will be higher.¹³ With an increase in the temperature, the polymorph with higher entropy will become the more stable form. The distinction between enantiotropic and monotropic conversion is dependent on where this transformation takes place. In a monotropic system all the polymorphs can be found below their particular melting points.¹⁴ This means that below the melting point only one of the two forms is stable and the other form is metastable.¹³ The metastable form can convert to the thermodynamically more stable form, but this process is irreversible and the transition normally occurs above the melting points.¹⁵ In the case of enantiotropic polymorphs, the different polymorphs can also be present below the melting point, but there is a transition temperature (T_t) where a conversion from one form to the other can occur.¹³ However, this process is reversible.^{13, 14} At temperatures above T_t polymorph A is more stable than polymorph B, and at temperatures below T_t polymorph B is more stable than A.

3.2. Single crystal X-ray diffraction studies of the monoclinic phase of hexakis(4-fluorophenoxy)cyclotriphosphazene

During the course of this study, a novel polymorph of **12** was isolated. Under certain crystallisation conditions (which will be discussed in section 3.3.1) a triclinic phase was isolated, as well as the known monoclinic phase that was first characterised by Allcock.³

The monoclinic phase will from here on be referred to as **M**, and the triclinic phase will be referred to as **T**.

The structure published by Allcock³ crystallises in the monoclinic crystal system in the space group $P2_1/n$ (Figure 3.1). The phosphazene ring is slightly puckered, with the *p*-fluorophenyl rings perpendicular to the phosphazene ring. The molecules close-pack through intermolecular stacking of the *p*-fluorophenyl groups³ and this leads to the formation of ribbons throughout the crystal structure (Figure 3.1b). These ribbons stack one behind the other to fill all possible voids.

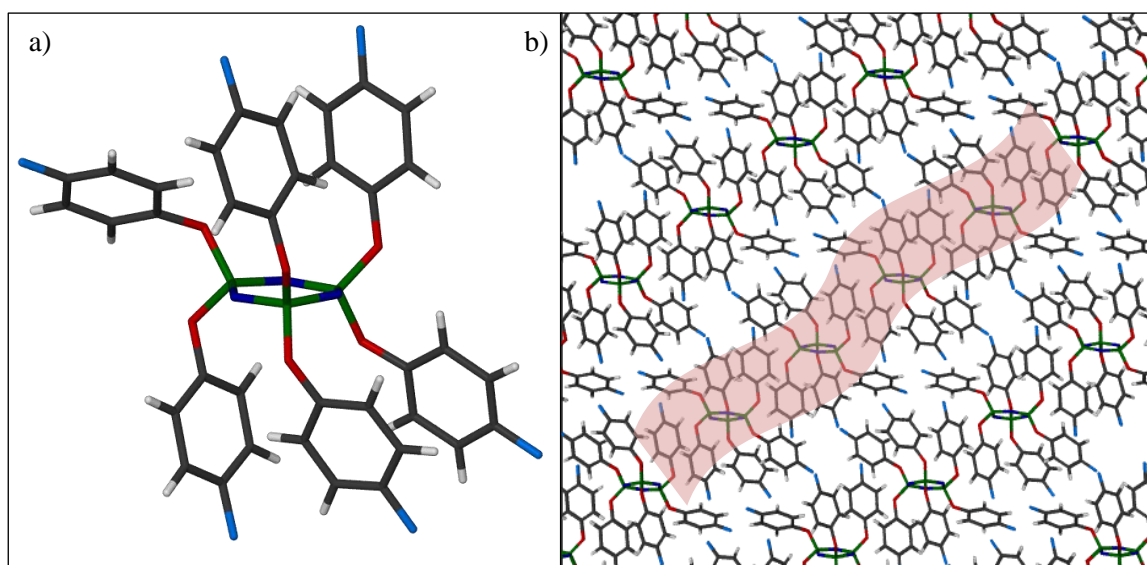


Figure 3.1 a) The structure of the known fluorophenyl derivative, **M**. (b) Ribbon-like packing of **M**, viewed down the crystallographic *b*-axis.

The data for **M** was originally collected at room temperature (RT, referred to as **M_{RT}**); therefore a low temperature structure (referred to as **M_{100K}**) was also collected to determine if there are any structural differences between the room temperature and low temperature structures. It would be logical to assume that there would be minor differences, mostly due to movement of the atoms at a higher temperature because they have more kinetic energy, consequently moving more. It was rather surprising to discover that the two structures are nearly identical regarding the position of the *p*-fluorophenyl rings and the torsion angles in the molecule. Figure 3.2 illustrates the similarities in the conformation of the two molecules. In Figure 3.2b it is evident that the unit cells are not an exact match. But the differences in the unit cell parameters can be attributed to the large temperature difference between the two data collections. Upon cooling, the axes and

β angle of M_{RT} become smaller. The unit cell parameters of the two structures can be found in Table 3.1.

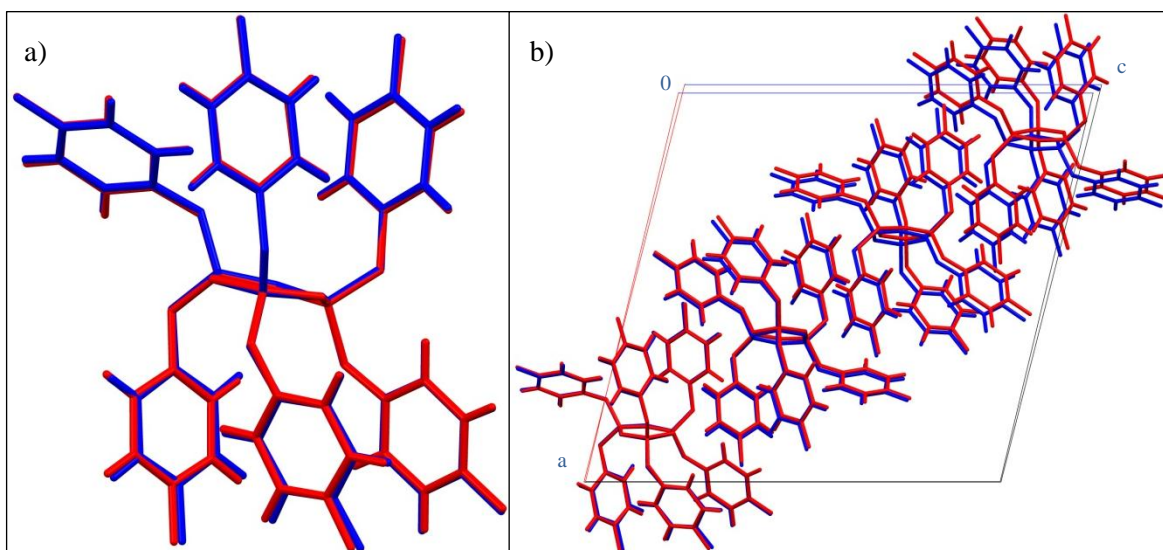


Figure 3.2 (a) The structure overlay of M_{RT} (in red) and M_{100K} (in blue). (b) The packing overlay of M_{RT} and M_{100K} . The difference in the unit cell parameters is due to the temperature as there is a contraction of the unit cell on cooling. This results in the offset of the overlay.

Table 3.1 The unit cell parameters of M_{RT} and M_{100K} .

Parameters	M_{RT}	M_{100K}
Crystal system	Monoclinic P	Monoclinic P
Space group	$P2_1/n$	$P2_1/n$
a (Å)	20.860(5)	20.323(2)
b (Å)	8.085(1)	8.051(8)
c (Å)	21.813(5)	21.694(2)
α (°)	90	90
β (°)	104.62(3)	103.831(1)
γ (°)	90	90
Z	4	4
$R1$ ($[I > 2\sigma(I)]$)	5.68	3.44

The simulated powder patterns of the room temperature and 100 K crystal structures were also compared for further validation that they are the same. The powder patterns were simulated using Mercury¹⁶⁻¹⁹ and visualised in X'Pert HighScore (Figure 3.3).

At first glance the powder patterns of the two structures seem identical (Figure 3.3a). On closer inspection, minor differences in the patterns become apparent – especially in the region between $2\theta = 19^\circ$ and $2\theta = 30^\circ$ (Figure 3.3b). A general shift in the pattern is expected due to the change in temperature. From Figure 3.3 it is clear that the peaks from **M_{100K}** are shifted to the right, relative to the peaks of **M_{RT}**. Further analysis shows that some peaks disappear (i, ii, v), while the shape of other peaks change (iii, iv). This could be attributed to the slight changes in the bond lengths of the molecules and the molecules moving closer to each other on cooling of the crystal. The slight shortening of the unit cell axes and β angle seen in Table 3.1 and Figure 3.2b could also cause the slight differences in the peak positions of the simulated powder patterns.

To ensure that there was not some anomaly in the data collected at low temperature, another data collection was performed on a crystal of the monoclinic phase, but this time it was carried out at room temperature. The powder patterns of the room temperature structures were once again simulated by Mercury¹⁶⁻¹⁹ and analysed using X'Pert HighScore (Figure 3.4). In this case, the two simulated patterns overlay perfectly. The peak shapes are consistent in both traces and the each peak correlates perfectly between the two patterns.

The difference in the patterns of **M_{RT}** and **M_{100K}** could indicate that the molecules in the crystal undergo a conformational change between RT and 100 K. This was investigated using variable temperature (VT) PXRD and is discussed in sections 3.4 and 3.6.

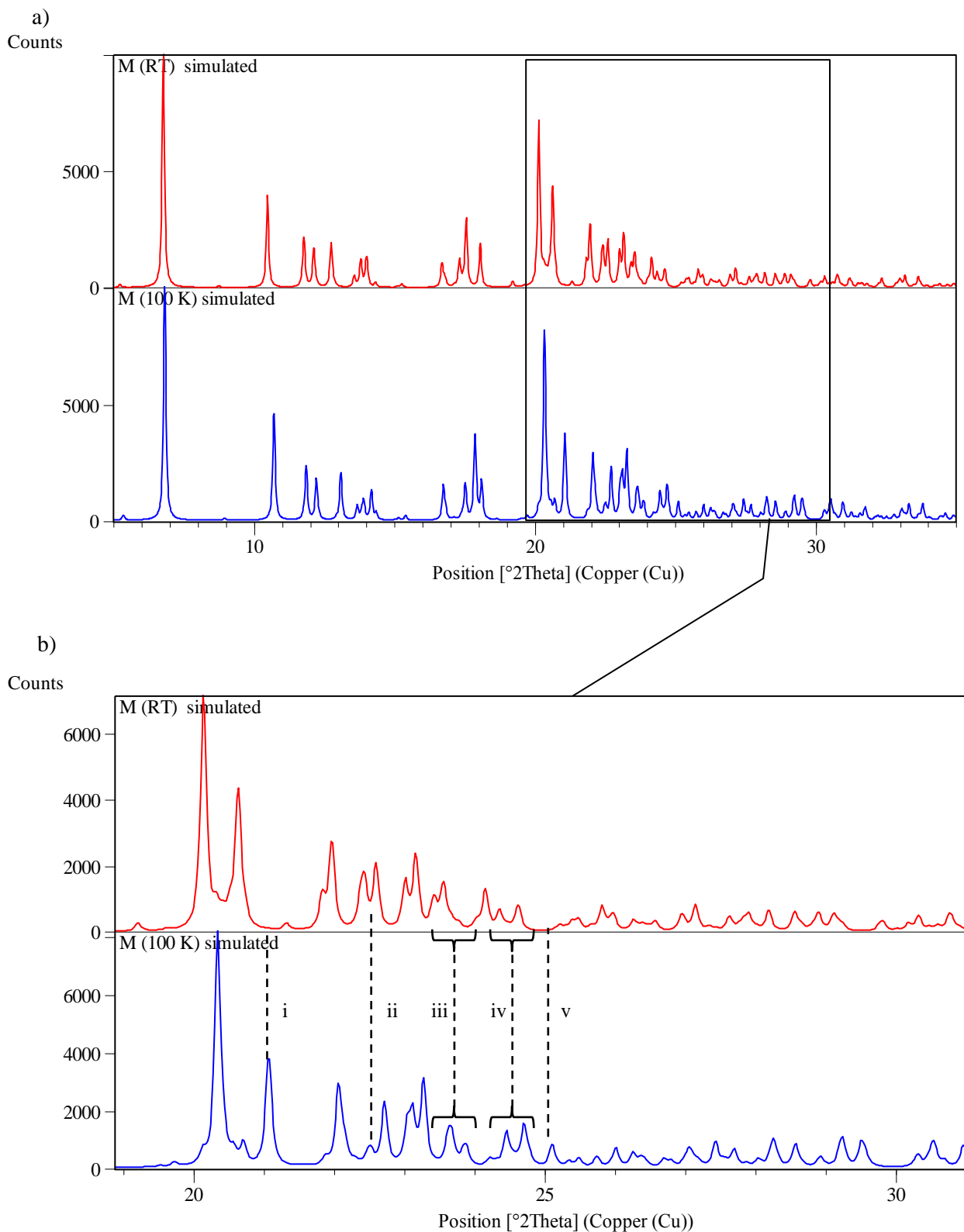


Figure 3.3 (a) Comparison of the simulated powder patterns of M_{RT} (in red) and M_{100K} (in blue). There appears to be a very good correlation between the patterns. (b) Small differences are noted where peaks are missing (i, ii, v) and where the peak shape has changed (iii, iv).

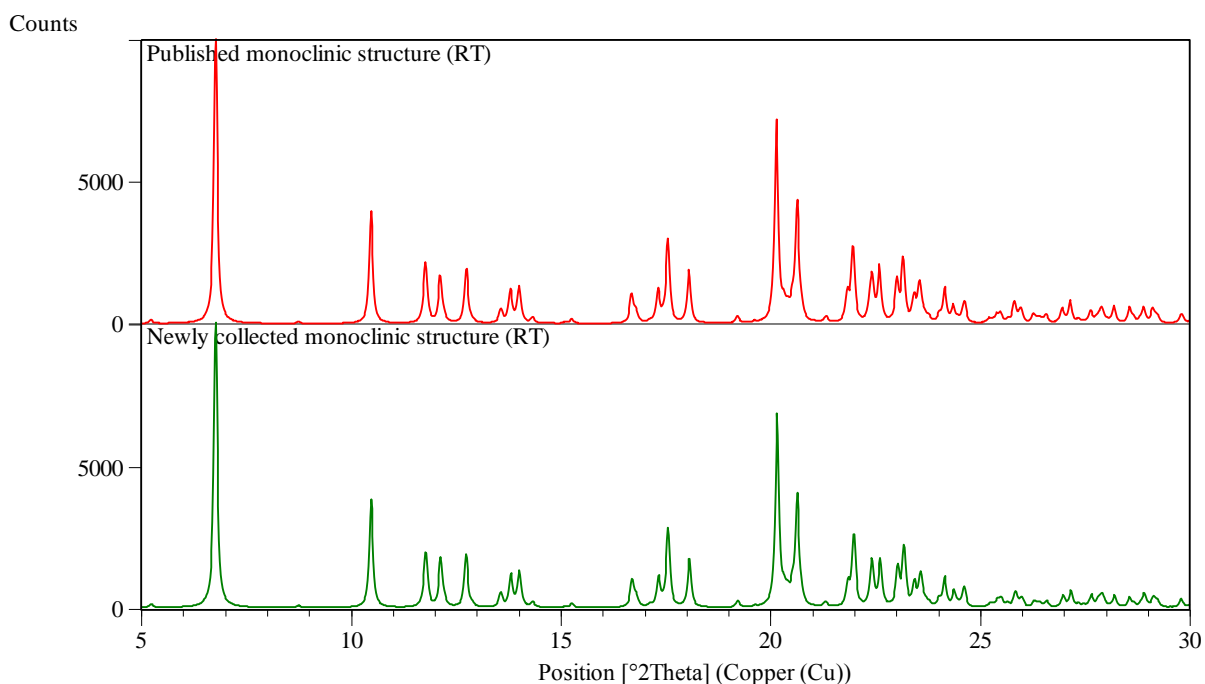


Figure 3.4 The simulated powder patterns of the monoclinic phase. The top diffractogram (red) is the simulated pattern of the structure published by Allcock³ that was collected at room temperature. The bottom diffractogram (green) is the simulated pattern of the data collected on a crystal of the monoclinic phase in this study, also at room temperature.

3.3. The novel triclinic phase of 12

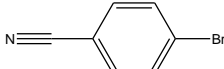
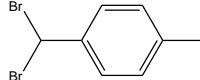
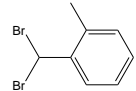
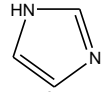
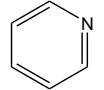
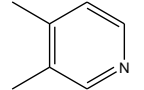
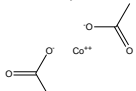
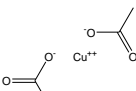
This section will describe the studies performed on the triclinic phase (**T**) of the fluorophenoxy derivative. First, the crystallisation experiments that were conducted from which **T** was isolated will be discussed. Thereafter, the structure of **T** will be described and the monoclinic phase (**M**) and **T** will be compared. PXRD, single crystal X-ray diffraction and DSC studies will also be discussed.

3.3.1. Crystallisation experiments

The aim of this study was to investigate co-crystal formation with cyclotriphosphazenes. The halophenoxy derivatives were used to determine whether halogen bonding would be a successful driving force for co-crystallisation with small molecules containing either halogen or nitrile groups. The halophenoxy derivatives are not air sensitive compounds, therefore crystallisations were not performed under inert conditions. The fluorophenoxy derivative and the co-crystallisation agent were dissolved separately in a suitable solvent, added together and left to stand until crystals formed. Table 3.2 outlines some of the

crystallisations that were performed as well as the solvent systems used in each case. The ratio of cyclotriphosphazene to co-crystallisation agent is also indicated, as well as which polymorph was obtained from each co-crystallisation experiment.

Table 3.2 Co-crystallisation experiments conducted with hexakis(4-fluorophenoxy)cyclotriphosphazene.

Co-crystallisation agent		Ratio of 12:co-crystal former	Solvents	Polymorph
4-bromobenzonitrile		1:3	acetonitrile/DCM	triclinic <i>P</i>
α -dibromo- <i>p</i> -xylene		1:1	acetonitrile/DCM	triclinic <i>P</i>
α -dibromo- <i>o</i> -xylene		1:1	acetonitrile/DCM	triclinic <i>P</i>
imidazole		1:2	THF	triclinic <i>P</i>
pyridine		1:2	THF	monoclinic <i>P</i>
3,4-lutidine		1:2	THF	monoclinic <i>P</i>
cobalt(II)acetate		1:1	THF/methanol	triclinic <i>P</i>
copper(II)acetate		1:1	THF/methanol	triclinic <i>P</i>

From Table 3.2 it is clear that there does not seem to be a significant pattern regarding which polymorph crystallises from which co-crystallisation conditions. Crystallisations were therefore set up again with the co-crystallisation agents and it was noted that the vials from which solvent evaporated the quickest, tended to form the triclinic phase. The fast evaporation rate could possibly trap the molecule in a conformation that does not pack efficiently. To ensure that this was definitely not a co-crystallisation agent effect, crystallisations were set up from different pure solvents and solvent mixtures. The solvents are however quite volatile, therefore evaporation tended to occur quickly. The results are summarised in Table 3.3.

Table 3.3 Crystallisation experiments of **12** from pure solvents.

Solvents	Polymorph	Conditions
acetonitrile/DCM	triclinic <i>P</i>	
acetonitrile	triclinic <i>P</i>	
DCM	triclinic <i>P</i>	Vial covered with parafilm, placed in a warm environment
THF/methanol	triclinic <i>P</i>	
THF	monoclinic <i>P</i>	

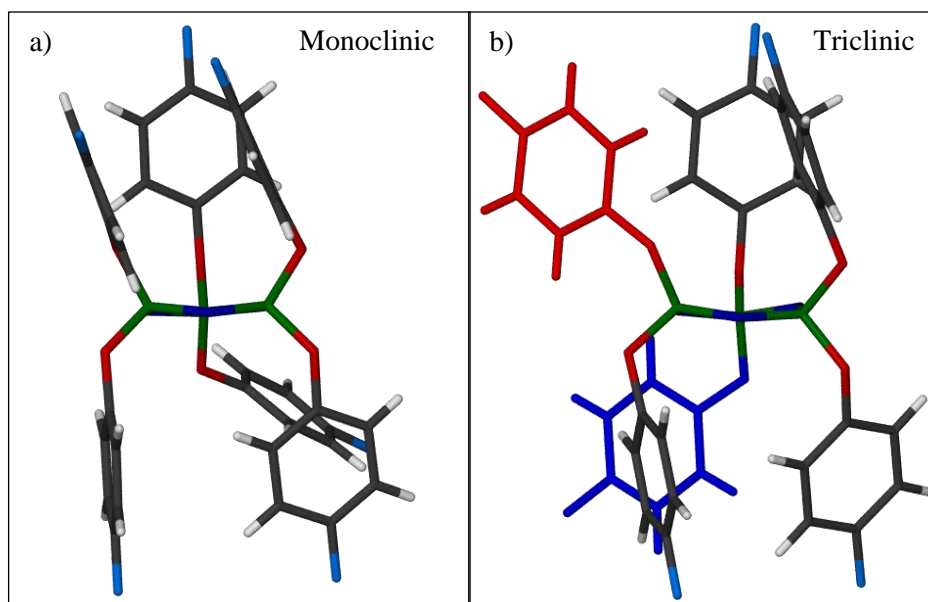
It can be concluded that the triclinic form will crystallise from most volatile solvents, especially when evaporation occurs at a high rate. However, it appears that the monoclinic form will crystallise from THF even under fast evaporation conditions.

3.3.2. Single crystal X-ray diffraction studies of the triclinic phase, **T**

The novel polymorph that was isolated crystallises in the triclinic crystal system in the space group $P\bar{1}$. The unit cell parameters for the triclinic polymorph **T** (collected at 100 K and room temperature) can be found in Table 3.4. In this molecule, one of the fluorophenoxy rings has rotated away from the other fluorophenoxy ring (shown in red in Figure 3.5b), essentially disrupting the close contact (3.735 Å between the centroids) between two of the fluorophenoxy rings in the molecule that is seen in **M** (Figure 3.5a). Another fluorophenoxy ring is now twisted in the opposite direction (shown in blue in Figure 3.5b).

Table 3.4 The unit cell parameters of **M** and **T** at 100 K and room temperature.

Parameters	M _{100K}	T _{100K}	T _{RT}
Crystal system	Monoclinic <i>P</i>	Triclinic <i>P</i>	Triclinic <i>P</i>
Space group	<i>P</i> 2 ₁ / <i>n</i>	<i>P</i> $\bar{1}$	<i>P</i> $\bar{1}$
<i>a</i> (Å)	20.323(2)	9.444(9)	9.596(2)
<i>b</i> (Å)	8.051(8)	9.925(1)	10.056(2)
<i>c</i> (Å)	21.694(2)	18.669(2)	18.910(3)
α (°)	90	103.683(1)	103.575(2)
β (°)	103.831(1)	96.009(1)	97.097(2)
γ (°)	90	91.803(1)	93.100(2)
Z	4	2	2
R1 [<i>I</i> > 2 σ (<i>I</i>)]	3.44	3.87	4.67

**Figure 3.5** (a) The known monoclinic phase **M**, with two fluorophenoxy rings forming a close contact (3.735 Å between the centroids) in the molecule. (b) In the triclinic phase this close contact is disrupted (shown in red). The fluorophenoxy ring shown in blue has also twisted.

This causes the molecules to pack in columns rather than the ribbon-like sheets of the monoclinic phase, as can be seen in Figure 3.6a. These columns are related by an inversion centre. This means that the symmetry operator x,y,z describes the green molecules, and the symmetry operator $1-x, 1-y, 1-z$ describes the orange molecules (Figure 3.6b).

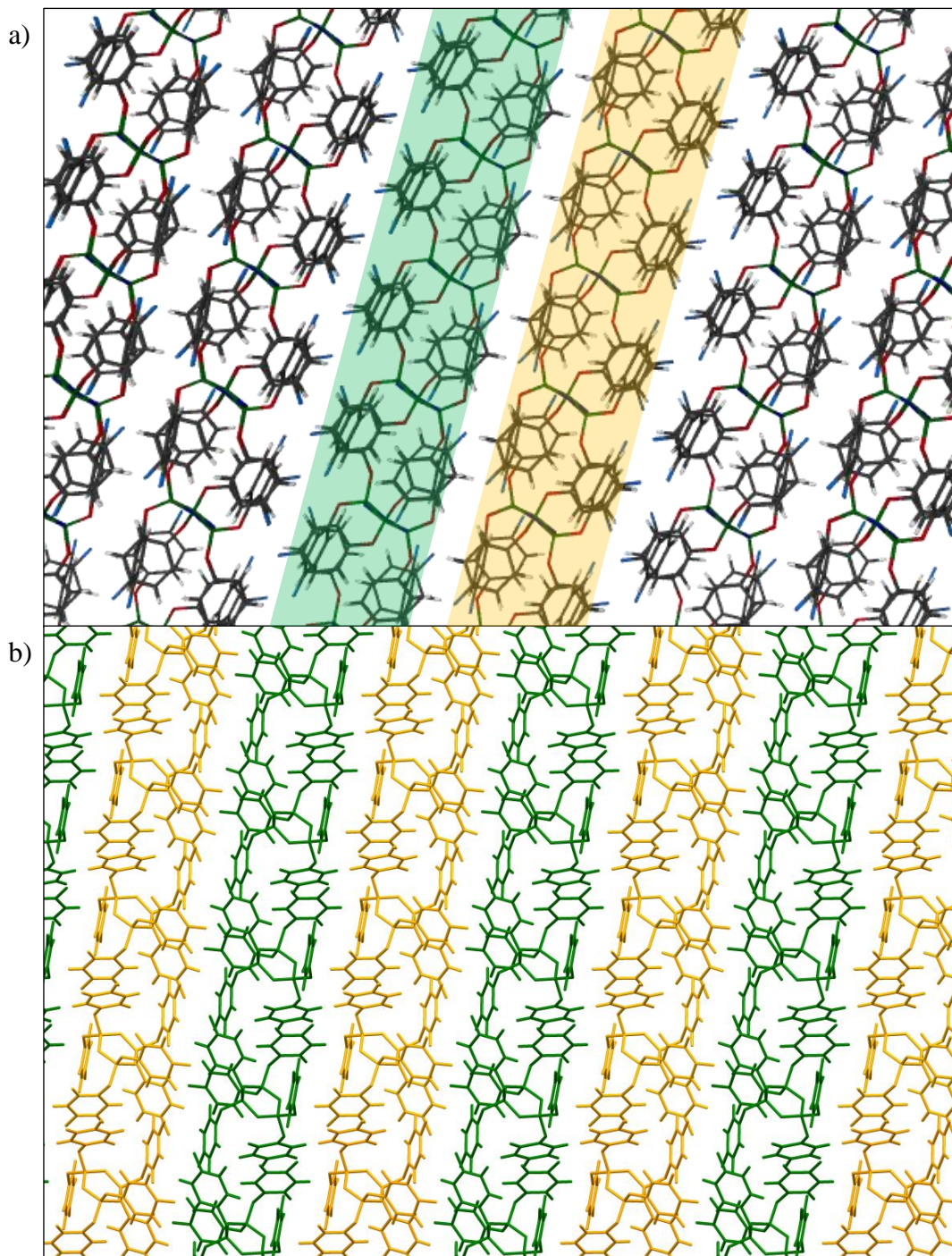


Figure 3.6 (a) The molecules in the triclinic phase pack in columns. (b) These columns are related by symmetry operations, where the orange molecules are the inversion of the green molecules. This packing diagram is viewed down the b -axis.

In order to better understand the intermolecular interactions at play in each polymorph, CrystalExplorer 2.1²⁰⁻²⁴ was used to visually represent these interactions. This program generates a Hirshfeld surface.²⁵ The Hirshfeld surface defines the space occupied by a molecule within a crystal structure.²⁶ It partitions the crystal space into molecular volumes that are smooth and interlock, but do not overlap.²⁷ Inside the Hirshfeld surface the electron distribution due to a sum of spherical atoms for the molecule (promolecule) dominates the corresponding sum over the crystal (procrystal).²⁷ The Hirshfeld surface is then implied where the ratio of promolecule to procrystal electron density is equal to 0.5.²⁷ The Hirshfeld surface visualises the relationship between different atoms and intermolecular contacts in the crystal.²⁷ This information is then used to generate a fingerprint plot that creates a visual representation of possible interactions or contacts in the crystal structure. These plots map the distance from the Hirshfeld surface to either *the nearest nucleus inside the surface* (d_i) or *outside the surface* (d_e).²⁶ This means that fingerprint plots are used to show the relation of d_i and d_e . Fingerprint plots are also especially useful in the analysis of polymorphs, as they are highly dependent on the environment surrounding the molecule.²⁶ Therefore a change in the packing arrangement will have a large effect on the fingerprint plot. Fingerprint plots were generated for both the known monoclinic and triclinic form of **12** (Figure 3.7).

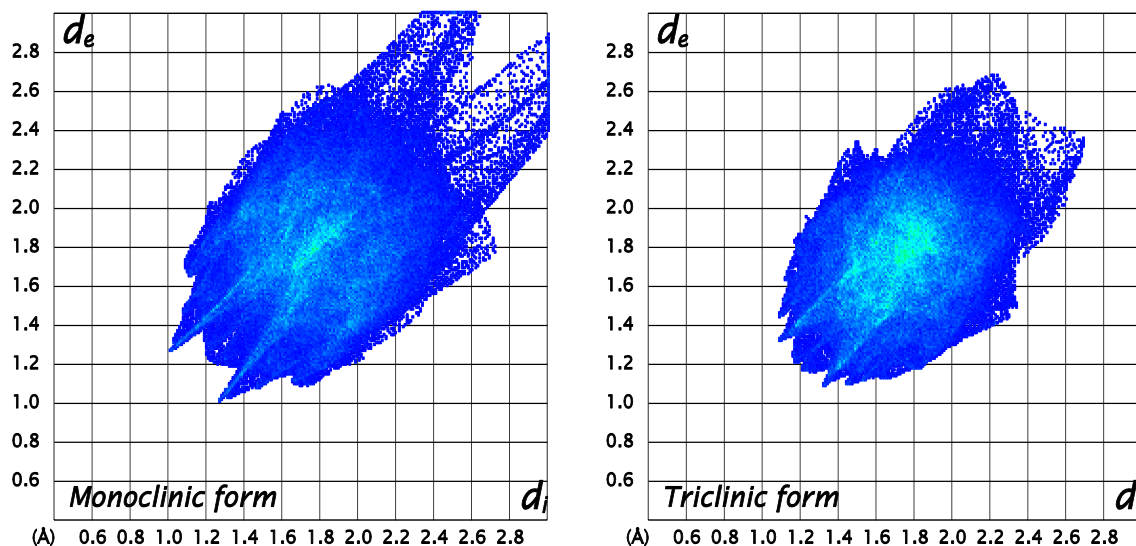


Figure 3.7 Fingerprint plots of the monoclinic and triclinic forms of hexakis(4-fluorophenoxy)-cyclotriphosphazene

It is clear from Figure 3.7 that there is a large difference in the intermolecular interactions present in each crystal structure. The change in the conformation of the fluorophenoxy groups in the triclinic form has a large influence on the intermolecular interactions that can now be formed. But this can be better understood by looking at a breakdown of the fingerprint plots (Figure 3.8). These fingerprint plots will highlight specific interactions or close contacts in each crystal structure.

The first intermolecular interaction that will be discussed is the F...F interaction. It is a somewhat controversial interaction and mostly believed to be very weak if it is in fact observed.²⁸ According to Ramasubbu *et al*,²⁹ F...F interactions can be classified into two types, namely type I which is caused by close packing within the crystal structure, and therefore not a true intermolecular interaction, and type II which is caused by polarisation of the fluorine atoms.^{28,29} Type II is considered to be an intermolecular interaction. While studying the fingerprint plot (Figure 3.8) of the possible F...F interactions, along with the crystal structure of both forms, it is evident that the F...F contacts are a result of close packing in the crystal structure. Distances between F atoms are longer than 3 Å. This also explains why this type of contact occurs more readily in the monoclinic phase than the triclinic phase. In the monoclinic phase, the molecules close pack in such a way, due to the molecular conformation, that more fluorine atoms are close together. However, in the triclinic structure, due to the twisting of two of the fluorophenoxy rings, the shape of the molecule is now so awkward that the fluorophenoxy groups cannot pack as closely as before. Although there are examples in the literature³⁰ of F...F interactions, they do not feature in these two polymorphs.

The F...H interaction is considered to be a type of intermolecular interaction for distances up to 2.9 Å,²⁸ and studying the fingerprint plots and the crystal structures, it is evident that this is a much more robust interaction in these two crystal structures. It even outweighs the occurrence of C...H interactions (π -stacking interactions). From Figure 3.8, it is also clear that this is the dominant interaction, especially in the case of the triclinic form where 29.6% of the possible intermolecular contacts are F...H interactions.

The remaining close contacts are mainly O...H, N...H and H...H close contacts in both structures.

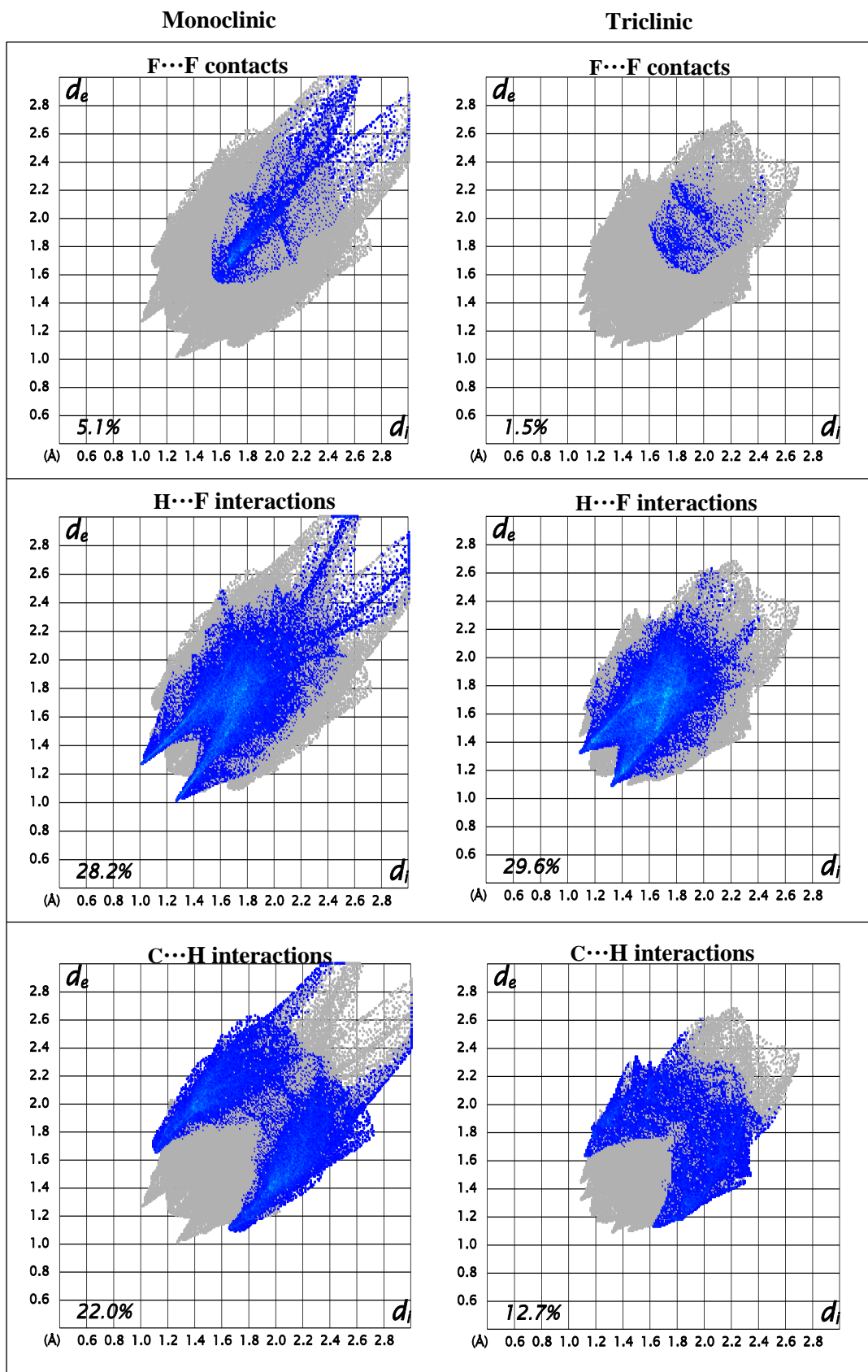


Figure 3.8 Distribution of intermolecular interactions in each polymorph. This shows that in both structures H...F interactions are the dominating intermolecular interaction. In the monoclinic phase C...H interactions are also abundant. This is due to π - π stacking interactions.

PXRD analysis was used to compare the low temperature (100 K) and room temperature structures of the triclinic form. These patterns correspond very well, with minor differences in peak form and peak splitting, which could be due to the change in temperature and vibration of the molecule (Figure 3.9).

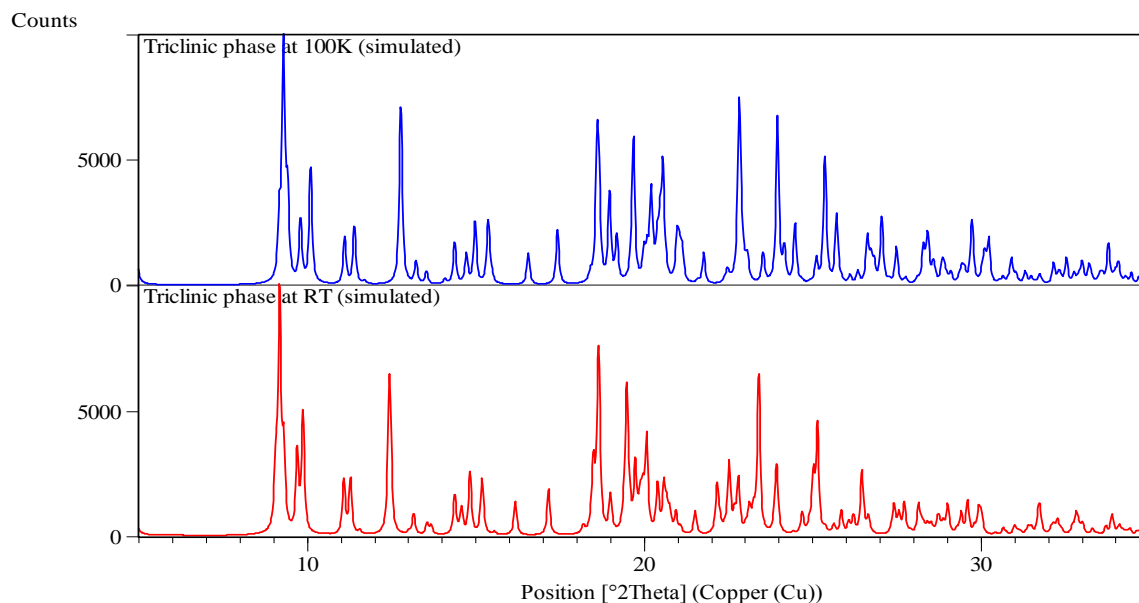


Figure 3.9 The simulated powder patterns of the crystal structures at 100 K (blue) and room temperature (red).

PXRD analysis of a vial of crystals, from which the triclinic form was isolated, showed that only the triclinic form crystallised in the vial (Figure 3.10). This implies that the two phases crystallise separately in pure phases, and not as concomitant polymorphs.

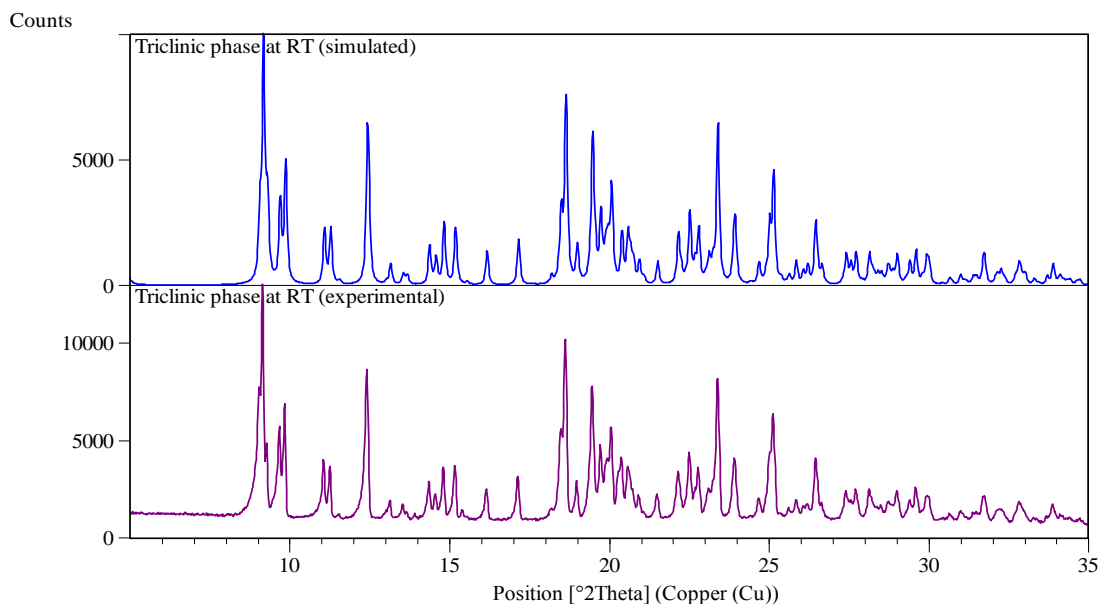


Figure 3.10 The simulated and experimental patterns of the triclinic phase. The two patterns correspond very well, indicating that all the crystals in the vial are of the triclinic phase.

3.4. Differential scanning calorimetry (DSC) and PXRD studies of crystal forms **M** and **T**

Polymorphic compounds often exhibit interesting properties that differ vastly from each other. In-depth analysis of polymorphic compounds is therefore very important. DSC analysis was performed on both crystal forms, **M** and **T** (Figure 3.11 and Figure 3.12). DSC analysis can help to identify whether two polymorphs are part of a monotropic or enantiotropic system. A DSC plot can give an indication of whether or not the different polymorphic forms can interconvert, i.e. change from the triclinic to the monoclinic form or vice versa – depending on which polymorph is the more stable form. This analysis will also be able to show which polymorphic form, **M** or **T**, is in fact the more stable form.

In each case, the sample was heated to the desired temperature at 10 °C/minute and then cooled to the desired temperature at 5 °C/minute. The sample was then heated to room temperature at 10 °C/minute.

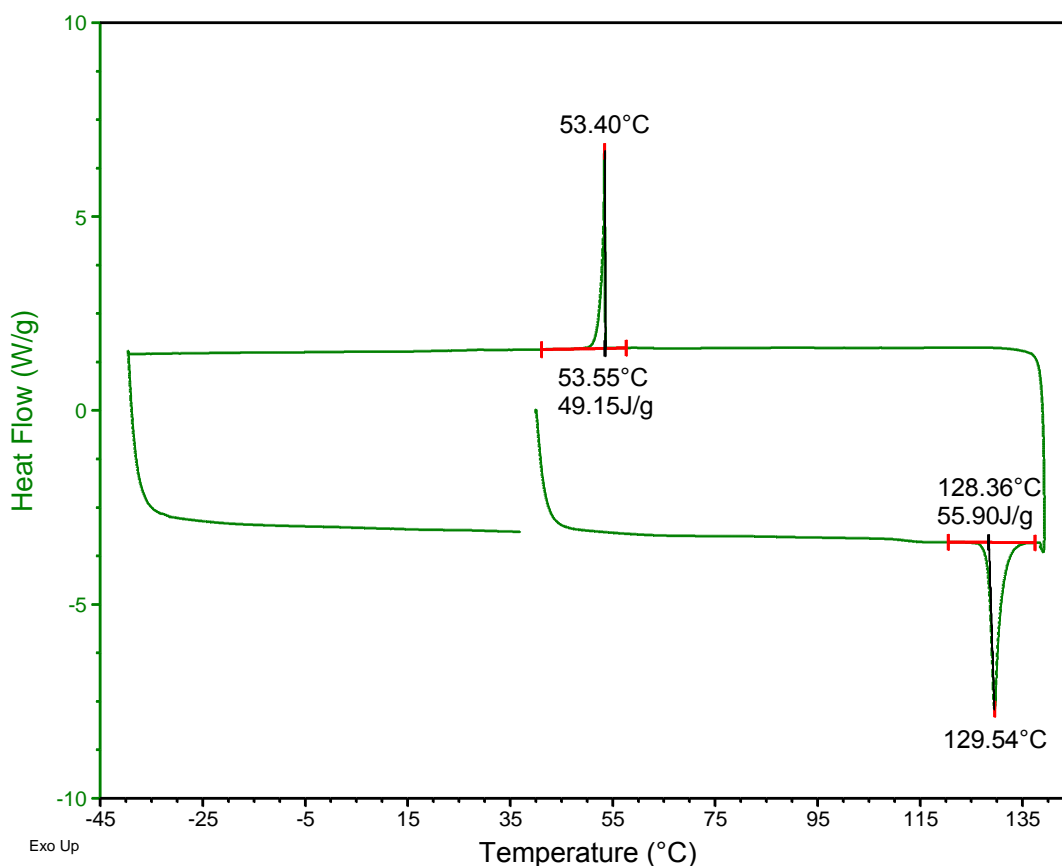


Figure 3.11 DSC of **M**. Melting of the monoclinic form occurs at the onset temperature of 128.4 °C as an endothermic event. Recrystallisation occurs at 53.4 °C as an exothermic event.

The monoclinic polymorph melts at 128.4 °C, after which it recrystallises at 53.4 °C (Figure 3.11). The triclinic form shows two events in the DSC – the first occurs at 98.4 °C, which could indicate a phase change (Figure 3.12). The second event occurs at the same temperature where the monoclinic form undergoes melting. This could mean that at 98.4 °C the triclinic form converts to the monoclinic form, then melts at 128.7 °C. On cooling, there is only one recrystallisation event at 45.9 °C.

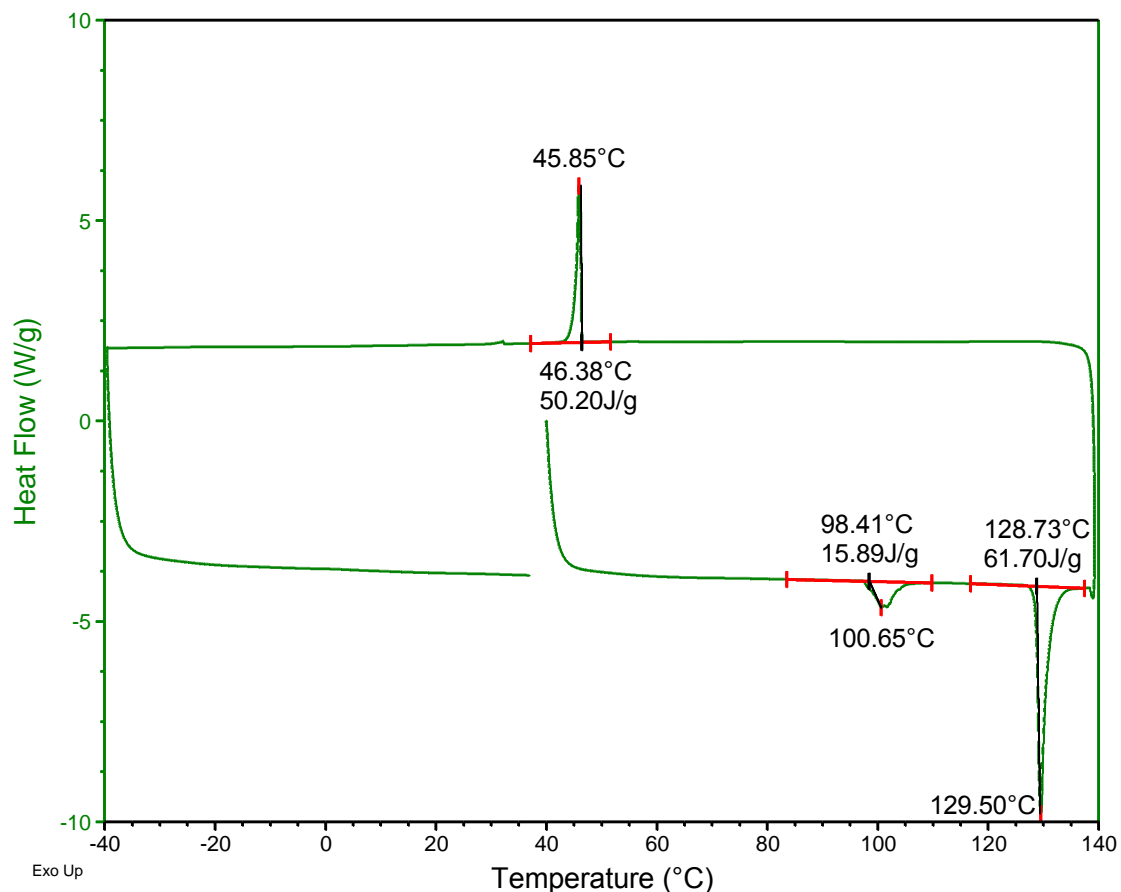


Figure 3.12 DSC of the triclinic form. The first event occurs at 98.4 °C and the second event at 128.7 °C. The second event corresponds to the melting of the monoclinic form.

When the DSC run is cycled, i.e. the sample is heated up to 140 °C, cooled down to -60 °C and heated again to 140 °C, the first event does not occur again (Figure 3.13). This indicates that the monoclinic form does not convert back to the triclinic form.

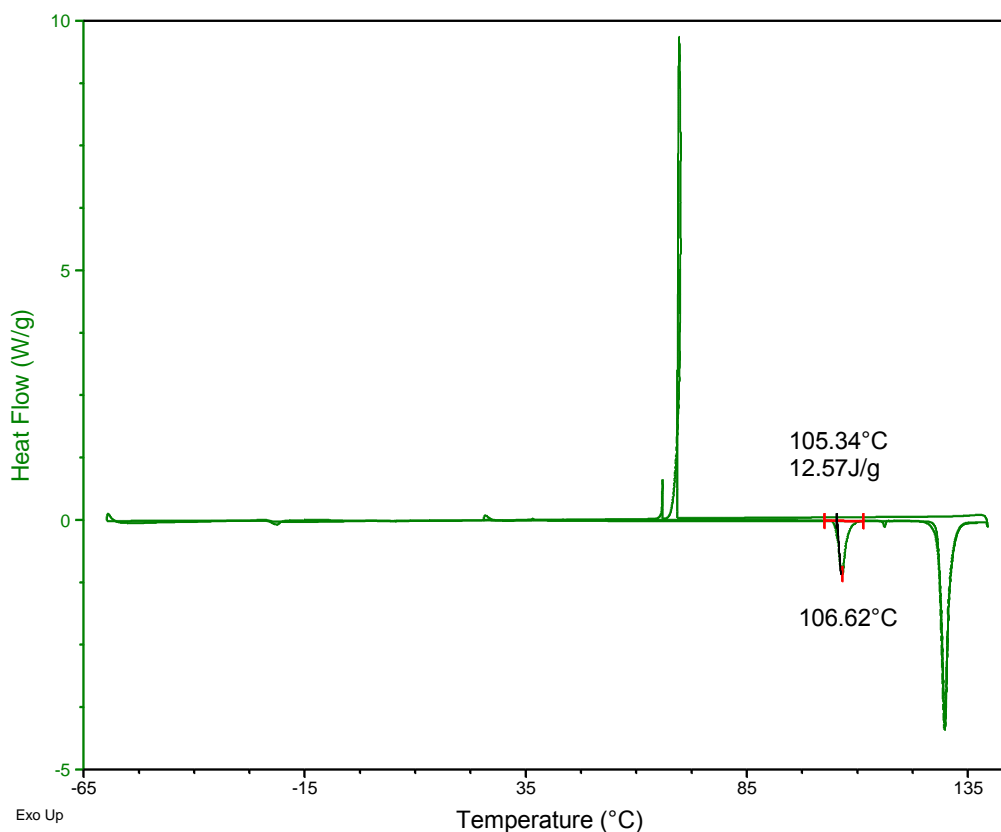


Figure 3.13 The cycled DSC run of **T**. The sample was heated to 140 °C, cooled to -60 °C and then these two steps were repeated. The DSC trace shows that the triclinic form does not appear again in the second cycle after the phase transformation and the melt.

Variable temperature PXRD (VT PXRD) analysis was used to further study this phenomenon (Figure 3.14). Crystals of the triclinic form were ground to a powder and placed in a capillary. The sample in the capillary was allowed to equilibrate at 25 °C and a measurement was taken. The sample was then heated and measurements were taken at approximately 20 °C increments. In the region of the phase transformation (85 °C to 115 °C) measurements were taken every 5 °C. Thereafter measurements were taken at 10 °C intervals up to 135 °C. The sample was cooled and measurements were taken at approximately 20 °C intervals to 25 °C. After each temperature change, the sample was allowed to equilibrate for two minutes.

PXRD analysis indicates that the triclinic structure undergoes a phase change between 90 °C and 95 °C, where it converts to the monoclinic phase. The discrepancy in the temperatures between the DSC and PXRD results could be due to the sample size, or the

temperature calibration of the instruments. Melting occurs after 125 °C and on cooling only the monoclinic phase recrystallises. There appear to be a number of peaks missing in the pattern after the sample melted at 135 °C, but this could be due to preferred orientation as the sample is now in crystalline form as opposed to the fine powder it was before. Preferred orientation occurs when crystals orientate themselves along the same flat surface which causes that crystal surface to be preferentially exposed to the X-ray beam. This leads to increased intensity in some reflections, whereas other planes get little or no exposure, causing a decrease or absence of a peak in the powder pattern.³¹

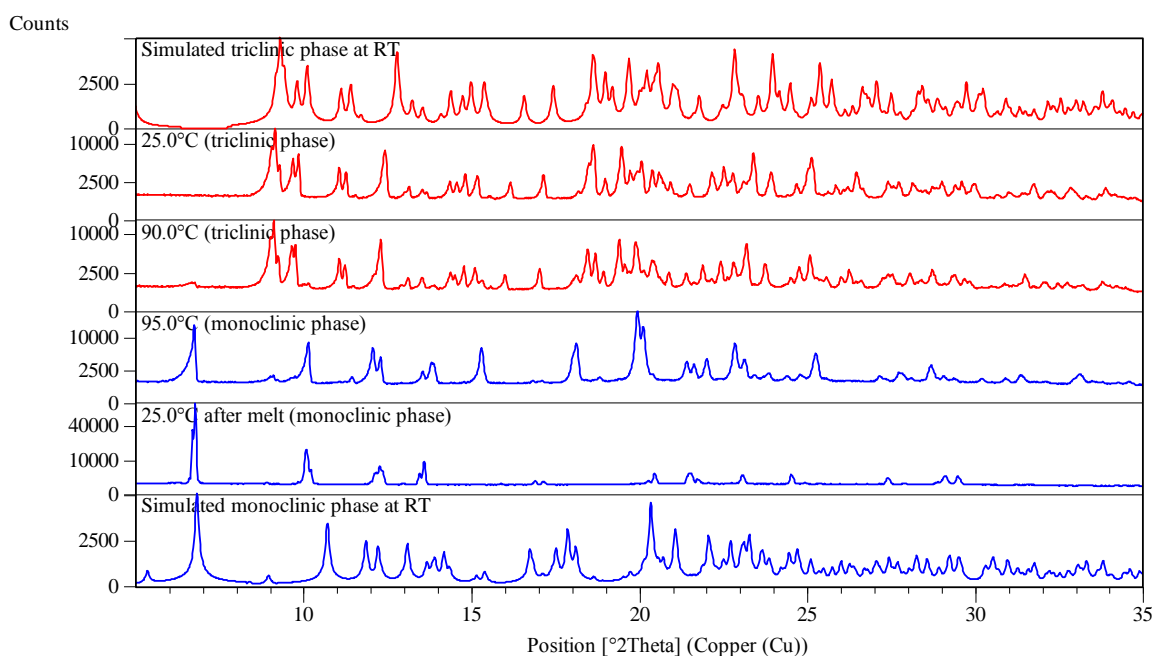


Figure 3.14 The PXRD shows that **T** converts to **M** between 90 and 95 °C. Between 125 and 135 °C the sample melts and recrystallises as the monoclinic form. It does not convert back to **T** on cooling.

As further confirmation that **T** can only convert to **M**, a VT PXRD study was carried out on the monoclinic phase (Figure 3.15). This clearly shows that at no point does the monoclinic form convert to the triclinic form. This indicates that the conversion from **T** to **M** is an irreversible phase change and that the triclinic form is the metastable polymorph. As was mentioned previously, the change in the pattern after the melt could be due to preferred orientation.

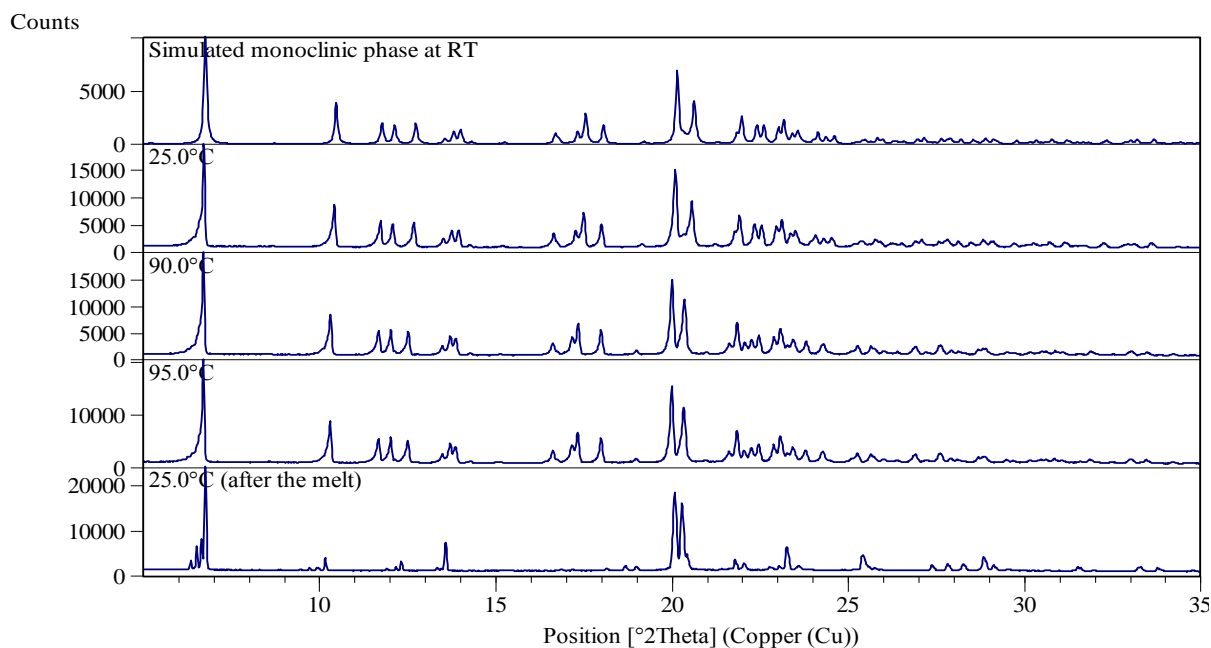


Figure 3.15 The VT PXRD experiment that was done on the triclinic form was repeated on the monoclinic form. There does not appear to be a significant change in the patterns, indicating that no phase change occurred. This implies that the monoclinic form is the more stable form of the two polymorphs.

3.5. Hot stage microscopy

Hot stage microscopy allows the direct observation of the crystals during heating. The crystals are placed on a slide and covered with a cover slip. In some cases the crystals can be placed in silicone oil. This is especially useful if the crystals contain solvent or gas molecules – when the gas or solvent starts to escape, it can be observed in the form of bubbles in the oil. The crystals of **M** and **T** do not contain any solvent or gas therefore it was not deemed necessary to place them in oil. The crystals of **T** were heated to 140 °C at 10 °C per minute and pictures were taken every thirty seconds.

Figure 3.16 illustrates how the phase change takes place and the change it causes in the crystal. At first the crystals are clear and remain clear up to 100 °C. During the phase transition around 100 °C the crystals start to turn opaque and at 130 °C one of the crystals has already melted. Hot stage microscopy clearly shows that the triclinic phase does not melt for the conversion to occur. However, once the crystals have melted they can only recrystallise in the monoclinic phase, according to VT PXRD and DSC analyses. This system can therefore be classified as a case of monotropic polymorphism. The transition is from a less stable phase, the meta-stable phase (**T**), to the stable phase (**M**). This transition is also not reversible, which is why it is classified as a monotropic phase transformation.

Single crystal X-ray diffraction studies were attempted on the crystals before and after phase transformation to study the conformational changes in the molecule. This will be discussed in section 3.6.1.

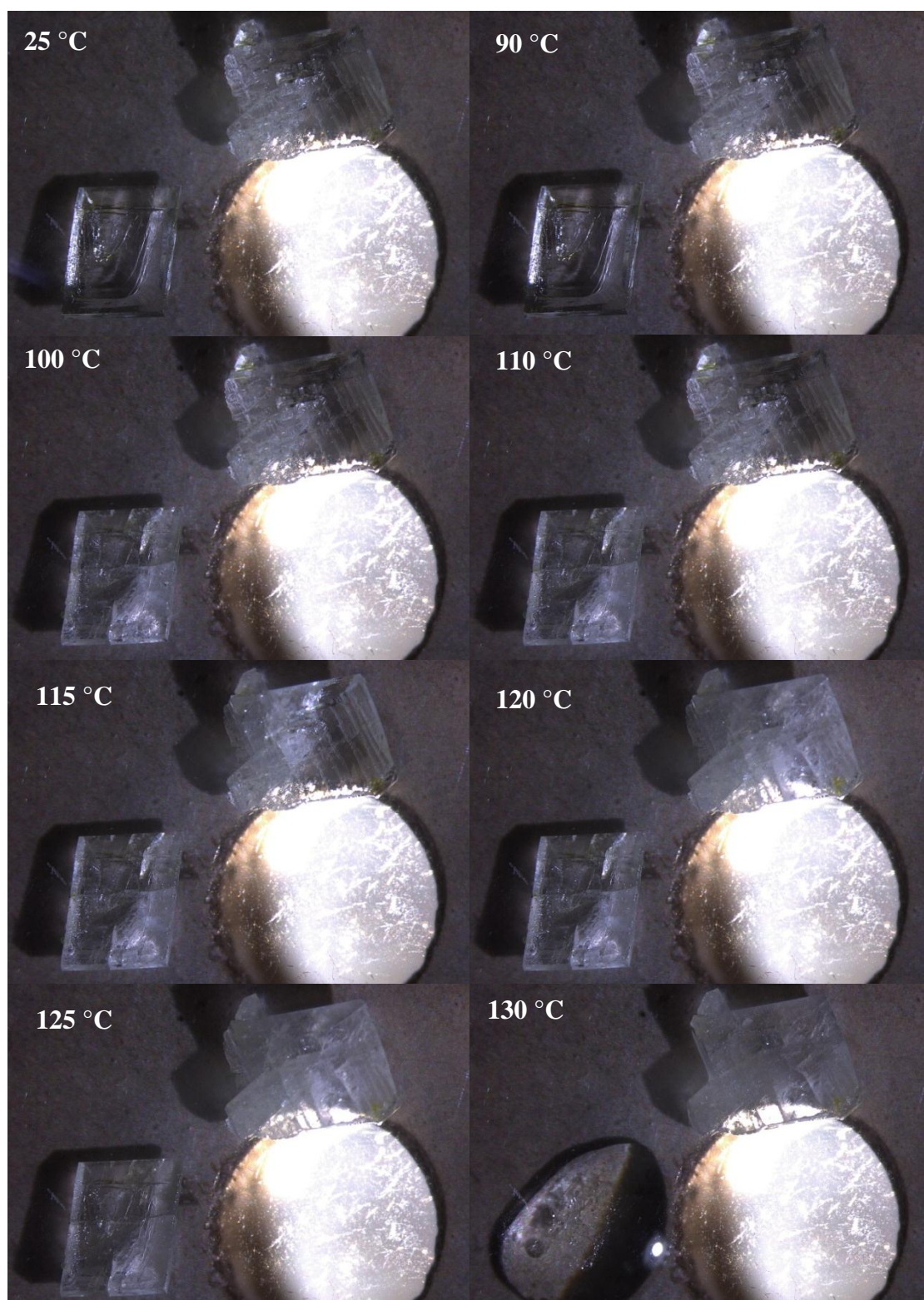


Figure 3.16 The crystals of the triclinic phase are clear until the phase transformation at 100 °C, after which they become opaque. Cracking of the crystal also appears in places. At 130 °C the crystals begin to melt.

3.6. Investigation into the phase transformation of the monoclinic *P* polymorph

3.6.1. Variable temperature studies on the conversion from triclinic to monoclinic

During the investigation into the relationship between the triclinic and monoclinic phase and studying the phase transformation from **T** to **M**, an interesting discovery was made regarding the behaviour of the crystals on heating. A sample of the triclinic phase was heated to 118 °C – just after the phase transition, but before melting occurred – then cooled to -40 °C and heated again to room temperature. Figure 3.17 shows that the conversion of the triclinic form to the monoclinic form takes place around 100 °C, as was previously seen. A new exothermic event occurs at -22.1 °C, which could indicate another phase change.

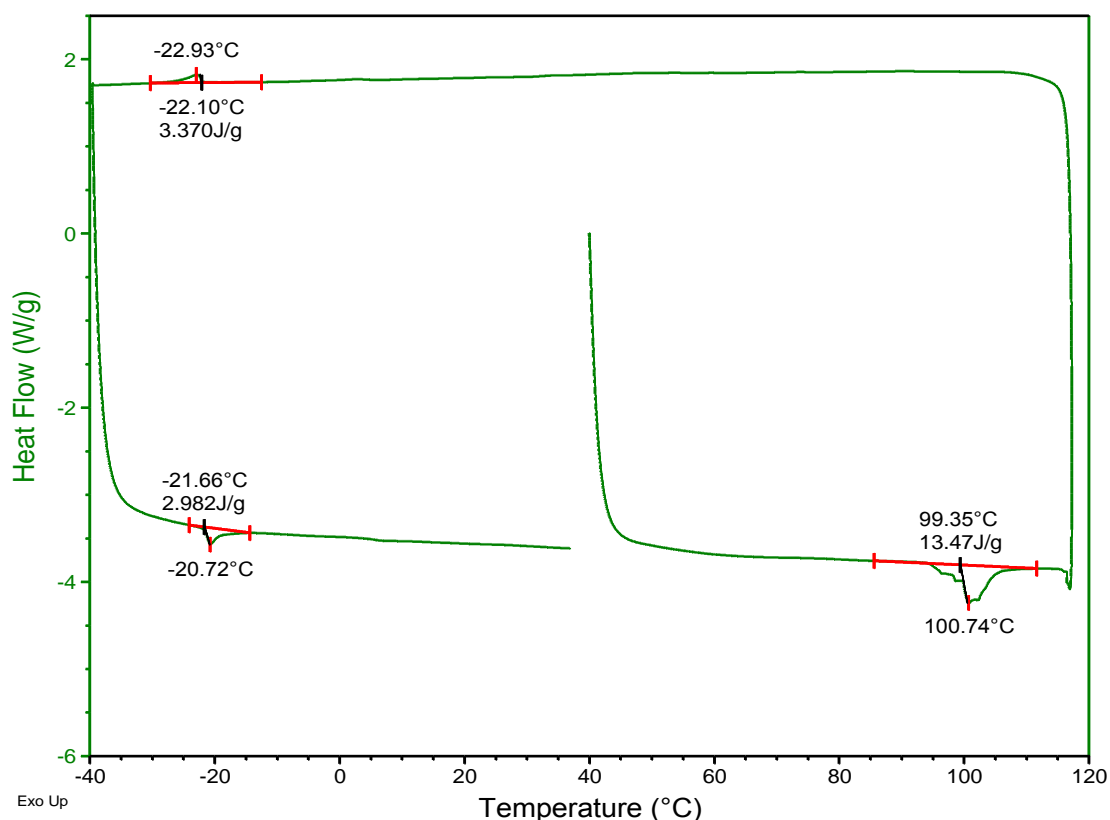


Figure 3.17 The sample was heated to 118 °C, cooled to -40 °C and heated to room temperature again. On cooling, an exothermic event occurs at -22.9 °C, possibly indicating a phase change.

In order to investigate whether the event on cooling is related to the behaviour of the triclinic form or the monoclinic form, the DSC run was cycled. The sample was heated to 118 °C, cooled to -40 °C, heated to 118 °C again, and then cooled again. The results are illustrated in Figure 3.18. It appears that after the phase change around 100 °C, the triclinic form does not reappear in the second cycle. This can be concluded from the fact that the peak at 96.1 °C (Figure 3.18) is not seen in the second cycle. The peak at 96.1 °C is the temperature where the triclinic form **T** converted to the monoclinic form **M**. Therefore, the events occurring around -20 °C and 0 °C can be attributed to the monoclinic form of the crystal structure.

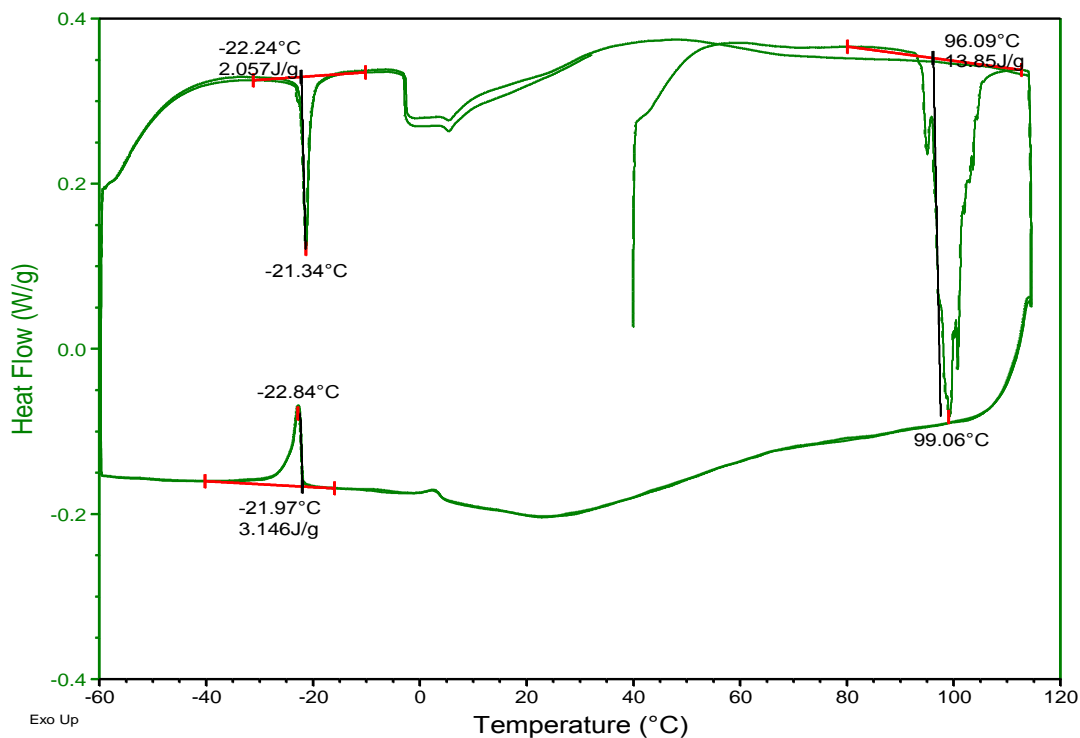


Figure 3.18 The endotherm indicating the phase transition from triclinic to monoclinic does not appear on heating the sample for the second cycle to 118 °C. The events around -20 °C do however reoccur in the second cycle.

The events at $-20\text{ }^{\circ}\text{C}$ and $0\text{ }^{\circ}\text{C}$ only occur if the triclinic phase is first heated to the point after the phase transformation. If the triclinic phase is cooled to $-40\text{ }^{\circ}\text{C}$ first, the peaks do not appear. Although, once the sample has been heated again the peaks reappear on cooling in the second cycle (Figure 3.19).

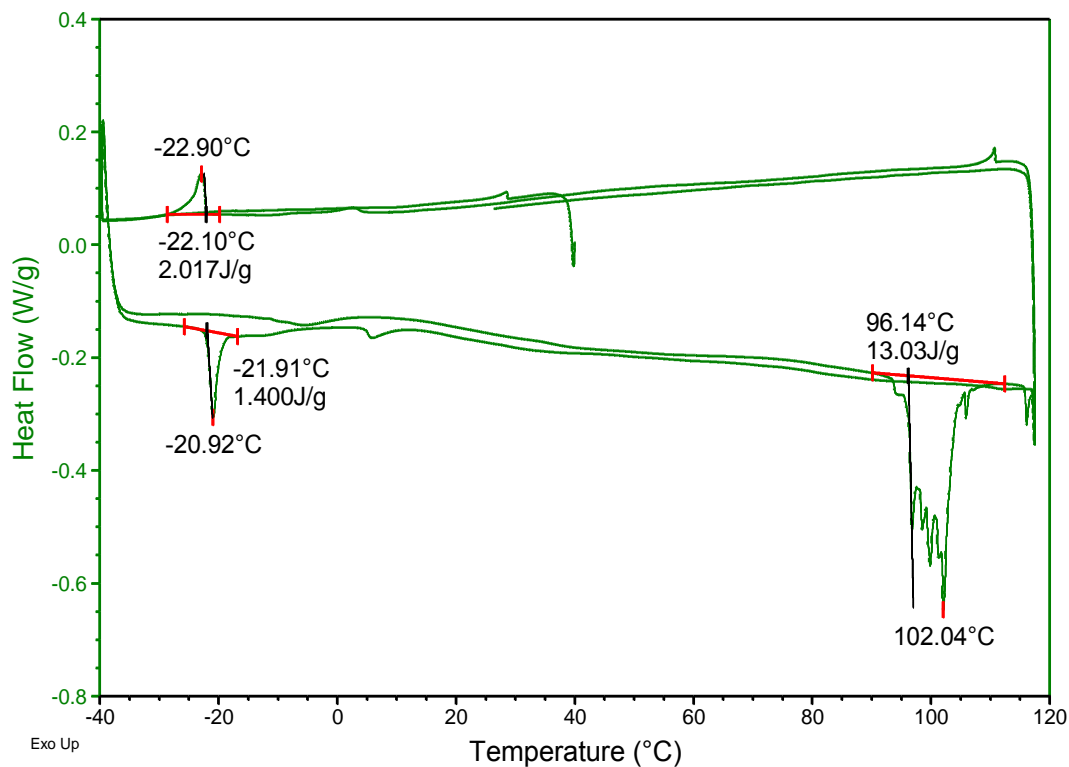


Figure 3.19 The peaks do not appear if the sample of the triclinic phase is cooled first. The peaks reappear once the sample has been heated to the transition point and then cooled.

VT PXRD analysis once again supplemented DSC analysis to attempt to understand the exo- and endothermic events around $-20\text{ }^{\circ}\text{C}$. The triclinic phase was heated to the temperature of the conversion, and then cooled to $-45\text{ }^{\circ}\text{C}$ (Figure 3.20). At first glance it appears that nothing out of the ordinary is taking place. The triclinic phase once again converts to the monoclinic phase between 90 and $95\text{ }^{\circ}\text{C}$ and remains monoclinic on cooling to $-45\text{ }^{\circ}\text{C}$. On closer inspection, small differences in the fine structure of the patterns taken at 95 , -45 and $25\text{ }^{\circ}\text{C}$ become apparent (indicated in Figure 3.20).

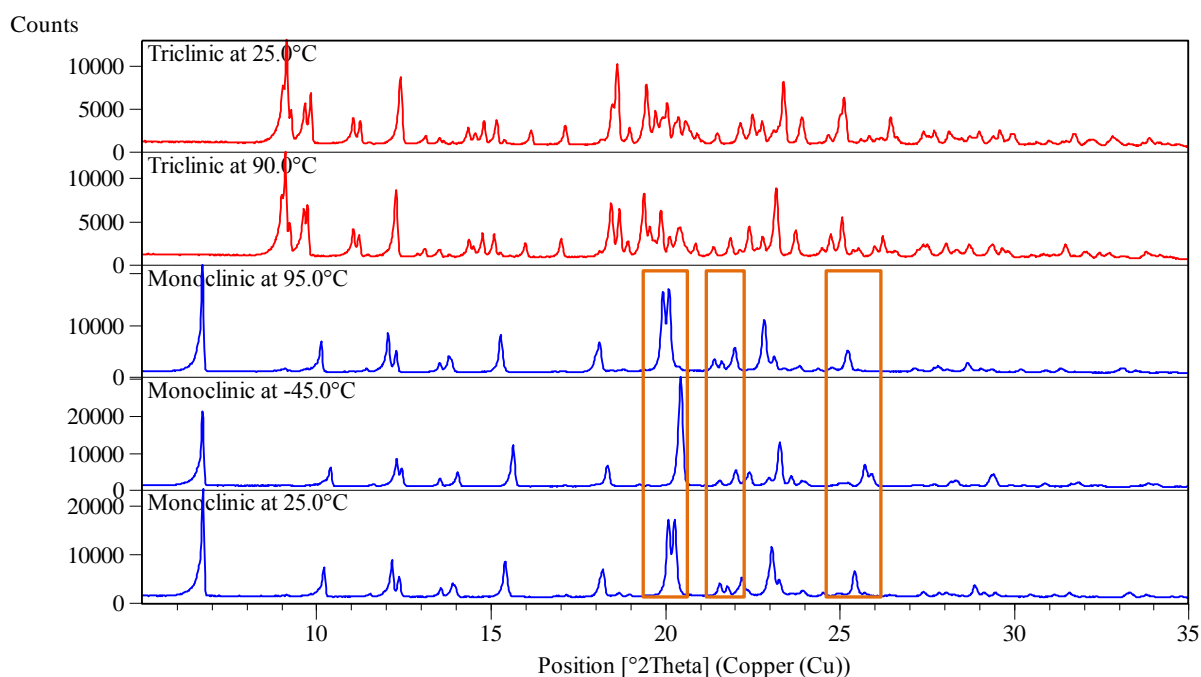


Figure 3.20 The conversion from triclinic to monoclinic takes place between 90 and $95\text{ }^{\circ}\text{C}$. At $-45\text{ }^{\circ}\text{C}$ there appears to be minor differences in the fine structure of the powder pattern compared (as indicated) to the monoclinic phases at 95 and $25\text{ }^{\circ}\text{C}$.

VT PXRD analysis was also done in the range between 0 and $-45\text{ }^{\circ}\text{C}$ to investigate the changes taking place. These are analysed in Figure 3.21. On expansion of the patterns, the fine structure differences become more apparent (Figure 3.21b). In some cases peaks that were split become one and sharpen. It appears to be a reversible process, as peaks that had become one and sharpened at $-45\text{ }^{\circ}\text{C}$, are once again split at $-25\text{ }^{\circ}\text{C}$.

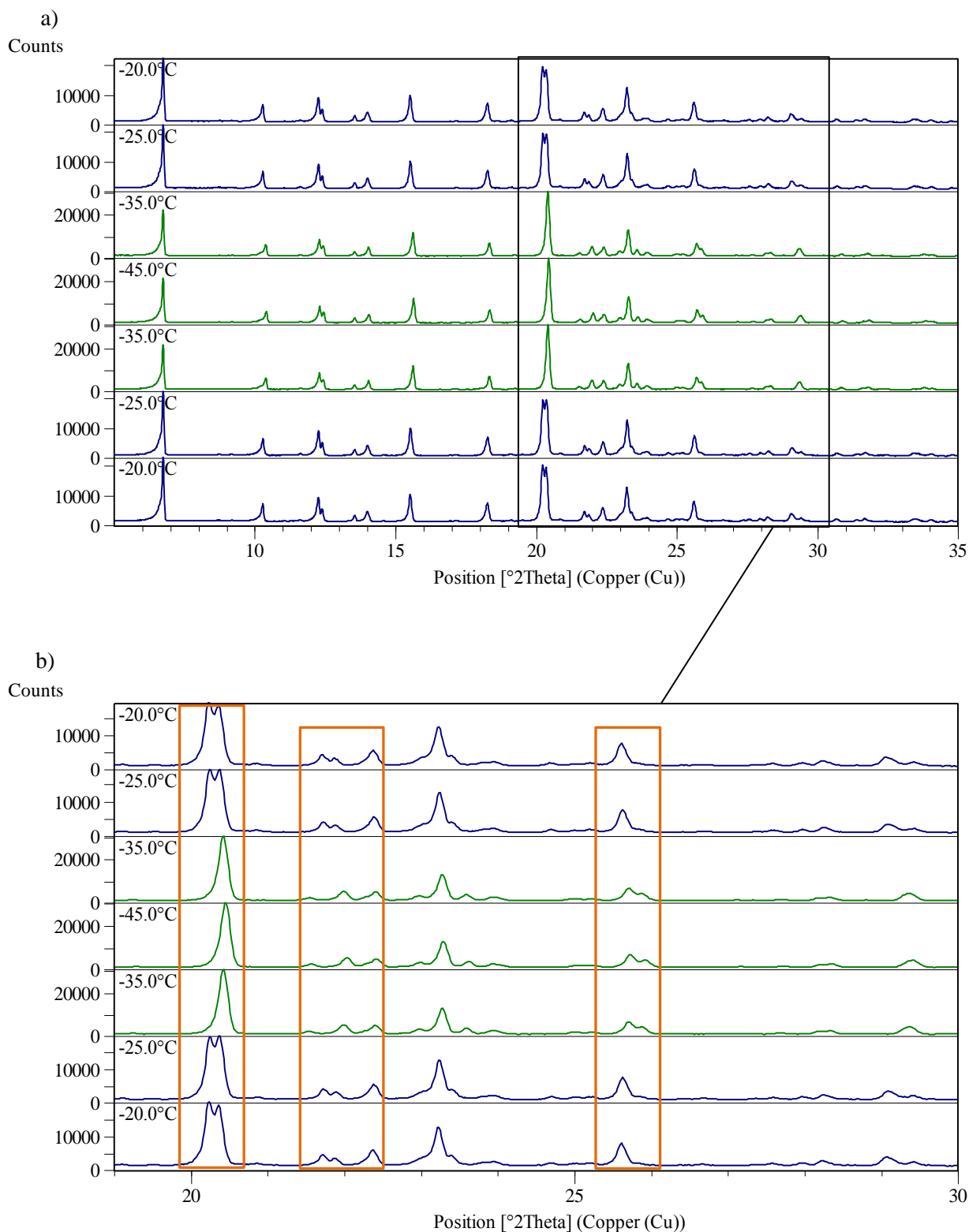
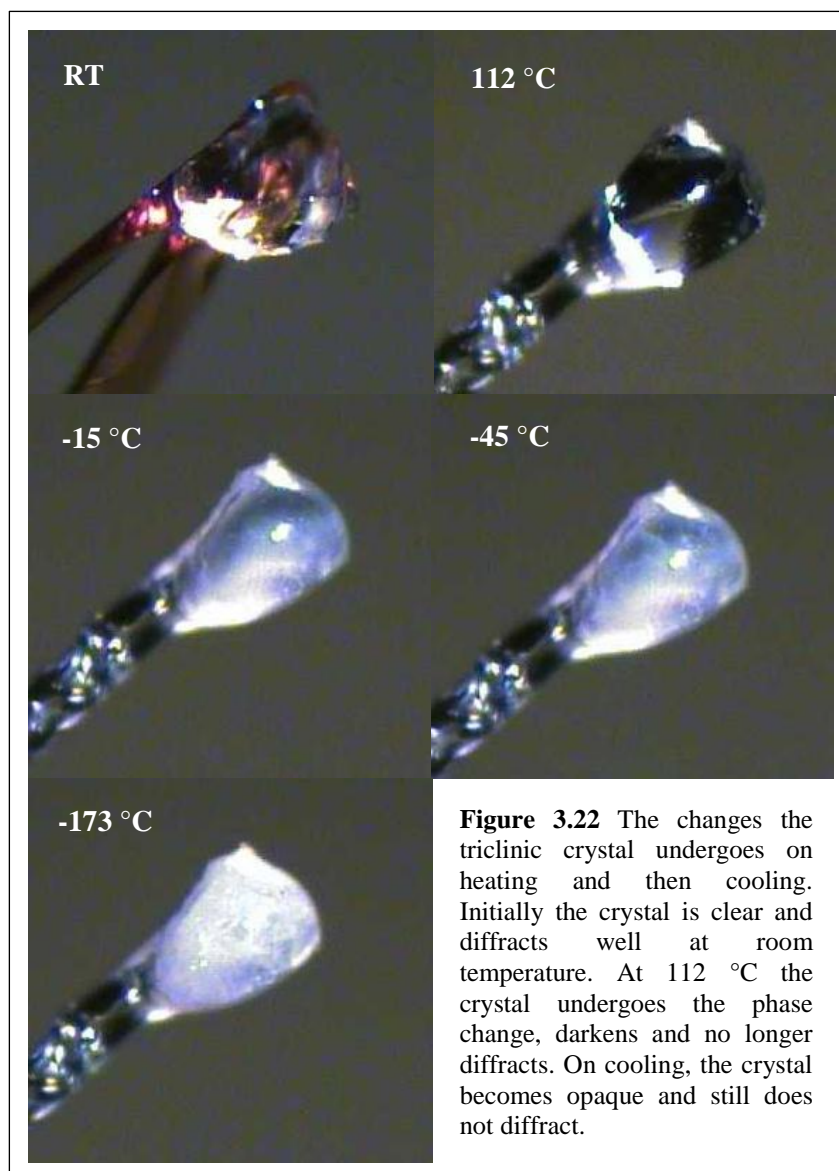


Figure 3.21 (a) Low temperature powder patterns of **M** after converting from **T** to **M**. (b) The fine structure differences include peak splitting and peaks that become one. This appears to be reversible, as the patterns at -45°C revert to that of the patterns at -25°C when the sample is slowly heated again.

Further single crystal X-ray diffraction studies were performed with the goal of obtaining structural data to explain these observations. First a room temperature structure of the triclinic form was obtained. The crystal was then heated to the phase transformation temperature and another dataset was collected. This procedure was repeated at -15, -45 and -173 °C. Unfortunately, after heating the crystal to 112 °C to induce the phase change, the crystal became dark and it no longer diffracted. Cooling the crystal did also not improve the situation, as it still did not diffract. Around 0 °C it turned slightly opaque, and by -15 °C it was almost light blue. At -45 °C it was more opaque than before, but still did not diffract. At -173 °C (100 K), the crystal was completely white and appeared to be cracked inside. Crystal videos were taken after every temperature step to record what was happening to the crystal. Selected highlights of the videos are shown in Figure 3.22.



3.6.2. Variable temperature studies of the transformations in the monoclinic phase, M

Since it was not possible to collect single crystal X-ray diffraction data observed in the DSC and VT PXRD of the triclinic crystals, the same series of experiments were conducted on the monoclinic crystals. This was done to investigate whether the events observed in the DSC and PXRD data only occurred with the triclinic form. DSC analysis was first performed on a few crystals of the monoclinic phase. The sample was heated to 118 °C (as was done with the triclinic crystals) and then cooled to -40 °C before being heated to room temperature. The results are shown in Figure 3.23. The peaks around -20 °C are once again visible, and peaks around 4 °C are now also much more prominent. This result confirms that the peaks previously seen in the DSC analysis are definitely related to the monoclinic phase. It appears to be dependent on heating of the crystals as the same events do not occur if **M** is first cooled to -40 °C.

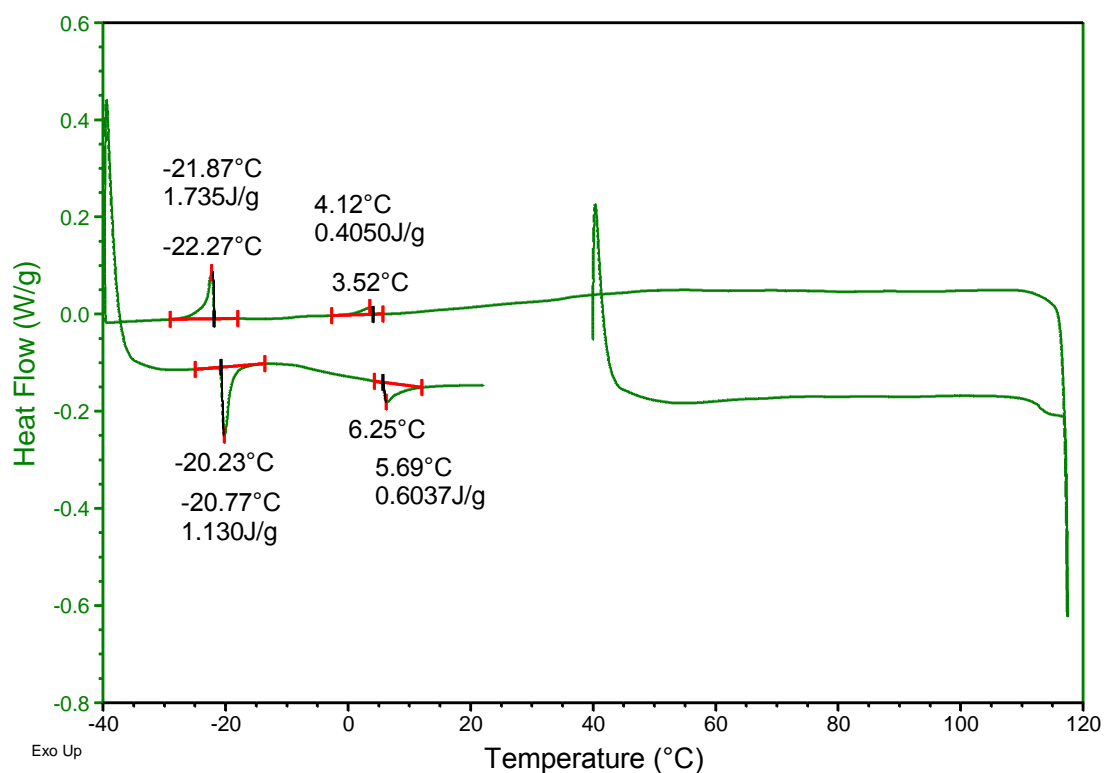


Figure 3.23. DSC results of the monoclinic phase. The sample was heated to the point where the phase transition from triclinic to monoclinic normally occurs, and then cooled to -40 °C. The peaks around -20 °C are there again and the peaks around 4 °C are now much more prominent than before.

VT PXRD experiments further analysed this interesting result. A sample of monoclinic crystals were crushed to a fine powder and loaded into a glass capillary. The sample was equilibrated at 25 °C and a measurement was taken. Further measurements were taken at approximately 10 °C intervals and the sample was allowed to equilibrate for two minutes after each temperature increase or decrease. The sample was heated to 95 °C and then cooled to -45 °C. The results are shown in Figure 3.24. There are no obvious differences in the powder patterns of the sample at different temperatures. These patterns correspond well with the simulated patterns from the crystal structures at room temperature and 100 K.

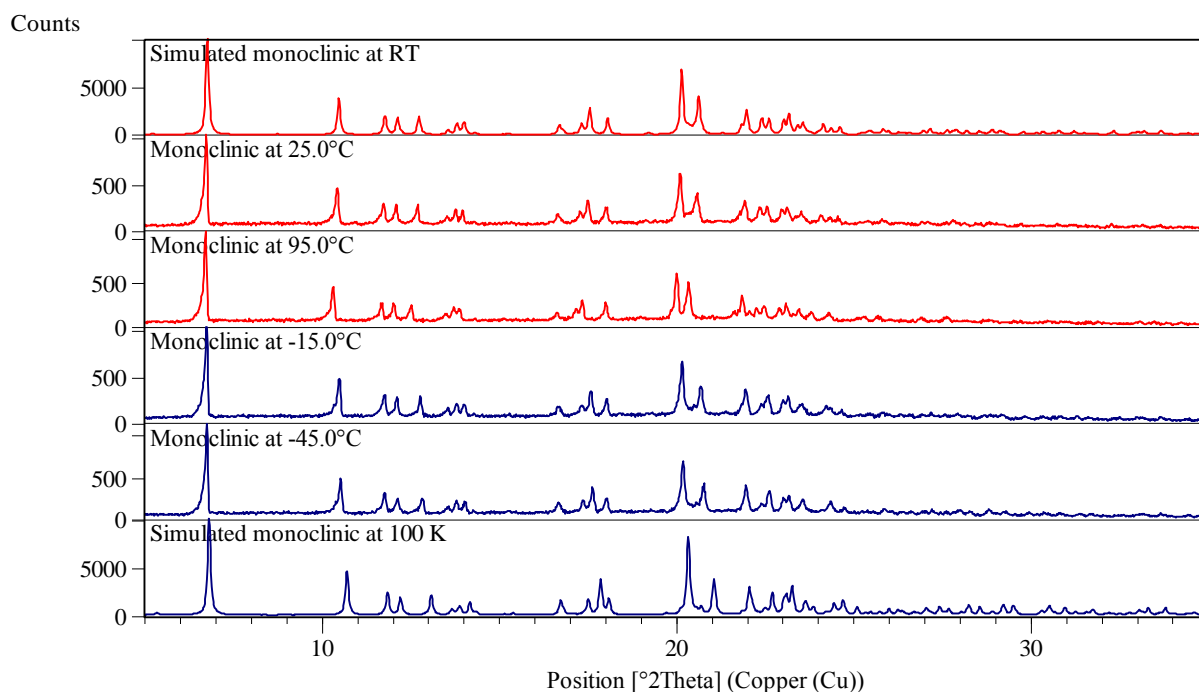


Figure 3.24. VT PXRD analysis of the monoclinic phase. There does not appear to be any obvious changes in the powder patterns at different temperatures. The simulated patterns from the crystal structures at RT and 100 K are also included for comparison.

When the patterns from Figure 3.24 are compared to the patterns from the experiment where the triclinic phase was converted to the monoclinic phase and then cooled, it is clear that these patterns do not match (Figure 3.25). There are peaks in the spectra in red that are not present in the navy spectra. DSC analysis definitely shows an event occurring at -20 °C, so the question arises whether a phase change did in fact occur, but it was not clearly identified by VT PXRD analysis.

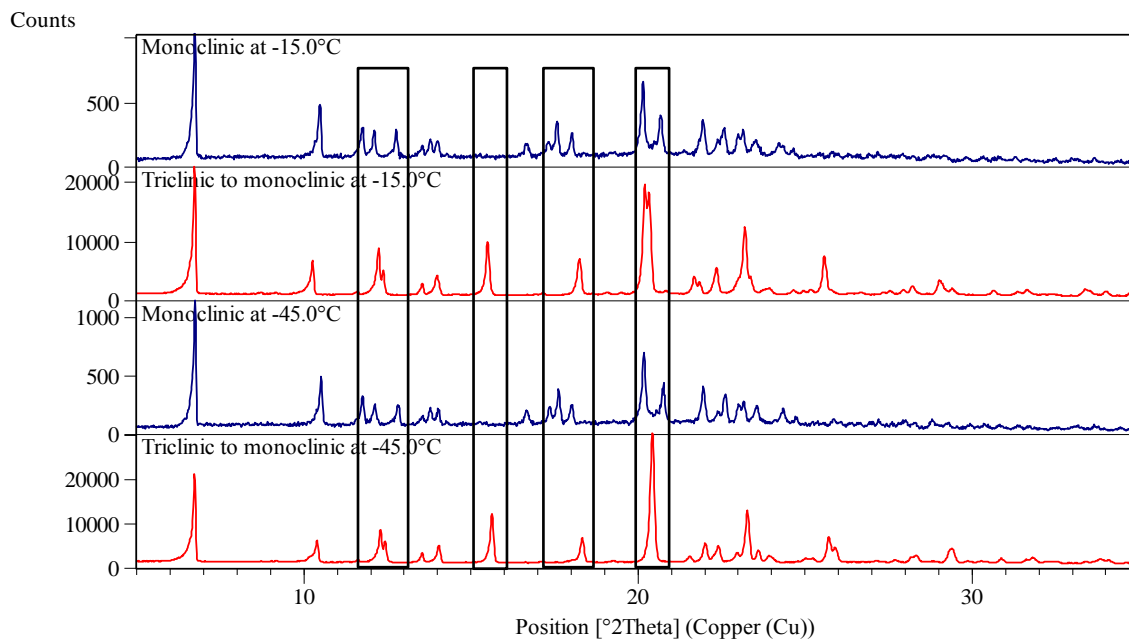


Figure 3.25. Comparison of the patterns of the triclinic sample that was converted to the monoclinic phase (in red), and the patterns of the experiment conducted on the monoclinic phase (in navy).

However, when results from a previous VT PXR D study of the monoclinic phase are compared to the results from Figure 3.24, it becomes evident that the pattern does indeed change. For the VT PXR D data that was previously collected, the monoclinic phase was heated until the sample melted. When the patterns at 125 °C are compared to the patterns of Figure 3.24, small differences are apparent (Figure 3.26).

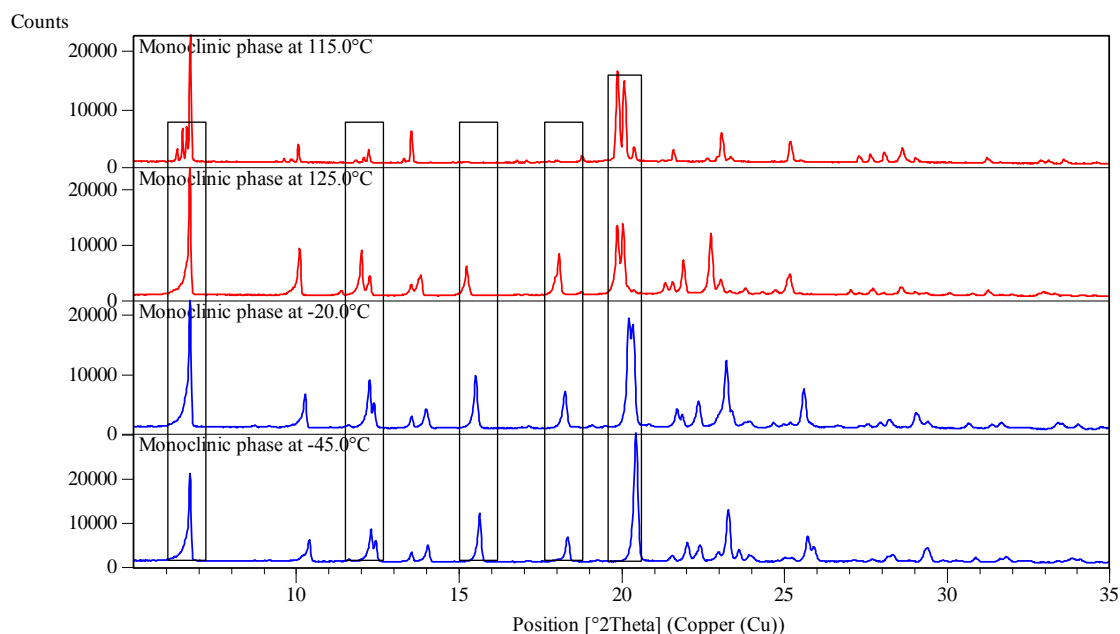


Figure 3.26 There is a difference in the patterns of **M** at 115 °C and 125 °C. The patterns at 125 °C do in fact correspond with the low temperature data.

The same single crystal X-ray diffraction studies that were performed on a triclinic crystal were performed on a monoclinic crystal with the aim to try and better understand what was happening in this system. The crystal was glued to a glass fibre as the high temperature would cause the crystal to move on a normal mount due to the decreasing viscosity of the paratone oil normally used to secure the crystal to the mount. Unit cells were collected at room temperature and 100 °C. Small changes were noted in the crystal morphology as the temperature increased. It appeared to become slightly opaque. Interestingly, the unit cell parameters changed from a monoclinic *P* cell at room temperature, to a monoclinic *C* cell at 100 °C. After the unit cell was collected, the crystal was cooled to 0 °C so as not to cause too much stress in the crystal, rendering it essentially useless. At 100 °C it was not diffracting very well. The unit cell remained monoclinic *C* at 0 °C and data was collected at this temperature. Data collections were also done at -20 °C and -45 °C. Although the crystal diffracted well at -45 °C, a suitable space group could not be found. Trying to solve the data in a low symmetry class such as *P1* did also not yield any positive results. The crystallographic data is summarised in Table 3.5. Crystal videos were also taken at each temperature before a data collection to track the visible changes (if any) in the crystal. These results are shown in Figure 3.27.

Table 3.5 Crystallographic data for the variable temperature SCD studies of the monoclinic phase.

Parameters	RT	100 °C	0 °C	-20 °C	-45 °C
Crystal system	Monoclinic <i>P</i>	Monoclinic <i>C</i>	Monoclinic <i>C</i>	Monoclinic <i>C</i>	Monoclinic <i>C</i> or <i>P</i>
Space group	<i>P2₁/n</i>	-	<i>C2/c</i>	<i>C2/c</i>	-
<i>a</i> (Å)	20.860(5)	31.01	30.970(3)	30.949(4)	-
<i>b</i> (Å)	8.085(1)	8.08	7.938(1)	7.916(1)	-
<i>c</i> (Å)	21.813(5)	17.37	17.159(2)	17.106(2)	-
α (°)	90	90	90	90	-
β (°)	104.62(3)	122.97	122.880(1)	122.820(2)	-
γ (°)	90	90	90	90	-
<i>Z</i>	4	-	4	4	-
R1 ($[I > 2\sigma(I)]$)	5.68	-	5.40	7.84	-

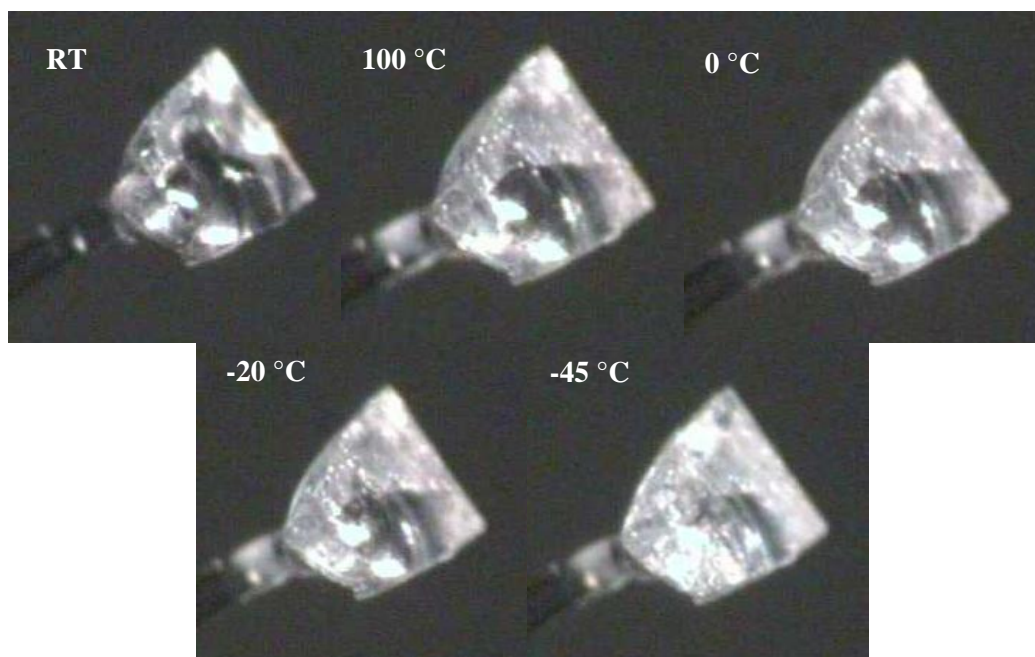


Figure 3.27 Images of the changes the crystal undergoes during heating and cooling. At 100 °C a clear crack has formed in the crystal. At -45 °C the crystal is less clear.

The crystal structures that were collected at 0 °C and -20 °C are both in the space group $C2/c$ and the packing arrangement is remarkably different to that of the structure originally collected at 100 K (M_{100K}). The asymmetric unit consists of half a cyclotriphosphazene molecule. Two of the fluorophenoxy rings are disordered over two positions, with approximately half occupancy for each position (Figure 3.28). The two disordered positions illustrate how the fluorophenoxy rings move at these higher temperatures (Figure 3.29). These conformations that the rings adopt, now allow the molecules to pack in a higher symmetry class.

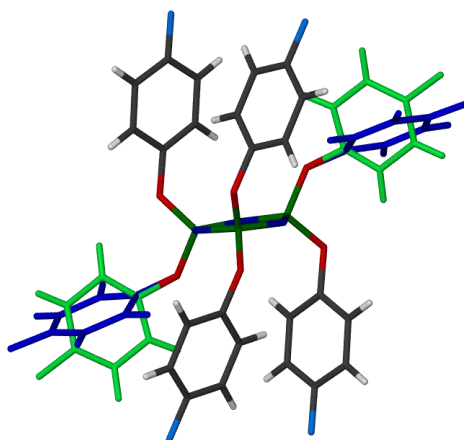


Figure 3.28 Capped stick representation of the monoclinic C polymorph. The two disordered fluorophenoxy rings are indicated in blue and green.

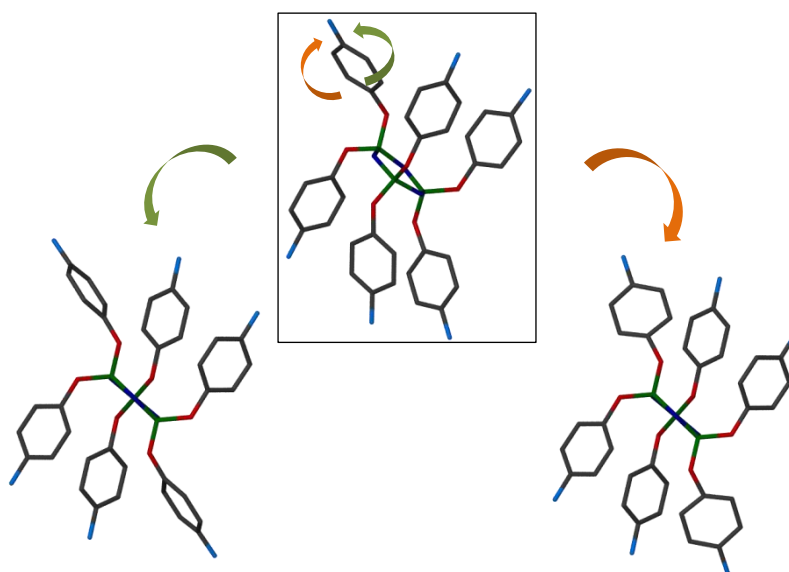


Figure 3.29 The different conformations the fluorophenoxy rings can adopt. This allows the molecules to pack in a higher symmetry class. Hydrogens have been omitted for clarity.

When viewed down the b -axis, the monoclinic C polymorph packs in a way that is reminiscent of the monoclinic P packing, viewed down the b -axis (Figure 3.30). When viewed down the a -axis, the cyclotriphosphazene rings all arrange in a pillar-like pattern along the b -axis.

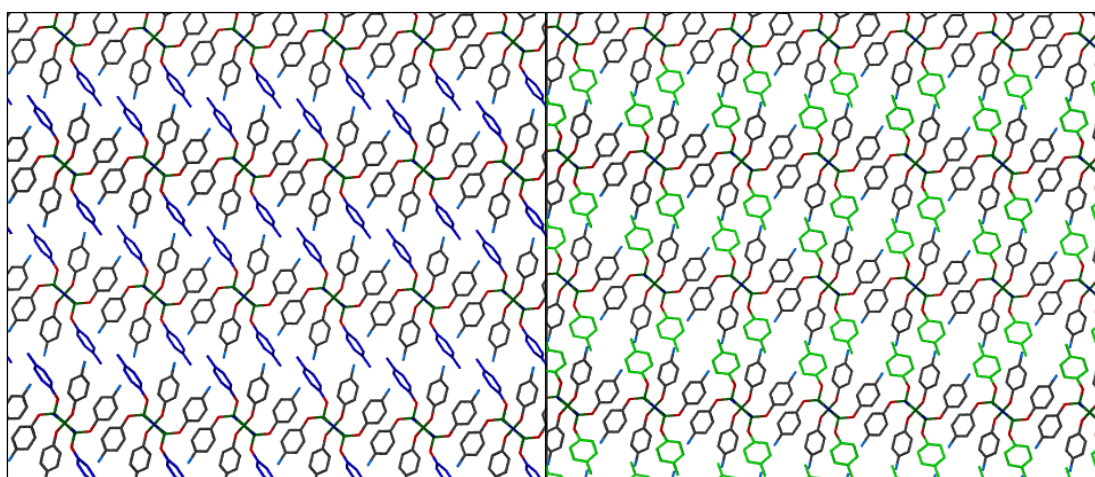


Figure 3.30 The packing of the monoclinic C polymorph viewed down the b -axis. The blue and green indicate the two different disordered positions.

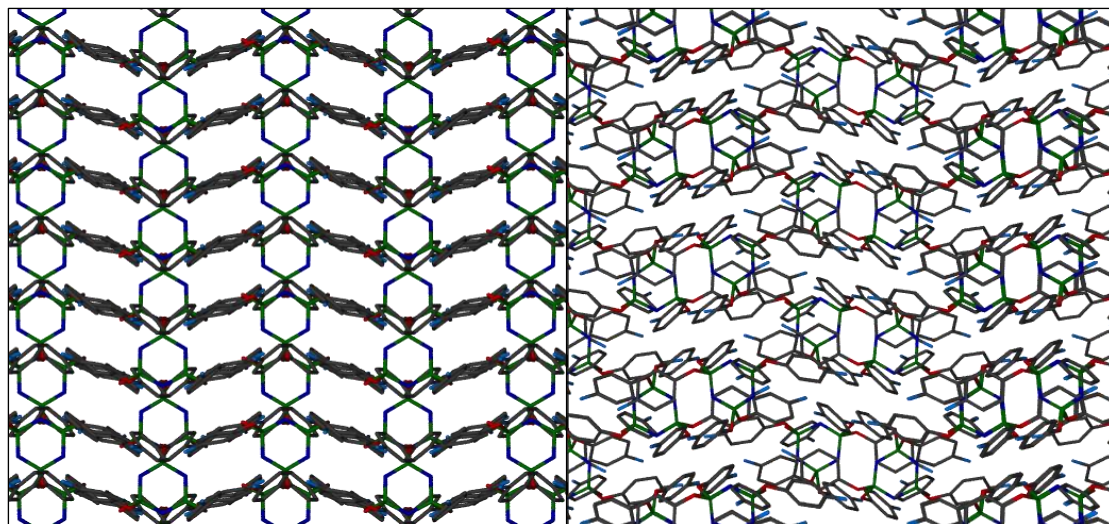


Figure 3.31 The pillar-like arrangement of the cyclotriphosphazene rings in the monoclinic *C* polymorph, viewed down the *a*-axis (left). The cyclotriphosphazene rings of the monoclinic *P* form on the right do not arrange in these pillars.

The simulated powder pattern of the monoclinic *C* polymorph was compared to the PXRD data collected on the triclinic sample. The triclinic sample was heated to the conversion temperature, and then cooled to $-45\text{ }^{\circ}\text{C}$. This experiment indicated that there could be another phase present. The VT SCD data collected on a monoclinic crystal confirms the suggestion of a new phase. The PXRD results are shown in Figure 3.32.

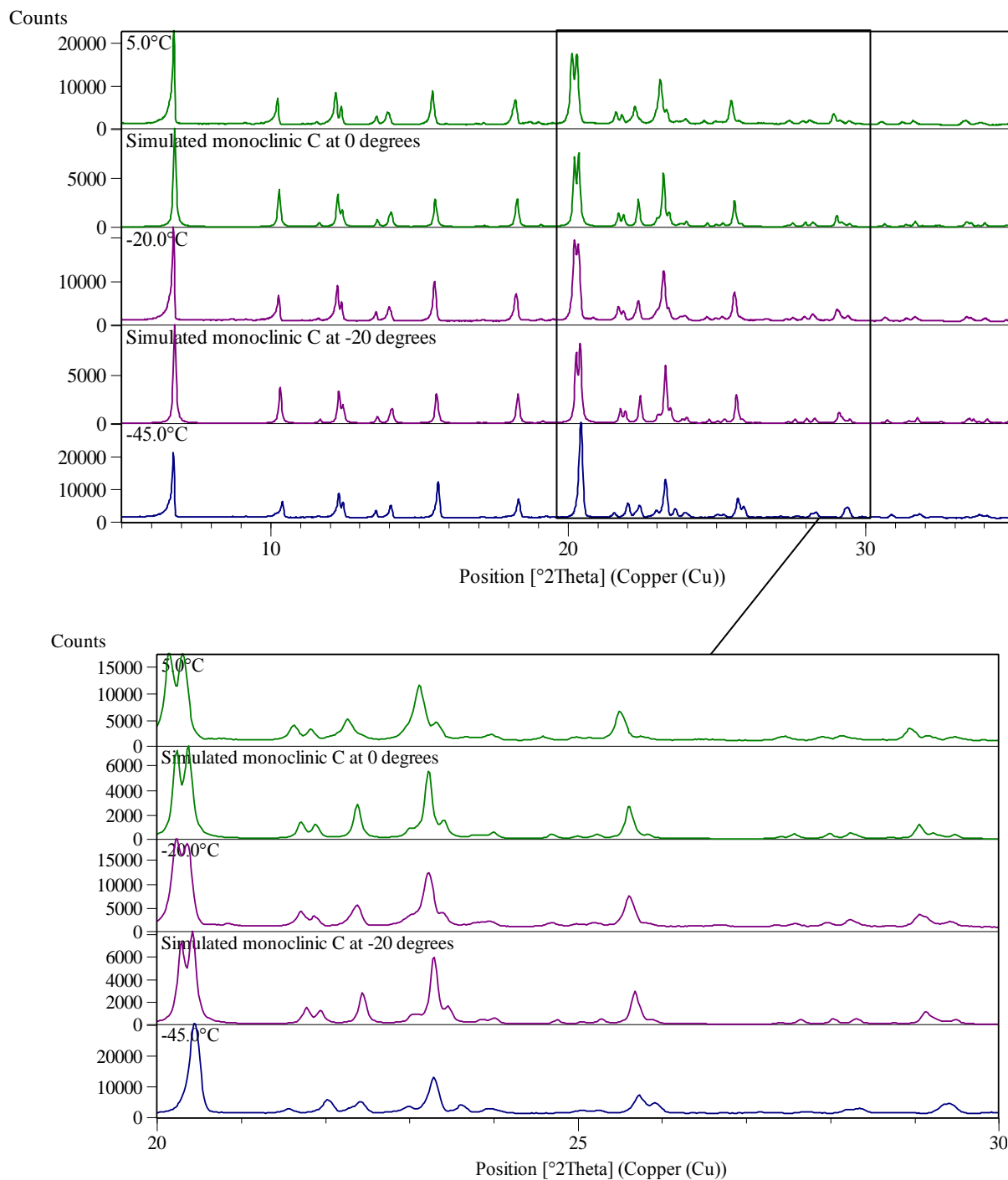


Figure 3.32 VT PXRD analysis of low temperature region after the triclinic form had been converted to the monoclinic phase. The simulated patterns from the crystal structures correspond well with experimental data collected at 5 and -20 $^{\circ}\text{C}$. There are still differences in the pattern at -45 $^{\circ}\text{C}$.

3.7. Conclusions and future work

In this study, two novel polymorphs of hexakis(4-fluorophenoxy)cyclotriphosphazene were discovered and extensive analysis was performed on this system.

The first polymorph that was identified was a conformational polymorph of **12** that crystallises in the triclinic crystal system. Crystals of the triclinic polymorph, **T**, were isolated from crystallisation experiments where the solvent has evaporated at a faster rate than the experiments that yielded the monoclinic form, **M**. DSC and PXRD analysis of **M** and **T** indicated that **T** converts to **M** at approximately 95 °C. The data also showed that it was not a reversible transformation, as **T** never reappeared on cooling. This leads to the conclusion that **T** is the metastable polymorph that converts to the more stable form **M** at higher temperatures. The endothermic conversion of **T** to **M** indicates that the two phases are enantiotropically related, but the reversibility of this conversion has not yet been observed.

An interesting observation was made when **T** was heated to a point after the phase transformation and cooled to -60 °C: two events were observed in the DSC data at -20 °C. It was suspected that these events indicated another phase change in the crystal. Close examination of the VT PXRD data showed a change in the fine structure of the powder patterns, possibly indicating that a change was taking place in the crystal structure. This could however not be confirmed by VT SCD studies as the crystal no longer diffracted after the phase transformation.

Further DSC analysis of the monoclinic form **M** did indicate that a phase change had taken place: the same events that occurred on cooling of **T** after the phase transformation occurred when **M** was heated to the same point and then cooled. VT SCD analysis was able to identify the new phase. The monoclinic *P* form converts to the monoclinic *C* polymorph. A lot of energy has to be introduced into the system to convert the primitive form to the *C*-centred form. The molecule has the energy to move around and twisting of the fluorophenoxy rings occurs. On cooling, the molecule then becomes trapped in this high symmetry conformation, consequently packing in the *C2/c* space group. Although the SCD data collected at -45 °C could not be solved, from numerous attempts it became clear that the difficulty of assigning a unit cell arose from the presence of extra reflections.

These reflections could be due to the crystal converting back to the monoclinic *P* form. The conversion was however not complete because the temperature was not low enough. This could indicate that the transformation between the monoclinic *P* and monoclinic *C* polymorphs is enantiotropic; therefore this could be a reversible process that occurs in a single crystal to single crystal fashion. In future, the crystal could be cooled to a lower temperature to investigate whether this allows the complete conversion from monoclinic *C* to monoclinic *P*. The same procedure can be followed with VT PXRD data where the sample could also be cooled to a lower temperature to study the peak splitting and peak deformation observed previously.

Since standard temperature and pressure conditions allow for only a limited amount of change, pressure DSC studies could be performed on this system to investigate if a change in pressure could result in the identification of more polymorphs. It would also be interesting to investigate if different pressures could induce the same type of polymorphism in the other halophenoxy cyclotriphosphazene derivatives, as various attempts to isolate polymorphs from crystallisations with these derivatives bore no fruit.

References

1. S. J. Coles, D. B. Davies, F. Hacivelioglu, M. B. Hursthouse, H. Ibisoglu, A. Kiliç and R. A. Shaw, *Acta Crystallogr., Sect. C: Cryst. Struct. Commun.*, 2007, **C63**, o152 - o156.
2. F. Hacivelioglu, R. Montis, D. B. Davies, A. Kiliç, M. B. Hursthouse and S. J. Coles, *CrystEngComm*, 2011, **13**, 4102 - 4109.
3. H. R. Allcock, D. C. Ngo, M. Parvez and K. B. Visscher, *Inorg. Chem.*, 1994, **33**, 2090 - 2102.
4. W. C. McCrone, in *Physics and chemistry of the organic solid state*, eds. D. Fox, M. M. Labes and A. Weissberger, Interscience, 1965, vol. 2, pp. 726 - 766.
5. R. Hilfiker, F. Blatter and M. v. Raumer, in *Polymorphism: in the pharmaceutical industry*, Wiley-VCH Verlag GmbH & Co. KGaA, 2006, pp. 1 - 19.
6. J. Bernstein, *Polymorphism in Molecular Crystals*, Oxford University Press, New York, 2008.
7. A. Nangia, *Acc. Chem. Res.*, 2008, **41**, 595 - 604.
8. G. Desiraju, *J. Chem. Sci.*, 2010, **122**, 667 - 675.
9. M. R. Caira, in *Encyclopedia of supramolecular chemistry*, eds. J. L. Atwood and J. W. Steed, M. Dekker, 2004, vol. 2, p. 1129.
10. D. Braga, F. Grepioni and L. Maini, *Chem. Commun.*, 2010, **46**, 6232 - 6242.
11. J. Bernstein, R. J. Davey and J.-O. Henck, *Angew. Chem., Int. Ed.*, 1999, **38**, 3440 - 3461.
12. S. M. Reed, T. J. Weakly and J. E. Hutchison, *Cryst. Eng.*, 2000, **3**, 85 - 99.
13. M. R. Caira, in *Design of organic solids*, ed. E. Weber, Springer, 1998, vol. 198, pp. 164 - 204.
14. D. Das, T. Jacobs, A. Pietraszko and L. J. Barbour, *Chem. Commun.*, 2011, **47**, 6009 - 6011.
15. F. H. Herbstein, *Cryst. Growth Des.*, 2004, **4**, 1419 - 1429.
16. C. F. Macrae, I. J. Bruno, J. A. Chisholm, P. R. Edgington, P. McCabe, E. Pidcock, L. Rodriguez-Monge, R. Taylor, J. van de Streek and P. A. Wood, *J. Appl. Crystallogr.*, 2008, **41**, 466 - 470.
17. C. F. Macrae, P. R. Edgington, P. McCabe, E. Pidcock, G. P. Shields, R. Taylor, M. Towler and J. van de Streek, *J. Appl. Crystallogr.*, 2006, **39**, 453 - 457.

18. I. J. Bruno, J. C. Cole, P. R. Edgington, M. Kessler, C. F. Macrae, P. McCabe, J. Pearson and R. Taylor, *Acta Crystallogr., Sect. B: Struct. Sci.*, 2002, **B58**, 389 - 397.
19. R. Taylor and C. F. Macrae, *Acta Crystallogr., Sect. B: Struct. Sci.*, 2001, **B57**, 815 - 827.
20. M. A. Spackman and J. J. McKinnon, *CrystEngComm*, 2002, **4**, 378 - 392.
21. J. J. McKinnon, M. A. Spackman and A. S. Mitchell, *Acta Crystallogr., Sect. B: Struct. Sci.*, 2004, **B60**, 627 - 668.
22. J. J. McKinnon, D. Jayatilaka and M. A. Spackman, *Chem. Commun.*, 2007, 3814 - 3816.
23. M. A. Spackman, J. J. McKinnon and D. Jayatilaka, *CrystEngComm*, 2008, **10**, 377 - 388.
24. M. A. Spackman and D. Jayatilaka, *CrystEngComm*, 2009, **11**, 19 - 32.
25. F. L. Hirshfeld, *Theor. Chim. Acta*, 1977, **44**, 129 - 138.
26. M. A. Spackman and D. Jayatilaka, *CrystEngComm*, 2009, **11**, 19 - 32.
27. J. J. McKinnon, F. P. A. Fabbiani and M. A. Spackman, *Cryst. Growth Des.*, 2007, **7**, 755 - 769.
28. K. Reichenbacher, H. I. Suss and J. Hulliger, *Chem. Soc. Rev.*, 2005, **34**, 22 - 30.
29. N. Ramasubbu, R. Parthasarathy and P. Murray-Rust, *J. Am. Chem. Soc.*, 1986, **108**, 4308 - 4314.
30. M. Barcelo-Oliver, C. Estarellas, A. Garcia-Raso, A. Terron, A. Frontera, D. Quinonero, I. Mata, E. Molins and P. M. Deya, *CrystEngComm*, 2010, **12**, 3758 - 3767.
31. J. L. Crisp, S. E. Dann and C. G. Blatchford, *Eur. J. Pharm. Sci.*, 2011, **42**, 568 - 577.

Chapter 4

Attempted co-crystal formation with cyclotriphosphazenes

This chapter will focus on the attempts to form co-crystals containing cyclotriphosphazenes. A large number of co-crystallisation experiments were conducted to study the conditions necessary for co-crystal and solvate formation, specifically with large, awkwardly shaped molecules such as cyclotriphosphazenes. These molecules seemed ideal for this type of study because their somewhat awkward shape could possibly cause inefficient packing in the solid state, leading to the formation of solvates. The range of substituents that can be placed on the cyclotriphosphazene ring creates the opportunity to incorporate various synthons into the structure to potentially form co-crystals.

Phenyl substituents that are placed on the cyclotriphosphazene ring tend to be perpendicular to the nearly planar ring. Three substituents point away from the ring on either side. This specific shape of the cyclotriphosphazene has been shown to crystallise in column-like structures in the solid state.^{1,2} Work done by Inoue and co-workers¹ described the co-crystallisation of hexakis(4-carboxyphenoxy)cyclotriphosphazene and hexakis(4-pyridylcarbonyl)cyclotriphosphazene from DMF, where these two cyclotriphosphazenes arrange in columns in the solid state *via* hydrogen bonds between the carboxylic acid and pyridyl moieties. The well-known tris(*o*-phenylenedioxy)cyclotriphosphazene (TPP) first published by Allcock in 1964,³ exhibits the remarkable ability to include a wide variety of solvents,^{4,5} methane and carbon dioxide⁶ and the ability to collect xenon atoms from the gas phase and subsequently orientating them on a macroscopic level.⁷ Although there are a few cyclotriphosphazene inclusion complexes and co-crystals present in the literature, it is a surprisingly small number compared to the vast amount of research conducted on cyclotriphosphazenes⁸ and the number of published structures in the Cambridge Structural Database (CSD)⁹⁻¹¹.

The aim of this study was to use the inherent properties of cyclotriphosphazene derivatives to form either solvates or co-crystals. These properties include the shape of the molecule, which is determined by the substituents on the phosphorus atoms. Therefore awkwardly shaped substituents were placed on the cyclotriphosphazene ring to prohibit efficient

packing in the crystal structure with the hope of including solvent in the crystal structure. Substituents containing functional groups with the potential to form supramolecular synthons in the solid state were used in order to engineer either pillared structures, or co-crystals.

First, the numerous co-crystallisation experiments conducted during this study will be described. The results from these experiments prompted a more in depth analysis of the CSD and results from this survey will be discussed. One novel co-crystal was isolated and the structure of this co-crystal will be described, as well as thoughts as to why this specific co-crystal was successfully engineered.

4.1 Co-crystallisation experiments

4.1.1 The trispiro and monospiro diaminoalkane cyclotriphosphazenes

The first crystallisation experiments were carried out with the diaminoalkane series of cyclotriphosphazenes. The diaminoalkane chain can coordinate through both the amine groups, forming spirocyclic compounds with the same paddle-wheel conformation as TPP (Figure 4.1). TPP has shown the remarkable ability to include a wide variety of solvents and gases. The diaminoalkane series was therefore chosen to mimic this inclusion ability of TPP. Figure 4.1a shows the structure of tris(1,3-diaminopropane)cyclotriphosphazene¹² (7).*

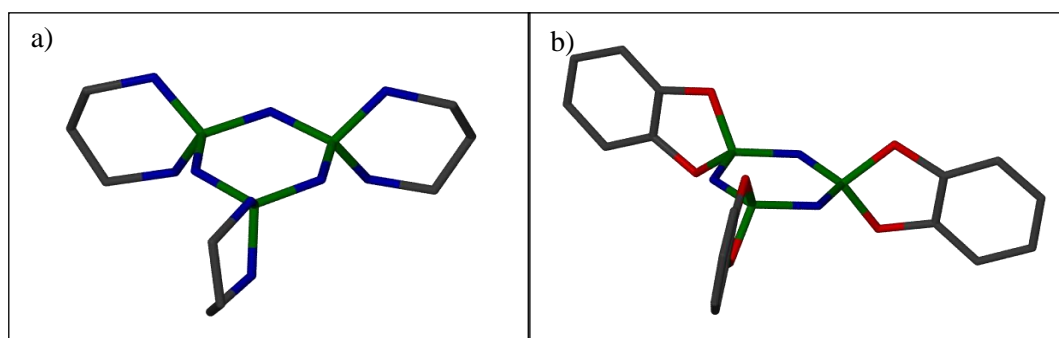


Figure 4.1 The crystal structures of (a) **7** and (b) TPP. Both molecules adopt a paddle wheel conformation. Hydrogens have been omitted for clarity.

The diaminoalkane derivatives also have the potential for hydrogen bonding through the nitrogen atoms on the diaminoalkane chain. Derivative **7** was synthesised and co-crystallisation experiments, as well as crystallisations from various solvents, were

* The numbering system used in this chapter follows from chapter 2.

conducted with this compound. These crystallisation experiments are listed in Table 4.1. The longer chain acids were chosen with the aim of forming a framework with the diacids acting as pillars between sheets of **7**. This was however not successful.

Table 4.1 Crystallisation experiments of **7** from different solvents and with different co-crystallisation agents.

Co-crystallisation agent	Ratio (7:co-former)	Solvent system	Crystallisation technique
isophthalic acid	1:1	methanol	slow evaporation
terephthalic acid	1:2	methanol	slow evaporation
trimesic acid	1:1	methanol	slow evaporation
succinic acid	1:3	methanol	slow evaporation
maleic acid	1:3	methanol/THF	slow evaporation
tartaric acid	1:3	methanol	slow evaporation
2,6-naphthalene dicarboxylic acid	1:1	methanol	slow evaporation
none	-	THF	slow evaporation
none	-	hexane/THF	slow evaporation
none	-	DCM	slow evaporation
none	-	DMSO	slow evaporation
none	-	acetonitrile	slow evaporation
none	-	methanol	slow evaporation
none	-	ethanol	slow evaporation
none	-	DMF	slow evaporation
none	-	NMP	slow evaporation
none	-	chloroform	slow evaporation

During the investigation into co-crystal formation with **7** it was observed that if **7** was not used in crystallisation experiments within three days, the compound would become paste-like and insoluble in most solvents.

Crystals were isolated from a THF/hexane mixture. These crystals proved to be the hydrate of **7** that has been reported in the literature¹² (Figure 4.2). It crystallises in the space group $P\bar{1}$.

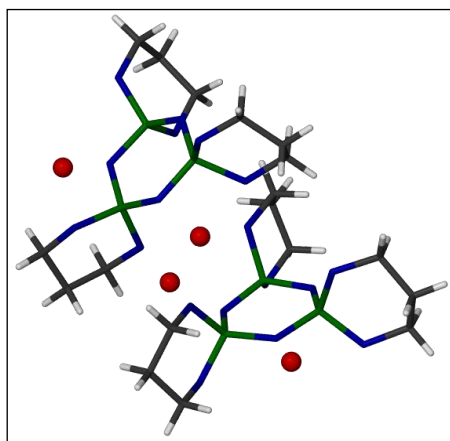


Figure 4.2 Capped stick representation of the hydrate of **7**.

The water molecules in the structure hydrogen bond to each other in a zig-zag fashion as shown in Figure 4.3. This type of hydrogen bond is represented by red dotted lines. Some of the water molecules hydrogen bond to the nitrogen atoms of the 1,3-diaminopropane chain, while others hydrogen bond to the nitrogen of the cyclotriphosphazene ring. Hydrogen bonding also occurs between cyclotriphosphazene rings where the nitrogen of the 1,3-diaminopropane chain interacts with the nitrogen of the next cyclotriphosphazene ring. An interesting feature of the structure is the fact that two cyclotriphosphazene rings will only interact through the 1,3-diaminopropane chains, but the next cyclotriphosphazene will interact through both the nitrogen of the 1,3-diaminopropane chain as well as the nitrogen of the cyclotriphosphazene ring. This is shown in blue in Figure 4.3. This causes the molecules to pack in stacks of dimers. The molecules in a dimer are related to each other through a centre of inversion.

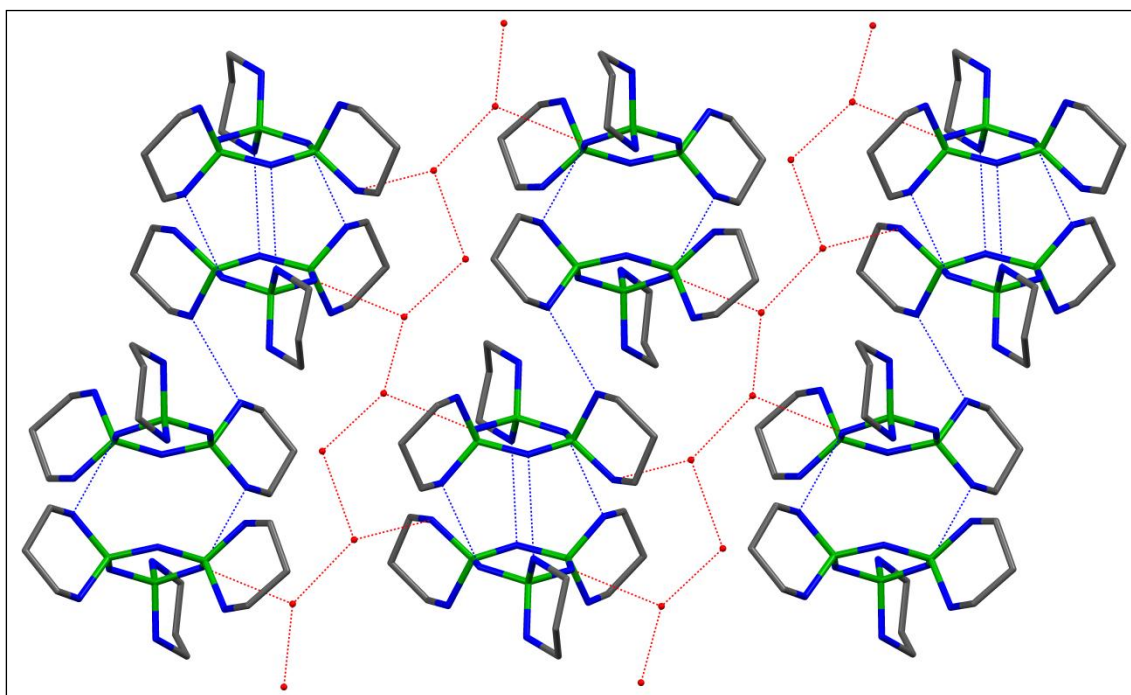


Figure 4.3 The hydrogen bonds found in the structure of **7**. The red dotted lines represent hydrogen bonding involving water molecules. The blue dotted lines represent hydrogen bonding between cyclotriphosphazenes. This causes the molecules to pack in stacks of dimers.

It was surprising that no solvates were formed with hydrogen bond donating solvents such as methanol and ethanol. According to El Murr and co-workers,¹² they were able to isolate crystals of **7** from the reaction mixture, but these crystals did not survive exposure to X-rays. However, the crystals grown from methanol that incorporated water into the structure (Figure 4.2) did not disintegrate upon exposure to X-rays. Therefore, it would be expected that it would be beneficial to the stability of the crystal structure to incorporate these solvents into the crystal structure. As this does not occur, it is suspected that more favourable interactions are formed between molecules of **7** than between **7** and other molecules. In other words, homomeric crystallisation is preferred to heteromeric crystallisation.

4.1.2 Crystallisation experiments with 2,2-bis(4-formylphenoxy)-4,4,6,6-bis[spiro(2',2''-dioxo-1',1''-biphenyl)]cyclotriphosphazene (**3**)

Co-crystallisation experiments were carried out with **3** (Figure 4.4) with the aim of using the awkward shape of the molecule to cause inefficient packing in the solid state in order to include solvent in the crystal structure. **3** was therefore crystallised from various solvents (Table 4.2). Although the aldehyde moiety is not considered to be a strong hydrogen bond acceptor it was co-crystallised with a wide range of hydrogen bond donors with the aim of forming co-crystals. The co-crystallisation experiments are listed in Table 4.3. The ratio of **3** to co-crystal former in each case is 1:2 as **3** has two aldehyde moieties that can potentially participate in hydrogen bonding interactions.

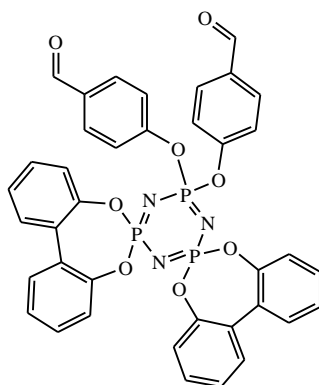


Figure 4.4 This molecule (**3**) was used in crystallisation experiments in the hope of forming solvates due to the awkward shape of the molecule.

Table 4.2 Crystallisation of **3** from a range of solvents. All crystalline products were shown to be crystals of **3**.

Solvent system	Crystallisation technique	Result
benzene	slow evaporation	Crystals of 3
toluene	slow evaporation	-
methanol	slow evaporation	-
NMP	slow evaporation	-
DMSO	slow evaporation	-
chloroform	slow evaporation	-
acetone	slow evaporation	Crystals of 3

Table 4.3 Co-crystallisation experiments with **3** from different solvent systems and using different crystallisation techniques.

Co-crystallisation agent	Solvent system	Crystallisation technique
pamoic acid	THF	slow evaporation
piperazine	THF	slow evaporation
2,6-diamino-pyridine	THF	slow evaporation,
trimesic acid	THF/hexane	slow evaporation
isophthalic acid	THF/hexane	layering
benzotrile	THF	layering
2,6-diaminopyridine	THF/diethyl ether	vapour diffusion
1,2-diaminoethane	THF/diethyl ether	vapour diffusion
1,3-diaminopropane	THF/diethyl ether	vapour diffusion
1,4-diaminobutane	THF/diethyl ether	vapour diffusion
1,5-diaminopentane	THF/diethyl ether	vapour diffusion
1,6-diaminohexane	THF/diethyl ether	Vapour diffusion
<i>p</i> -aminobenzoic acid	DCM	vapour diffusion
	DMF/diethyl ether	slow evaporation
2-aminothephtalic acid	THF	vapour diffusion
	DMF/diethyl ether	slow evaporation
2,6-dipicolinic acid	THF/DCM	vapour diffusion
		slow evaporation
3,5-dinitrobenzoic acid	THF	vapour diffusion
	DMF/diethyl ether	slow evaporation
1,6-dihydroxynaphthalene	THF	vapour diffusion
	DMF/diethyl ether	slow evaporation
<i>o</i> -phenylenediamine	THF	vapour diffusion
	DMF/diethyl ether	slow evaporation
phenol	THF	vapour diffusion
	DMF/diethyl ether	slow evaporation

Crystals were formed in a co-crystallisation with 1,6-dihydroxynaphthalene, as well as from benzene and acetone, and subsequent single-crystal X-ray diffraction analysis showed that these were crystals of pure **3**. The crystal structure of **3** was described in chapter 2, but selected features relating to possible reasons why it did not co-crystallise with any small molecules will be discussed here.

The biphenyl-2,2'-diol groups in **3** adopt a conformation that is seen in both the structures of 2,2-dichloro-4,4,6,6-bis[spiro(2',2''-dioxo-1',1''-biphenyl)]cyclotriphosphazene¹³ (**2**) and the triply substituted tris(2,2'-dioxybiphenyl)cyclotriphosphazene¹⁴ (**17**) (Figure 4.5).

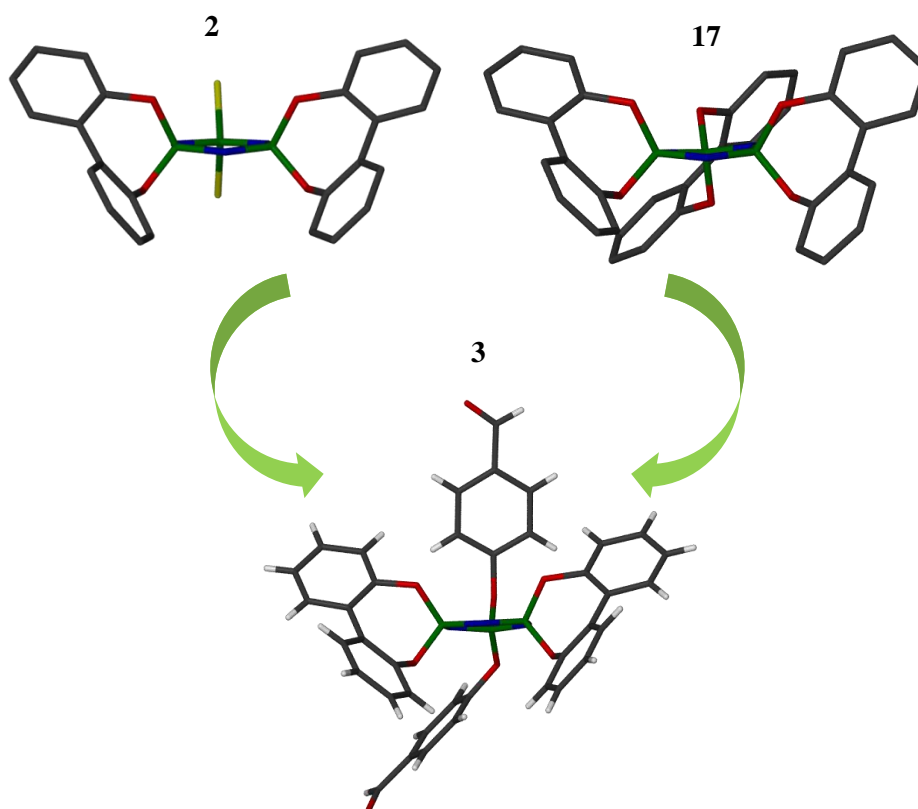


Figure 4.5 The conformation of the 2,2'-dioxybiphenyl groups in **3** is the same as in both structures of **2** and **17**.

In **2** the 2,2'-dioxybiphenyl groups are involved in π - π stacking interactions, causing the molecules to close-pack in the crystal structure despite the substituents being bulky. The benzaldehyde substituents of **3** also close pack by means of π -stacking interactions, therefore it can be concluded that these interactions (the π -stacking interactions of the 2,2'-dioxybiphenyl and the benzaldehyde groups of **3**) are more favourable than forming

hydrogen bonds with donor groups such as the carboxylic acids, amines and hydroxyl moieties.

The hexakis(4-hydroxyphenoxy)cyclotriphosphazene (**11**) was also used in co-crystallisation experiments with acids, amines, alcohols and hydrogen bond acceptors such as pyridine, but no crystals could be grown from these solutions. Some of the attempted co-crystallisation experiments are listed in Table 4.4. All of the attempts to grow co-crystals with hydrogen bonding being the driving force for co-crystal formation were not successful therefore it was decided to try to use either halogen-halogen interactions or halogen-nitrile interactions to construct co-crystals.

Table 4.4 Selected co-crystallisation experiments that were attempted with **11**. The ratio of **11** to the co-crystal former is indicated, as well as the solvent system used.

Co-crystal former	Ratio	Solvent system	Crystallisation technique
<i>p</i> -aminobenzoic acid	1:3	THF	slow evaporation
2-aminoterephthalic acid	1:3	THF	slow evaporation
3,5-dinitrobenzoic acid	1:3	THF	slow evaporation
phenol	1:3	THF	slow evaporation
<i>o</i> -phenylene diamine	1:3	THF	slow evaporation
2,6-dipicolinic acid	1:3	DMF	slow evaporation
pyridine	excess	THF	slow evaporation
4,4'-bipyridine	1:3	DMF	slow evaporation
4,4'-trimethylene dipyridine	1:3	DMF	slow evaporation
3,4-, 3,5-lutidine	1:3	DMF	slow evaporation
2,3-, 2,5- lutidine	1:3	THF	slow evaporation
2,4-, 2,6-lutidine	1:3	DMF	slow evaporation
2-, 3-, 4-picoline	1:3	THF	slow evaporation
2,6-diaminopyridine	1:3	DMF	slow evaporation
piperazine	1:3	THF	slow evaporation

4.1.3 Attempted co-crystallisation *via* halogen-halogen and halogen-nitrile interactions

The hexakis(4-halophenoxy)cyclotriphosphazene derivatives (**12** – **15**) were co-crystallised with a range of small molecules, including molecules with halogens, nitriles and nitrogen-containing heterocycles such as pyridine. The solvent systems that were used include acetonitrile, acetonitrile/DCM, DCM, THF, THF/methanol, chloroform, chloroform/acetone and DMSO, as well as combinations of these solvents.

In each case the halophenoxy cyclotriphosphazene preferred to crystallise by itself rather than co-crystallising with other small molecules. From these results it appears that the size and shape of the co-crystallisation agents do play a role. A study conducted by Anderson and co-workers¹⁵ found that molecules that crystallise with $Z' > 1$ (more than one chemical unit in the asymmetric unit) are generally small, awkwardly shaped molecules. They are also more conformationally restricted, which would explain why the cyclotriphosphazenes seldom co-crystallise with smaller molecules: cyclotriphosphazenes are much larger molecules with substituents that are more conformationally flexible. It is therefore possible that the flexibility of the molecule would allow only interaction with similarly-shaped molecules and the cyclotriphosphazene derivatives consequently crystallise without forming a co-crystal or inclusion compound.

Expanding on the idea that similarly-shaped molecules would prefer to co-crystallise, the crystal structures of the halophenoxy derivatives **12** to **15** were analysed. It was found that hexakis(4-fluorophenoxy)cyclotriphosphazene (**12**) and hexakis(4-chlorophenoxy)cyclotriphosphazene (**15**) are isostructural (Figure 4.6), and that hexakis(4-bromophenoxy)cyclotriphosphazene (**14**) and hexakis(4-iodophenoxy)cyclotriphosphazene (**13**) are isostructural (Figure 4.7).

These structures were originally collected at room temperature^{16, 17} therefore the structures were recollected at 100 K.

There are slight differences in the conformation of the chlorophenoxy rings relative to that of the fluorophenoxy rings, but the packing is identical when viewed down the *b*-axis (Figure 4.6).

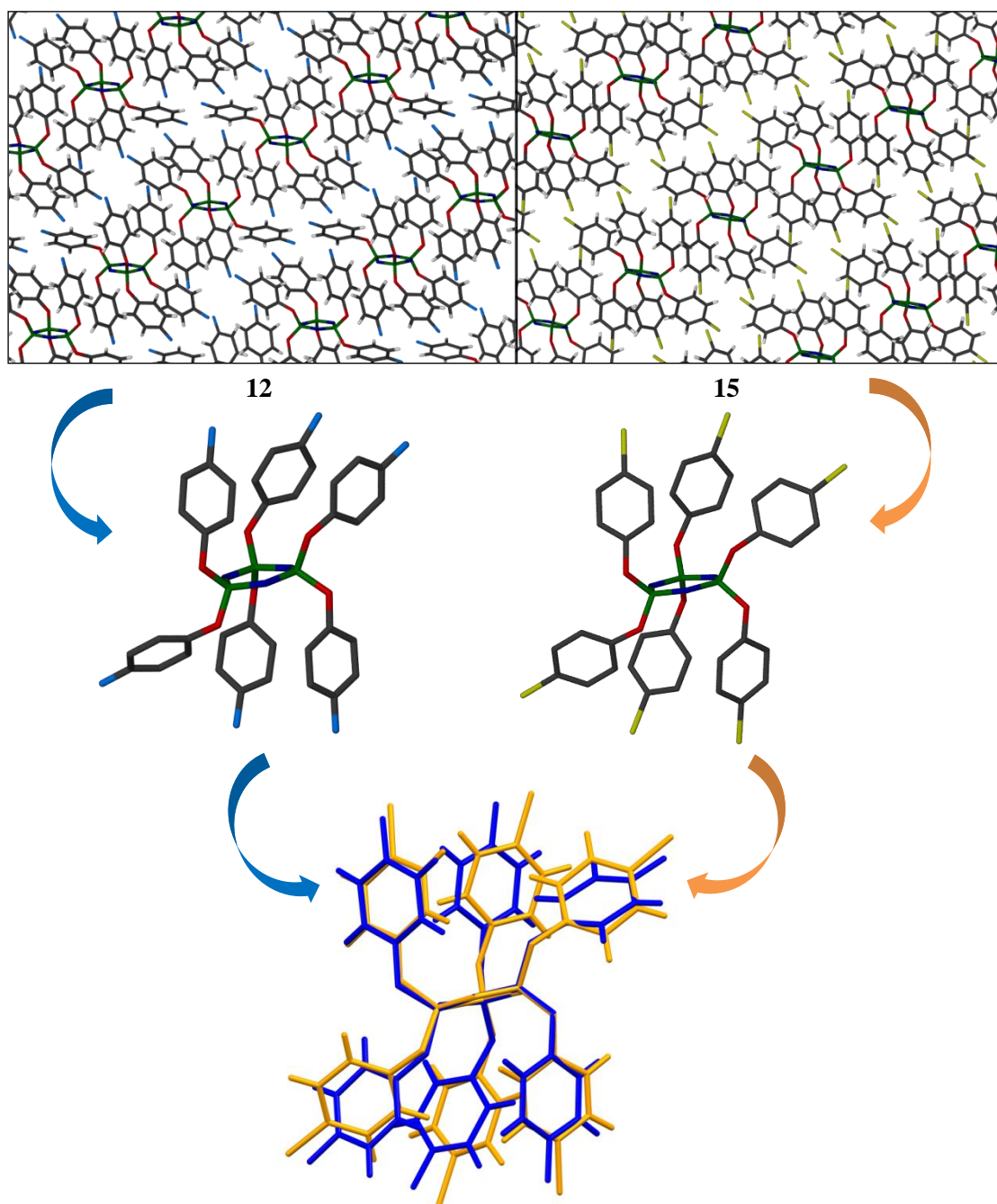


Figure 4.6 The isostructural hexakis(4-fluorophenoxy)cyclotriphosphazene (**12**) (left, blue) and hexakis(4-chlorophenoxy)cyclotriphosphazene (**15**) (right, orange). There are slight differences in the conformation of the chlorophenoxy rings relative to the fluorophenoxy rings.

The iodophenoxy ring of **13** is twisted relative to the bromophenoxy ring of **14** on the same phosphorus atom (Figure 4.7).

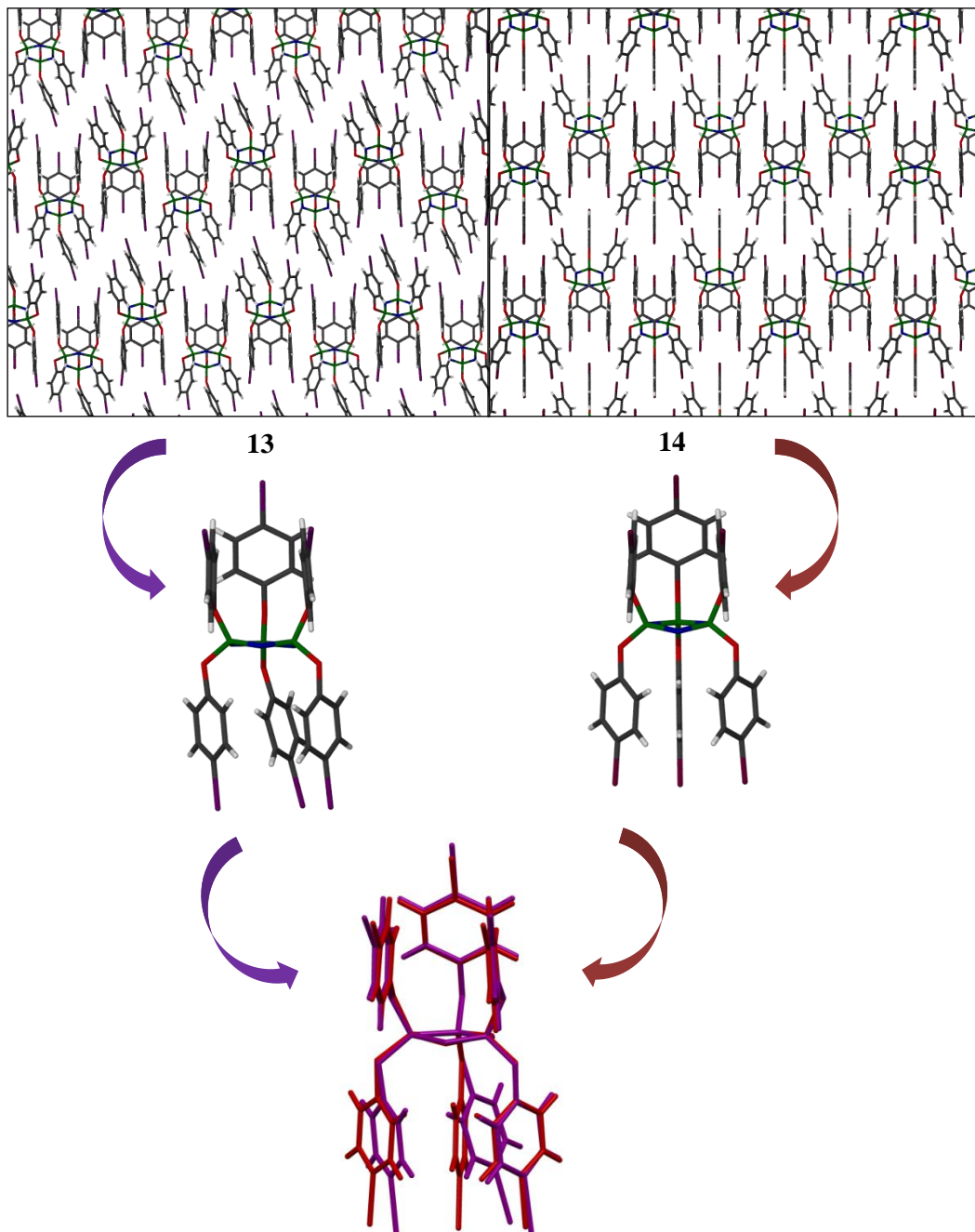


Figure 4.7 The isostructural hexakis(4-iodophenoxy)cyclotriphosphazene (**13**) (left, purple), viewed down the *b*-axis, and hexakis(4-bromophenoxy)-cyclotriphosphazene (**14**) (right, maroon), viewed down the *c*-axis. One iodophenoxy ring is slightly twisted relative to the bromophenoxy ring.

Unfortunately, co-crystals of **13** and **14**, or **12** and **15** could not be grown from solution. It was decided to try to grow co-crystals by melting the isostructural compounds together. This was done to investigate whether there was an energy barrier that had to be overcome before co-crystallisation could take place. Studies that were conducted on the polymorphs of hexakis(4-fluorophenoxy)cyclotriphosphazene (**12**) in chapter three showed the effect temperature has on the conformation of the molecule. It was surmised that to induce co-crystal formation, energy also had to be supplied to the system to allow the molecules to adapt their conformation to allow co-crystallisation with a different derivative.

Crystals of **12** and **15** were ground together in a 1:1 ratio, melted and DSC analysis was performed on the product. DSC analysis showed that the melting point of the product (referred to as **12/15**) is at 122.9 °C, which is lower than the melting point of **12** (129 °C) and **15** (152 °C). This is however not conclusive evidence that a co-crystal has formed, as melting of the one compound could possibly induce melting of the other at a lower temperature than expected (Figure 4.8).

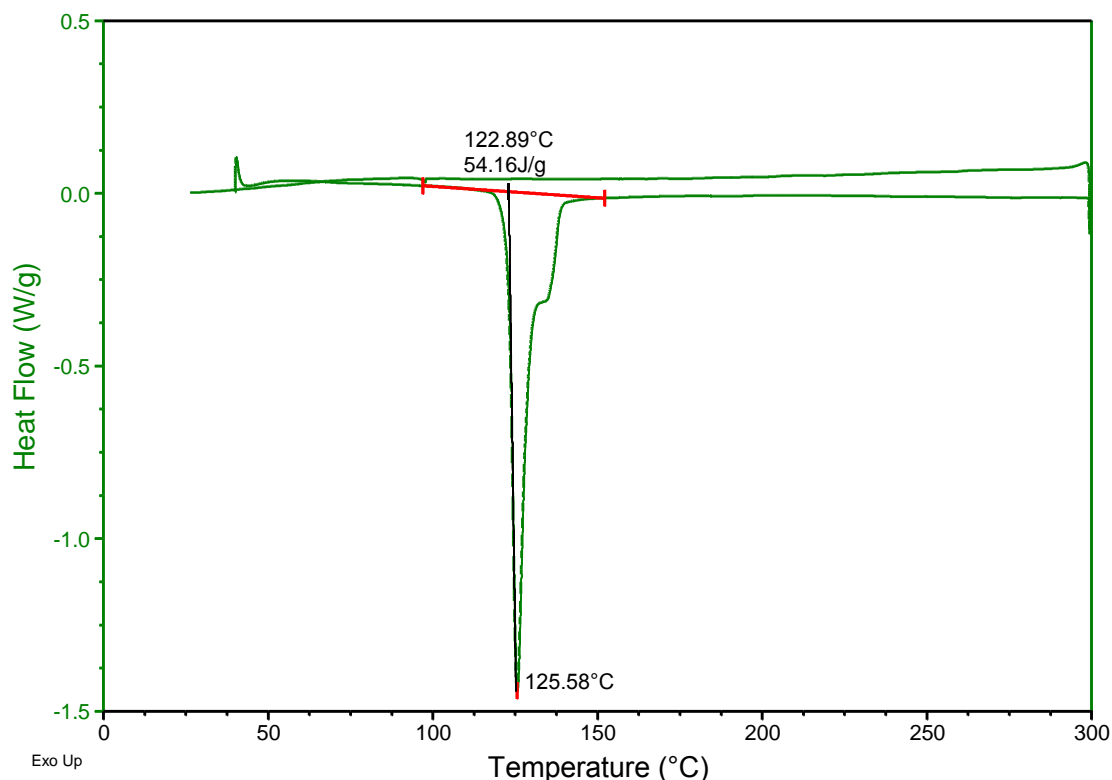


Figure 4.8 DSC analysis of the melt product (**12/15**) of the fluoro and chloro derivatives. Melting occurs before the melting point of the fluorophenoxy derivative (129 °C).

The same procedure was followed for **13** and **14** (Figure 4.9) and the same observation was made. Once again there is only one melting point at 173.1 °C. The melting point of **14** is at 176.8 °C and the melting point of **13** is at 187.6 °C. However, the melting point of the product (**13/14**) is again lower than both these temperatures. This could again be due to induced melting of **13** because of the small sample size.

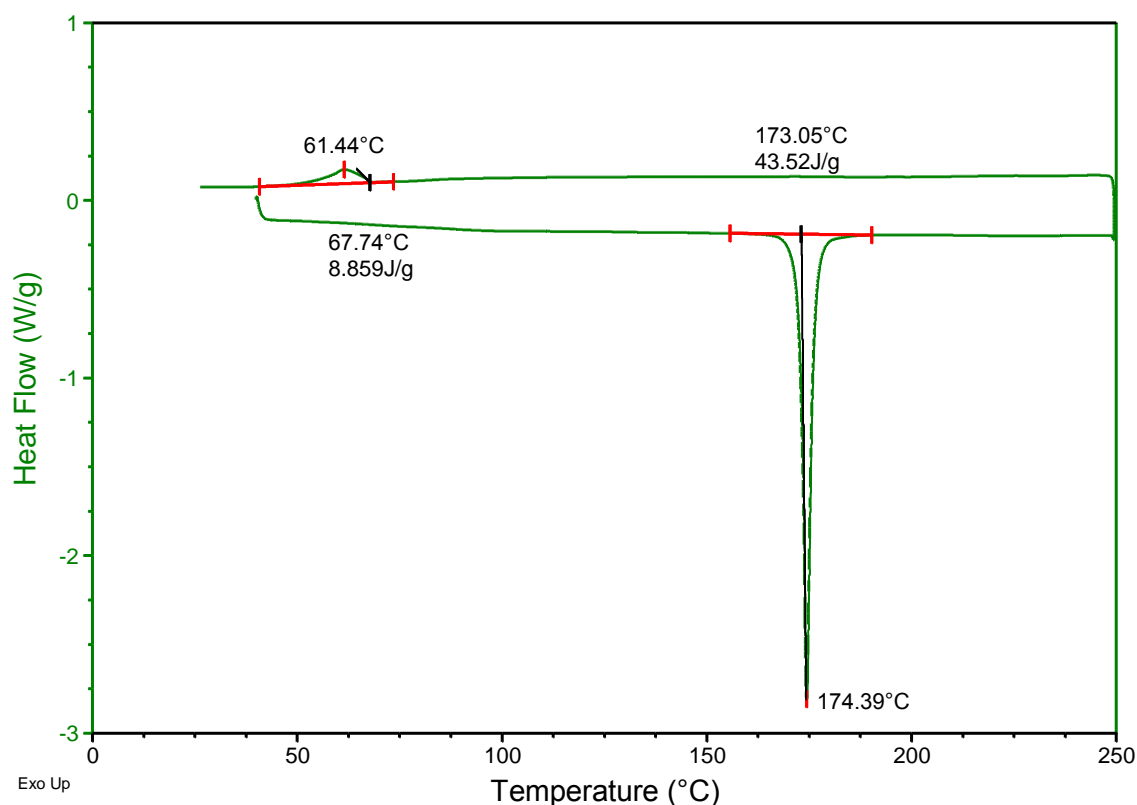


Figure 4.9 DSC analysis of the product of **13** and **14**. The melting point of **13/14** is lower than that of both the reagents.

DSC results indicate that a co-crystal could have been formed by melting the two isostructural components together. This is however not conclusive evidence. PXRD analysis was used to further study the melt products **12/15** and **13/14**. The results are shown in Figure 4.10 and Figure 4.11. PXRD analysis does unfortunately not deliver conclusive results. The powder patterns of the halophenoxy melt products **12/15** and **13/14** largely correspond to the simulated patterns of the halophenoxy derivatives. There are however minor differences between the patterns, therefore it is difficult to determine whether a novel co-crystal has in fact formed. It could also be possible that the co-crystals are isostructural to the co-crystal formers, and hence have similar powder patterns. This

could be further analysed by solid state NMR that could indicate if new intermolecular interactions have formed.

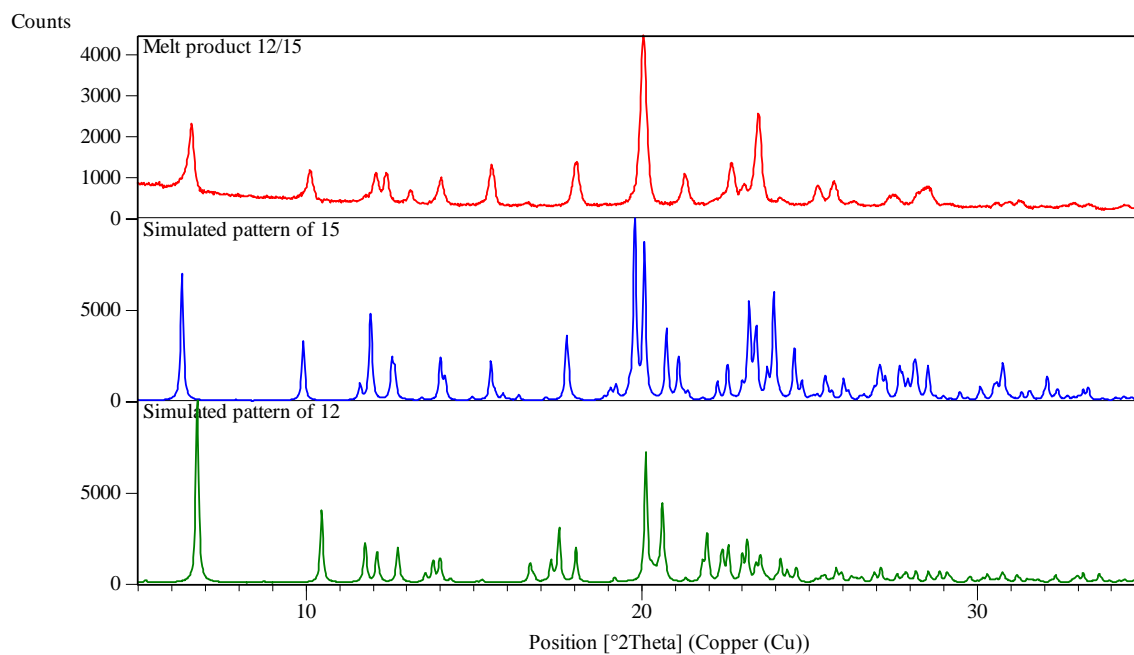


Figure 4.10 PXRd analysis of the melt product **12/15** of the fluorophenoxy and chlorophenoxy derivatives. The pattern of **12/15** corresponds with the patterns of **12** and **15** to a large extent, but the results are not conclusive.

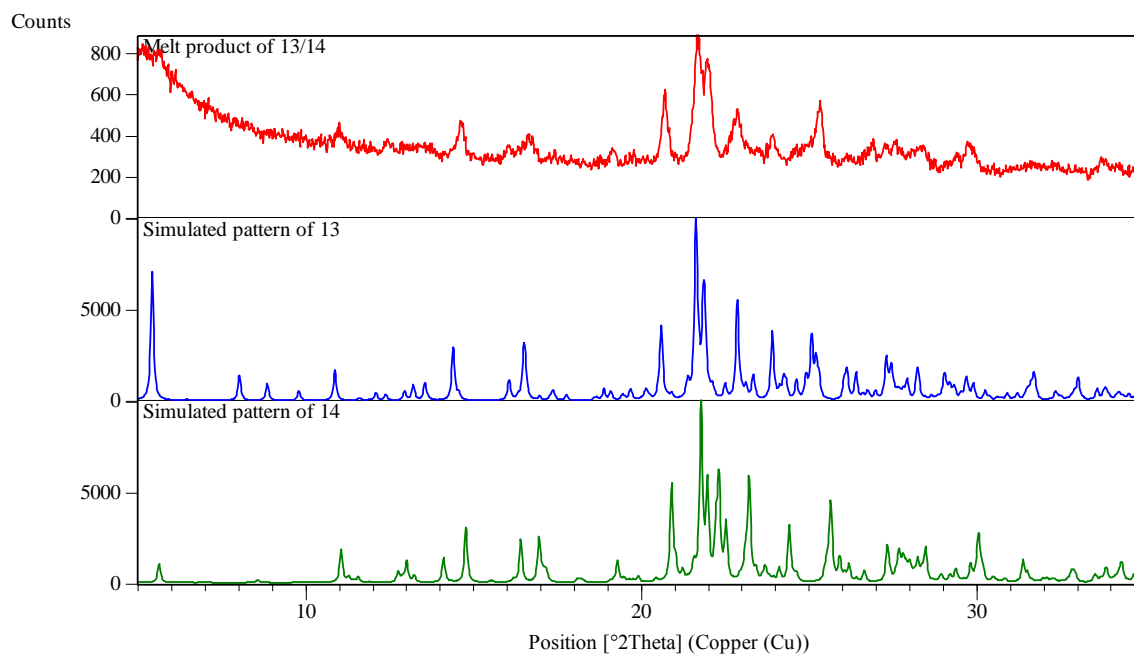


Figure 4.11 PXRd analysis of the melt product of **13/14** of the bromophenoxy and iodophenoxy derivatives.

4.1.4 Attempted mechanochemical synthesis of co-crystals

As part of the investigation into whether energy was required to induce the formation of co-crystals, mechanochemical synthesis was used. The cyclotriphosphazene derivatives **2** and **8** (Figure 4.12) were ground together with 4,4'-bipyridine, imidazole and benzimidazole (Table 4.5). In the case of imidazole, the products of the grinding experiments with both **2** and **8** were sticky white substances, whereas the other products were fine dry powders. The products of the grinding experiments were analysed by PXRD and the results for the experiments conducted with **2** are shown in Figure 4.13. The results show that the products are mainly a mixture of the reagents, as the peaks belonging to each reagent can be identified in the pattern of the product.

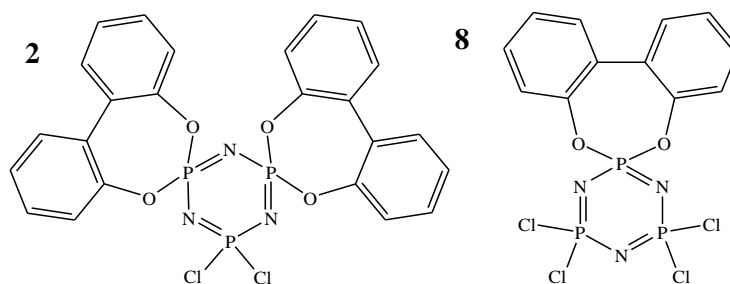
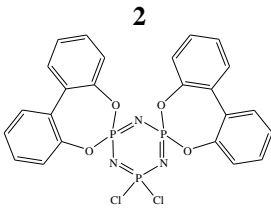
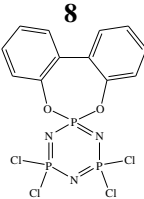


Figure 4.12 The structure of the cyclotriphosphazene derivatives **2** and **8**.

Table 4.5 The grinding experiments conducted with **2** and **8**. The ratio of cyclotriphosphazene to co-crystal former is also indicated.

Cyclotriphosphazene derivative	Co-crystal former	Ratio of cyclotriphosphazene: co-crystal former
 2	4,4'-bipyridine	1:2
	imidazole	1:2
	benzimidazole	1:2
 8	4,4'-bipyridine	1:4
	imidazole	1:4
	benzimidazole	1:4

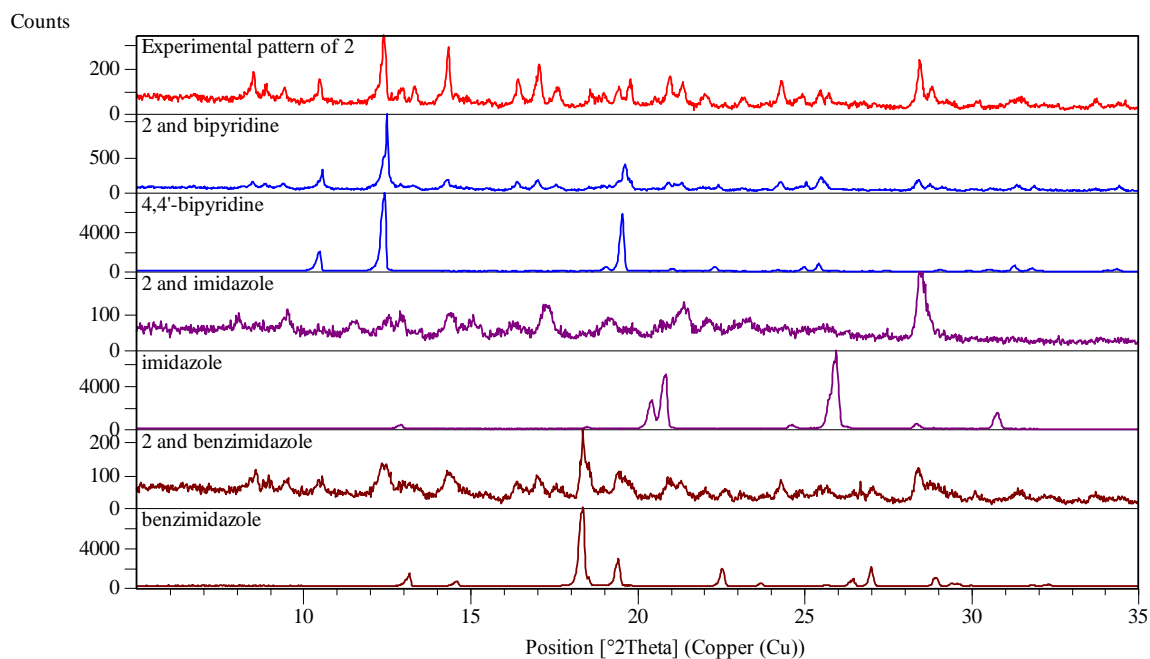


Figure 4.13 The PXRD results of the mechanochemical experiments between **2** and 4,4'-bipyridine, imidazole and benzimidazole. In most cases there appears to be an agreement between the patterns of the product and 4,4'-bipyridine, imidazole and benzimidazole.

The results of the attempted mechanochemical synthesis between **8** and 4,4'-bipyridine, imidazole and benzimidazole are generally the same (Figure 4.14), i.e. no co-crystals were formed. In the case of the reaction with benzimidazole, the product was dissolved in THF yielding a pink precipitate when the mixture was allowed to stand for a few days. The powder pattern of the precipitate differs from the powder patterns of the reagents. This is illustrated in Figure 4.15.

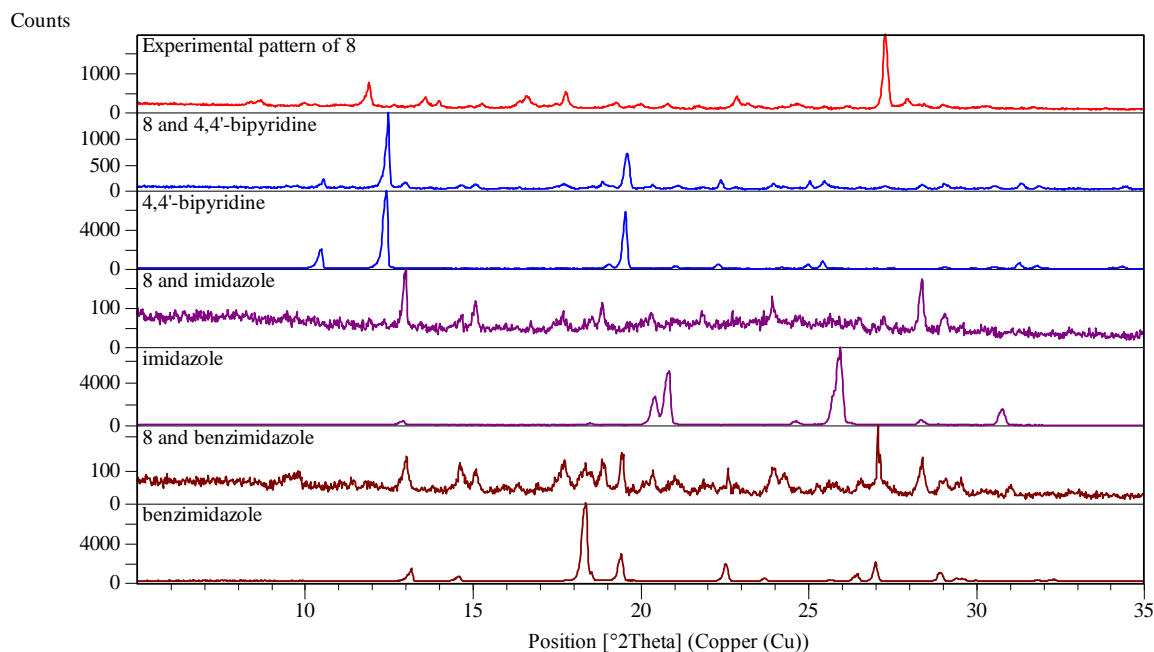


Figure 4.14 PXRD results of the grinding experiments with **8**. The powder patterns of the products either correspond to that of **8** or the co-crystal former.

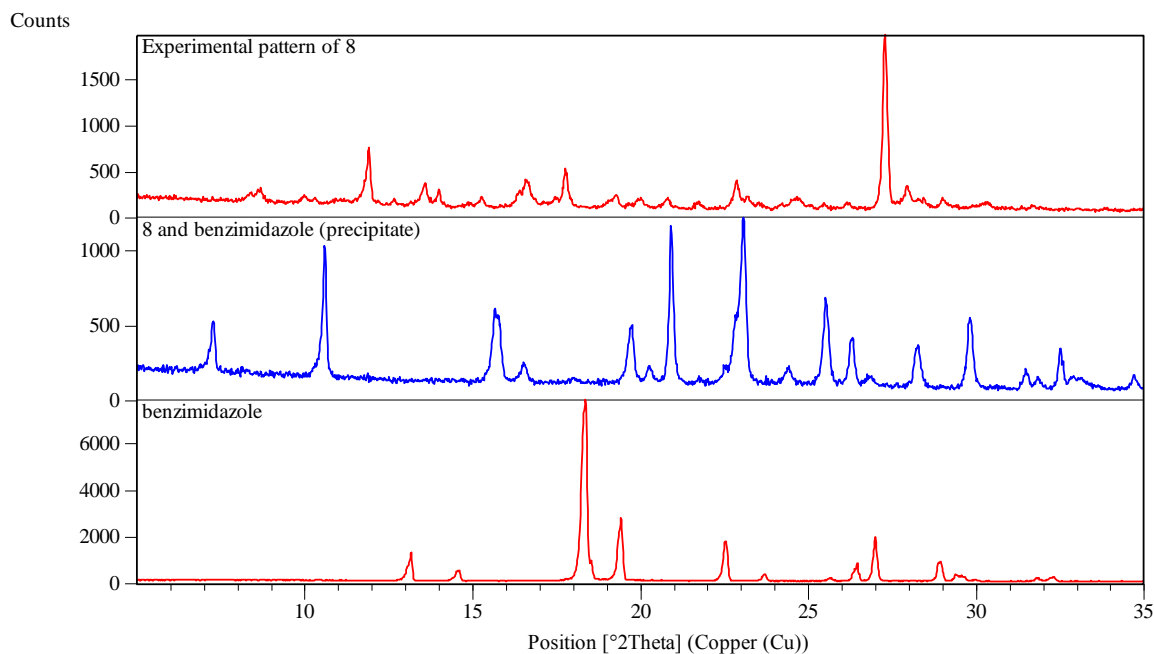


Figure 4.15 PXRD analysis of the precipitate formed when the product of grinding **8** and benzimidazole together is dissolved in THF. It is apparent that the peaks of the precipitate do not correspond with either of the patterns of the reagents.

NMR analysis of the precipitate showed numerous signals in the ^{31}P spectrum that do not correspond with the signals normally observed for **8**. This could possibly indicate that grinding the two components together resulted in substitution of the chloro groups with benzimidazole on the cyclotriphosphazene ring. It could also indicate a varying number of substituents, which could cause the multiple peaks seen in the spectrum (Figure 4.16).

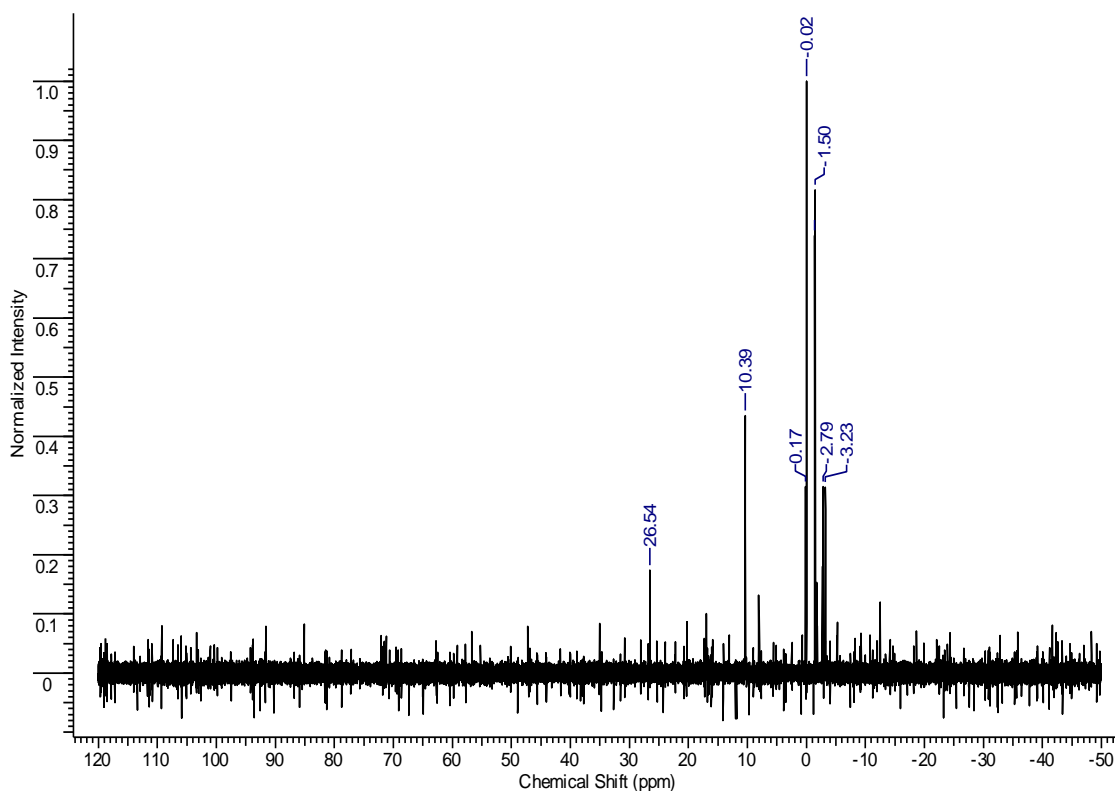


Figure 4.16 The ^{31}P spectrum of the pink precipitate. The peaks no longer correspond with the doublet and triplet usually observed for **8**.

4.2 The co-crystal with hexakis(4-pyridyloxy)cyclotriphosphazene

In the course of this study, more than 500 co-crystallisation experiments were carried out using methods such as slow evaporation, vapour diffusion, mechanochemical synthesis and crystallisation from the melt. One co-crystal of hexakis(4-pyridyloxy)cyclotriphosphazene (**4**) with terephthalic acid was however successfully isolated. This is the only example of a co-crystal with this particular hexasubstituted cyclotriphosphazene derivative. A list of the co-crystallisation experiments that were conducted with **4** can be found in Table 4.6.

The co-crystal of **4** and terephthalic acid was grown from a 1:2 ratio of **4**:terephthalic acid in a layered solution of chloroform and DMF. Crystals of **4** were dissolved in chloroform and the terephthalic acid in DMF. Care had to be taken to add the two solutions together slowly as terephthalic acid is insoluble in chloroform and precipitates out of solution when chloroform is added to DMF. These two compounds co-crystallise in the space group $P\bar{1}$.

No charge transfer has taken place in the structure, i.e. both carboxylic acid groups are protonated and only form hydrogen bonds with the pyridyl groups on the cyclotriphosphazene. The asymmetric unit contains one cyclotriphosphazene molecule and two and a half terephthalic acid molecules. One of the terephthalic acid molecules is on a special position, namely a centre of inversion, therefore only half a molecule is part of the asymmetric unit. This is illustrated in (Figure 4.17) where the part in green is the other half of the molecule that is generated by the inversion centre.

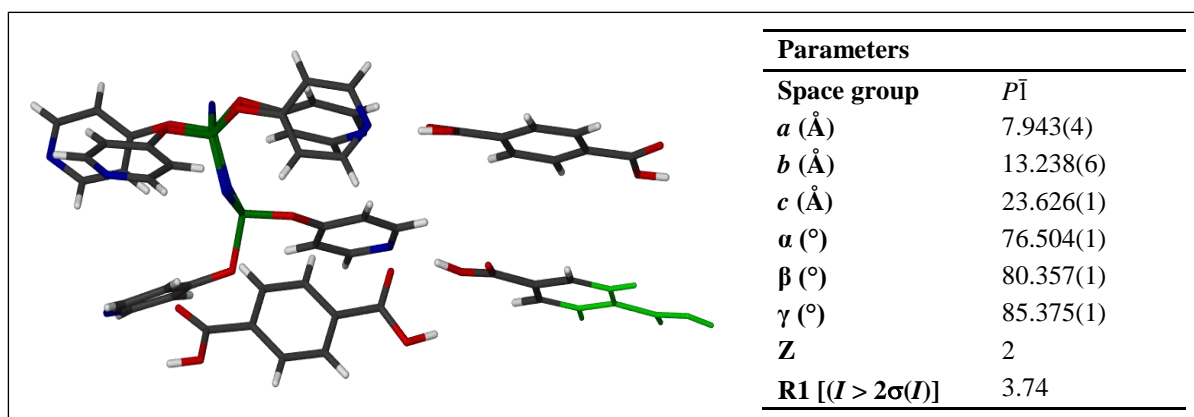


Figure 4.17 The asymmetric unit of the co-crystal of **4** and terephthalic acid along with the unit cell parameters and other crystallographic information.

Table 4.6 Co-crystallisation experiments with **4** and various diacids, amines and halophenoxy cyclotriphosphazene derivatives (**12 – 15**). The ratio of **4**:co-crystal former is indicated.

Co-crystal former	Ratio	Solvent
iodopentafluorobenzene	1:2	chloroform
bromopentafluorobenzene	1:2	chloroform
hexakis(4-iodophenoxy)- cyclotriphosphazene	1:1	chloroform
hexakis(4-bromophenoxy)- cyclotriphosphazene	1:1	chloroform
trimesic acid	1:2	chloroform/THF, layered
terephthalic acid	1:2	chloroform/DMF, layered
fumaric acid	1:3	THF/DMF
pamoic acid	1:3	THF/DMF
boric acid	1:3	THF/DMF
2-aminopyridine	1:3	THF/DMF
urea	1:3	THF/acetonitrile, layered
adipic acid	1:3	chloroform/DMF
tartaric acid	1:3	chloroform/DMF
maleic acid	1:3	chloroform/DMF
citric acid	1:3	chloroform/DMF
succinic acid	1:3	chloroform/DMF
trimesic acid	1:3	chloroform/DMF, layered
malic acid	1:3	chloroform/DMF, layered
pamoic acid	1:3	chloroform/DMF, layered
fumaric acid	1:3	chloroform/DMF, layered

Five out of the six pyridyl groups on the cyclotriphosphazene ring partakes in hydrogen bonding with a terephthalic acid molecule through a $\text{COOH}\cdots\text{N}$ interaction with the hydroxyl group of the carboxylic acid (Figure 4.18). This interaction causes the molecules to stack in an infinite hydrogen bonded chain throughout the crystal structure, alternating between two and three terephthalic acid molecules between each cyclotriphosphazene molecule (Figure 4.19).

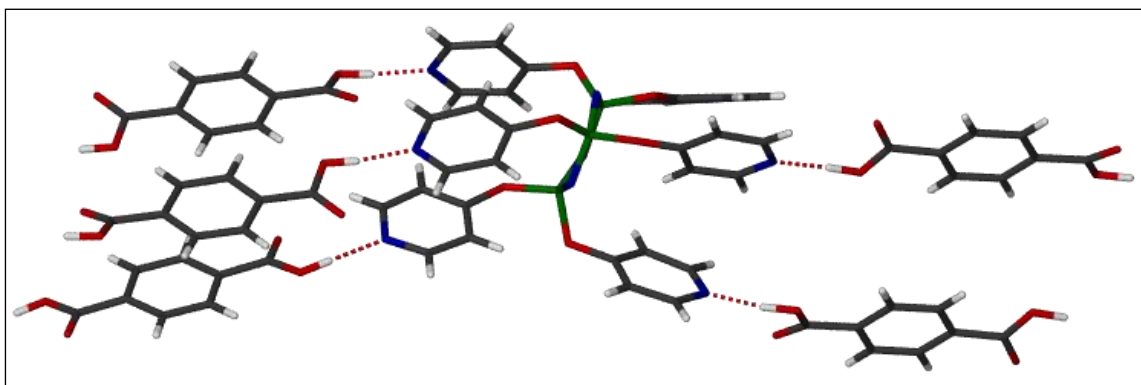


Figure 4.18 A capped stick representation of the five pyridyl groups each hydrogen bonding to a terephthalic acid molecule.

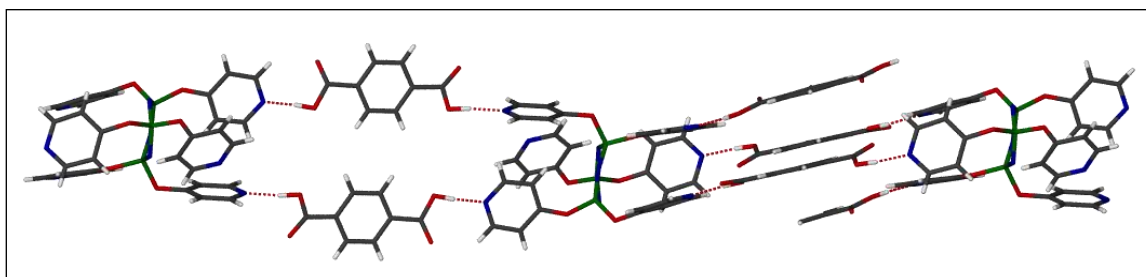


Figure 4.19 The infinite hydrogen bonded chain. The chain alternates between two and three terephthalic acid molecules between each cyclotriphosphazene molecule.

The terephthalic acid molecules shown in orange in Figure 4.20 link neighbouring chains by hydrogen bonding to a pyridyloxy group in the next chain.

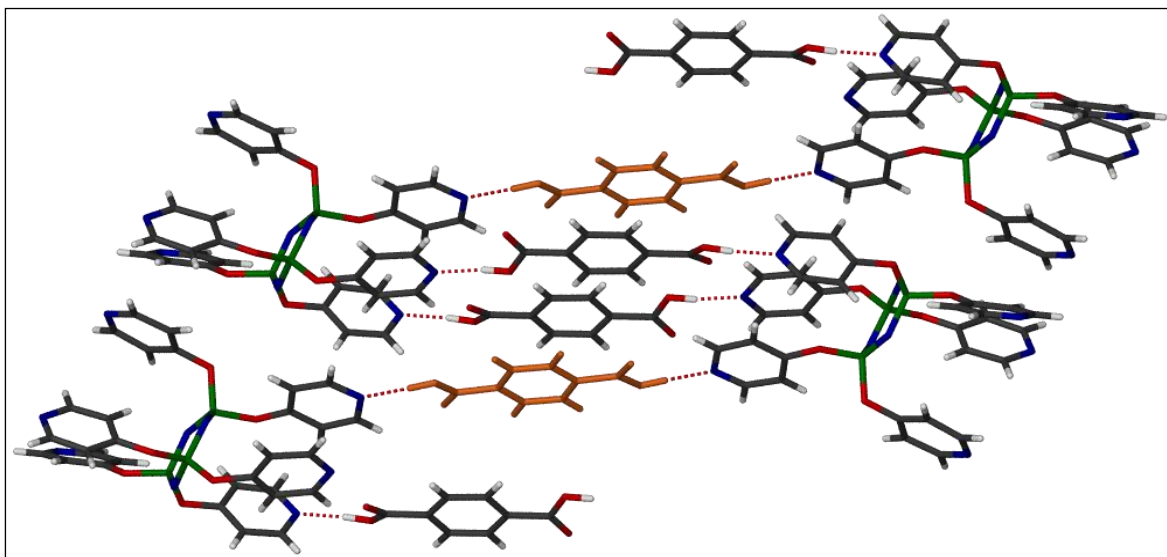


Figure 4.20 The hydrogen bonded chains are linked *via* a terephthalic acid molecule, shown here in orange, that hydrogen bonds to the pyridyloxy group of a neighbouring cyclotriphosphazene molecule.

After conducting a survey of the Cambridge Structural Database (CSD)^{10, 11}, it was noted that this is the only example of a co-crystal with the hexasubstituted pyridyloxy derivative. There is however a co-crystal with a derivative very similar to **4**. The only difference in the cyclotriphosphazene derivative is an extra carbon atom between the oxygen linker and the carbon atom of the phenyl ring (XUTLIH¹⁸), shown in Figure 4.21. In the case of this co-crystal, only four of the pyridylmethoxy groups each hydrogen bond to a 1,4-anthracenedicarboxylic acid. These infinite hydrogen bonded chains are also not connected to each other *via* hydrogen bonds.

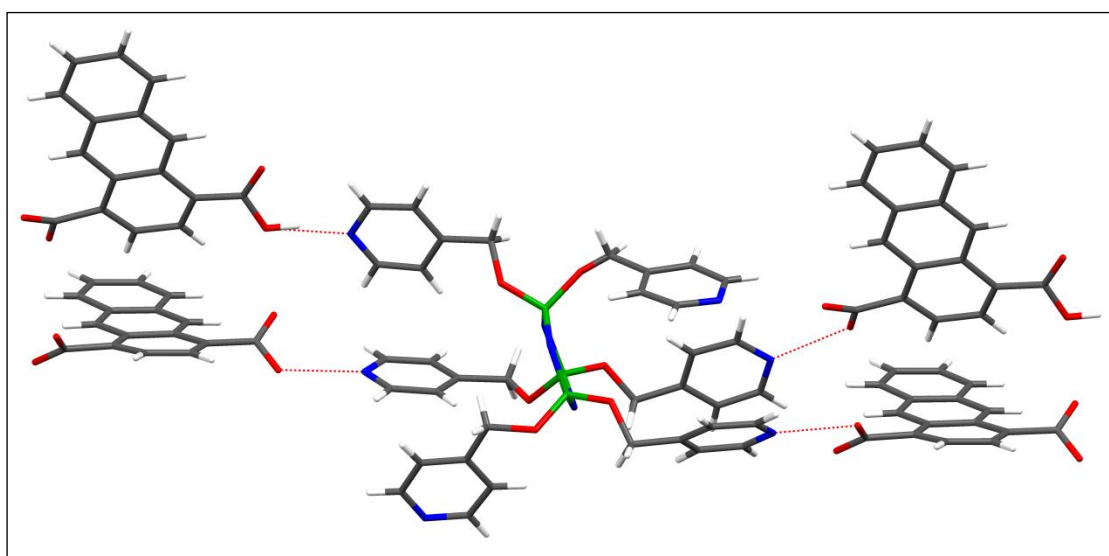


Figure 4.21 The hydrogen bonding motif of the co-crystal of hexakis(4-pyridylmethoxy)-cyclotriphosphazene and 1,4-anthracenedicarboxylic acid.

The hydrogen bond that is formed between **4** and terephthalic acid is clearly a very strong interaction, driving the formation of a co-crystal. It is surprising, however, that no other co-crystals with diacids were isolated with this derivative despite this seemingly strong interaction. This could indicate that the correct shape-match is very important.

4.3 A Cambridge Structural Database survey of co-crystal occurrence with cyclotriphosphazenes

The results of the investigation into co-crystal formation with cyclotriphosphazenes prompted another analysis of the CSD⁹⁻¹¹ in order to investigate whether co-crystal formation with cyclotriphosphazenes is as rare an occurrence as the results implied: one co-crystal from 500 co-crystallisation attempts.

First, a search was done to identify all cyclotriphosphazene derivatives in the CSD. This was done by drawing the base molecule as shown in Figure 4.22. The bond type is set as varying (indicated by dotted lines) because the cyclotriphosphazene ring has a pseudo-aromatic character often represented in different ways. The note “T4” indicates that four bonds are allowed to the atom, and “T2” indicates that only 2 bonds are allowed for the specific atom.

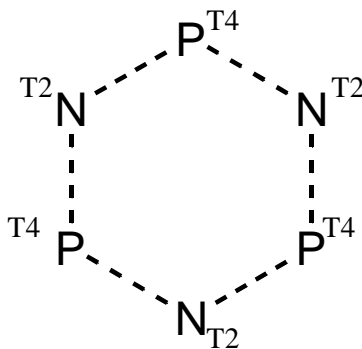
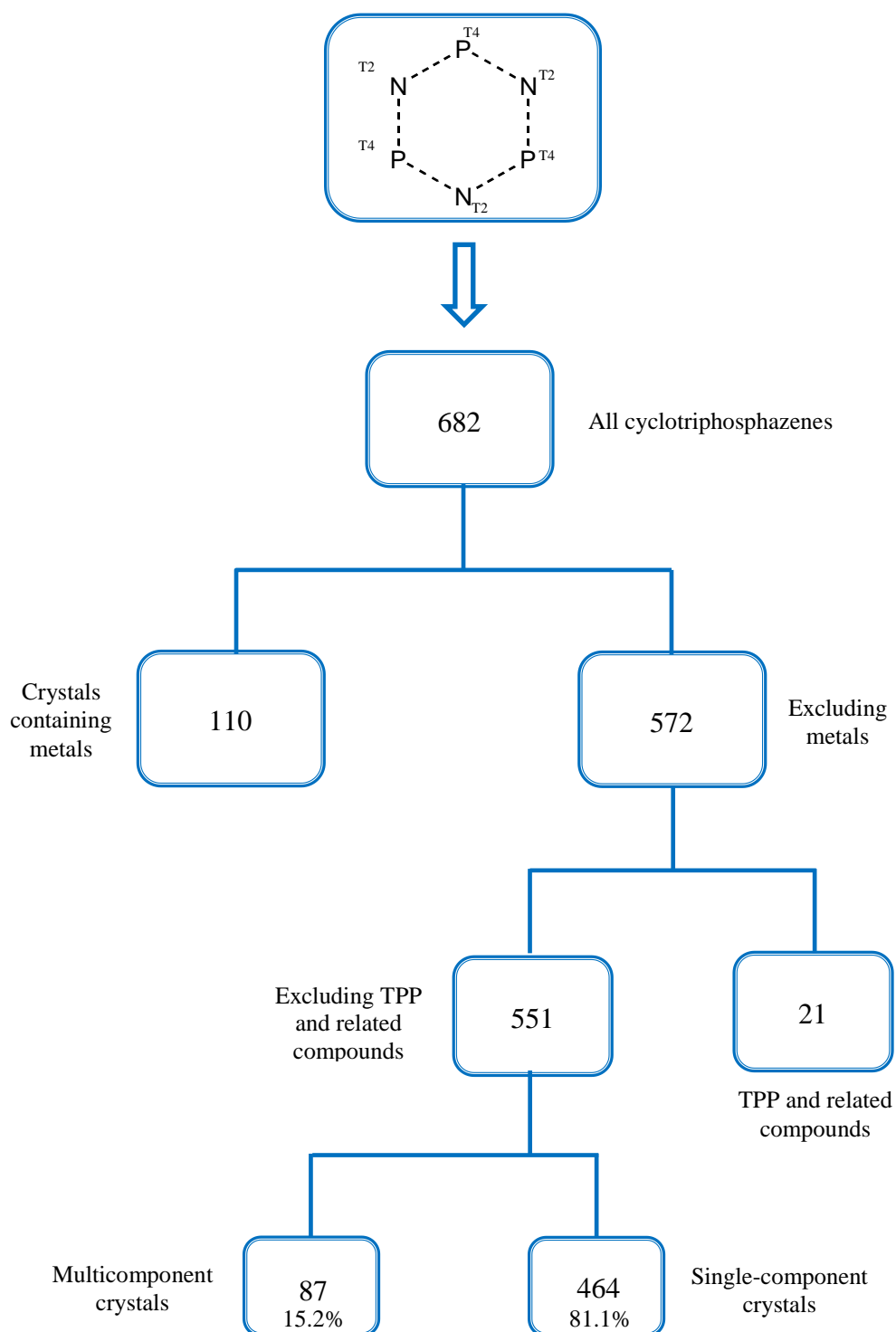


Figure 4.22 The cyclotriphosphazene ring is drawn in this way in order to identify all the cyclotriphosphazene derivatives. T4 implies 4 bonded atoms, and T2 implies 2 bonded atoms, as this is a pseudo-aromatic system.

When the search parameters are left as unrestricted as possible, but with 3D coordinates determined, 682 entries that meet the search parameters are identified in the CSD. Scheme 4.1 on the following page summarises the search process.



Scheme 4.1 This scheme outlines the CSD survey that was performed. Out of the 572 cyclotriphosphazene crystal structures that do not contain metals, only 87 (excluding TPP) have more than one chemical unit.

By analysing the crystal structures in the CSD, it becomes apparent that only 18.8% of the cyclotriphosphazene structures contain more than one chemical entity in the crystal structure. Surprisingly, there are quite a number of solvates with THF, toluene, DCM and chloroform, although no solvates were isolated during this study. Due to the fact that TPP is known to be a robust inclusion compound, it was decided that TPP and its related derivatives could bias the search for multicomponent crystals containing cyclotriphosphazenes in the CSD. These structures were therefore removed from the list of 572 structures containing cyclotriphosphazenes, resulting in 21 TPP and related structures being removed from the list. The remaining 551 structures were separated into structures containing more than one chemical unit and structures containing only one chemical unit. This left 87 compounds that crystallise with more than one chemical unit in the crystal structure. This implies that only 15.2% of the purely organic structures tend to form multicomponent crystals with cyclotriphosphazenes, excluding the solvates of TPP and related compounds. This is however a relative result, meaning that this result has to be compared to the occurrence of multicomponent crystals in all organic compounds. A search was therefore conducted for carbon and restricted to only organic compounds. There are a staggering 228 550 organic crystal structures in the CSD, of which 66 226 crystallise with more than one chemical entity. This is an occurrence of 29%. The crystallisation of more than one chemical unit in a crystal structure is therefore quite a rare event, and even more so with cyclotriphosphazenes.

4.4 Conclusions and future work

Co-crystal formation is not a phenomenon that often occurs, as is evident from the results of the CSD survey. For co-crystallisation to occur, the shape and size of the molecules have to match.¹⁵ However, shape and size similarity are not enough to induce co-crystallisation in the case of cyclotriphosphazenes. The conformational flexibility of cyclotriphosphazenes can allow the molecules to adapt a conformation that favours interaction between cyclotriphosphazene molecules, rather than other small molecules. The small organic molecules used in the co-crystallisation experiments could have caused a shape mismatch, which would not allow co-crystallisation to occur, even though there was the potential for strong hydrogen bonding interaction.

The halophenoxy cyclotriphosphazene derivatives **12** to **15** were used to study whether cyclotriphosphazenes with similar conformations would in fact co-crystallise. The derivatives **12** and **15** are isostructural, as are **13** and **14**. This did however not induce co-crystal formation from solution – in each case crystals of the pure derivative formed. An investigation into whether co-crystals could be grown from melting the two isostructural components together did not yield any conclusive results. DSC analysis showed only one melting point for each of the combinations, which could indicate the formation of a co-crystal. The co-crystal would have new properties such as a different melting point from the parent compounds. PXRD analysis did unfortunately not shed more light on the situation, as it could not clearly indicate whether the patterns of **12/15** and **13/14** were only a mixture of the two parent components or if a new product had formed. Infrared spectroscopy and solid state NMR would be good analytical methods to use to further characterise the products of the melt.

One novel co-crystal was synthesised and characterised in this study. Co-crystallisation with cyclotriphosphazenes is therefore possible, but a very strong interaction is clearly needed to drive the formation of the co-crystal. It is also possible that the solvent system plays a role in determining the pH and polarity of the solution, which could in turn determine how strongly a hydrogen bond donor would donate, and how strongly a hydrogen bond acceptor would accept. In other words, the solvent system can possibly determine the strength of the interaction and how favourable it is. It is interesting to note

that in the co-crystal of **4** with terephthalic acid, no proton transfer took place to form a salt.

A computational study could aid in the understanding of interactions at play in the crystal structures of single-component crystals and multicomponent crystals of cyclotriphosphazenes. It would be useful to calculate the lattice energies of the cyclotriphosphazene compounds that crystallise only as a single-component crystal.¹⁹ This could be compared to calculations of the lattice energy of a co-crystal in order to determine whether it is more favourable (lower energy) for cyclotriphosphazenes to crystallise as single component crystals. If this is in fact the case, then it would go a long way in explaining why the occurrence of co-crystals with cyclotriphosphazenes is relatively low. These computational studies can aid the design process by identifying which properties of cyclotriphosphazenes are critical in forming supramolecular architectures.

References

1. K. Inoue and T. Itaya, *Supramol. Sci.*, 1998, **5**, 163 - 166.
2. R. Bertani, F. Chaux, M. Gleria, P. Metrangolo, R. Milani, T. Pilati, G. Resnati, M. Sansotera and A. Venzo, *Inorg. Chim. Acta*, 2007, **360**, 1191 - 1199.
3. H. R. Allcock, *J. Am. Chem. Soc.*, 1964, **86**, 2591 - 2595.
4. H. R. Allcock, M. L. Levin and R. R. Whittle, *Inorg. Chem.*, 1986, **25**, 41 - 47.
5. H. R. Allcock, *Acc. Chem. Res.*, 1978, **11**, 81 - 87.
6. P. Sozzani, S. Bracco, A. Comotti, L. Ferretti and R. Simonutti, *Angew. Chem., Int. Ed.*, 2005, **44**, 1816 - 1820.
7. A. Comotti, S. Bracco, L. Ferretti, M. Mauri, R. Simonutti and P. Sozzani, *Chem. Commun.*, 2007, 350 - 352.
8. M. Gleria and R. De Jaeger, *J. Inorg. Organomet. Polym.*, 2001, **11**, 1 - 45.
9. F. H. Allen and O. Kennard, *Chem. Des. Autom. News*, 1993, **8**, 31 - 37.
10. Cambridge Structural Database Version 5.32 with 4 updates.
11. F. H. Allen, *Acta Crystallogr., Sect. B: Struct. Sci.*, 2002, **B58**, 380 - 388.
12. N. El Murr, R. Lahana, J.-F. Labarre and J.-P. Declercq, *J. Mol. Struct.*, 1984, **117**, 73 - 85.
13. I. Dez, J. Levalois-Mitjaville, H. Grützmacher, V. Gramlich and R. de Jaeger, *Eur. J. Inorg. Chem.*, 1999, **1999**, 1673 - 1684.
14. H. R. Allcock, M. T. Stein and J. A. Stanko, *J. Am. Chem. Soc.*, 1971, **93**, 3173 - 3178.
15. K. M. Anderson, M. R. Probert, A. E. Goeta and J. W. Steed, *CrystEngComm*, 2011, **13**, 83 - 87.
16. H. R. Allcock, D. C. Ngo, M. Parvez and K. B. Visscher, *Inorg. Chem.*, 1994, **33**, 2090 - 2102.
17. G. Bandoli, U. Casellato, M. Gleria, A. Grassi, E. Montoneri and G. C. Pappalardo, *J. Chem. Soc., Dalton Trans.*, 1989, 757 - 760.
18. T. Itaya, N. Azuma and K. Inoue, *Bull. Chem. Soc. Jpn.*, 2002, **75**, 2275 - 2281.
19. C. Ouvrard and J. B. O. Mitchell, *Acta Crystallogr., Sect. B: Struct. Sci.*, 2003, **B59**, 676 - 685.

Chapter 5

Summary and concluding remarks

Crystal engineering is an ever-growing field of research. The crystal engineer uses knowledge of the vast array of intermolecular interactions available to design specific molecular architectures in the solid state. This study focused specifically on using cyclotriphosphazenes to create supramolecular architectures. The goal was to modify cyclotriphosphazenes with substituents that contain functional groups that could participate in strong supramolecular interactions in the solid state. It was hoped that the strong hydrogen bonding interaction, as well as other interactions such as π - π stacking, would direct the cyclotriphosphazene molecules to arrange in columns in the solid state. If these cyclotriphosphazene molecules were co-crystallised with suitable co-crystal formers, the co-crystal formers could play the role of linkers between the pillars essentially forming a framework that could potentially include solvent. Solvate formation was therefore one of the design aims.

Co-crystals have been an area of intense interest for many years, especially because co-crystallisation has such a profound effect on the properties of the parent components. The co-crystal often has properties that completely differ from the properties of the co-crystal formers. It was therefore of interest to study this phenomenon in cyclotriphosphazenes. Such a wide variety of substituents can be placed on the cyclotriphosphazene ring that it lead to the theory that the inherent variety of the cyclotriphosphazenes would be ideal for co-crystal formation. It was hypothesised that the substituents on the ring are reasonably flexible to potentially allow small changes in the conformation of the cyclotriphosphazene to accommodate smaller molecules in the crystal structure. The range of substituents that could be placed on the cyclotriphosphazene ring would allow for a diverse set of molecules with which to perform many co-crystallisation experiments. Extensive research has been conducted on the synthesis of cyclotriphosphazenes, but not in the area of using these molecules to construct supramolecular architectures. We therefore aimed to fill this apparent gap in the literature and add to the small number of co-crystal structures initially identified in the CSD.

Of the sixteen target molecules, fifteen cyclophosphazene derivatives were successfully synthesised in this study. Although the original aim was to synthesise derivatives with functional groups that could participate in hydrogen bonding, this was not successful. The hexakis(4-hydroxyphenoxy)-cyclotriphosphazene does in fact have this potential, but no co-crystals could be grown with this derivative. The greatest stumbling block in the design of these derivatives was the synthesis of derivatives with hydrogen bonding functionality. Numerous attempts were made to synthesise the hexakis(4-carboxyphenoxy)cyclotriphosphazene, but none were successful. The most promising synthetic route is that of the conversion of hexakis(4-bromophenoxy)cyclotriphosphazene to the lithiated derivative and then converting it to the carboxylic acid through reaction with dry ice. This procedure has never before been attempted with cyclotriphosphazenes, but it is known to be highly successful with organic compounds. It would be worthwhile to optimise the reaction conditions by lengthening the reaction time and allowing the bromo derivative to react with excess *n*BuLi to ensure complete lithiation.

Mechanochemical synthesis is a method that has enjoyed great popularity in recent years. It would therefore be worthwhile to expand attempts at generating the cyclotriphosphazene derivatives via mechanochemical synthesis. Results from this study were inconclusive regarding the success of grinding PABA and the phosphonitric chloride trimer together in the presence of base. A different base could yield better results and should be explored further.

Although the occurrence of polymorphism in cyclotriphosphazenes was not part of the original study, a very interesting polymorphic system has been discovered. Two novel polymorphs of hexakis(4-fluorophenoxy)cyclotriphosphazene (**12**) have been identified and characterised with DSC, VT PXRD and SCD analyses. The original structure reported in the CSD crystallises in the monoclinic *P* system (**M**). The first polymorph of this structure that was discovered crystallised in the triclinic *P* system (**T**). The structures of these two polymorphs were discussed in detail in chapter 3, but the interesting feature of these two polymorphs is how they relate to each other. The triclinic phase undergoes an apparently irreversible phase transformation to the monoclinic phase at approximately 100 °C. However, if the triclinic phase is heated to just after the phase transformation and cooled to sub-zero temperatures, evidence of another phase is observed. This new phase

does not appear once the triclinic phase has been heated past the point of conversion and melted. At first it was thought that this behaviour is related to the triclinic phase, as the same was not observed for the monoclinic phase. SCD analysis of a triclinic crystal could however not shed light on this phenomenon, as the crystal did not diffract past the point of conversion from triclinic to monoclinic.

Fortunately, when the same experiment was conducted with a monoclinic sample (heated to approximately 100 °C and then cooled to -40 °C on the DSC) there was again evidence of another phase. SCD analysis was able to identify this phase as the crystal remained intact on heating to 100 °C. The new phase was a monoclinic *C* phase and data was collected at 0 °C. The molecule in this phase has higher symmetry than the monoclinic *P* molecule, although two of the fluorophenoxy rings are disordered over two positions. The conformation of the substituents causes the molecules to pack in such a way as to align the cyclotriphosphazene rings in columns in the crystal structure. Although the structure collected at -45 °C could not be solved, it is speculated that this could be due to a mixed phase present in the crystal, subsequently causing spurious reflections that make determining a unit cell difficult. This mixed phase possibly comprises the monoclinic *P* and monoclinic *C* phases. This could mean that this is in fact an example of an enantiotropic polymorphic system, where the monoclinic *P* polymorph converts to the monoclinic *C* polymorph, which in turn converts back to the monoclinic *P* form.

It would be interesting to examine whether it is necessary to cool the crystal to induce the phase change back to monoclinic *P*, or if it is possible to simply leave the crystal to allow it to slowly convert back to the monoclinic *P* under ambient conditions. It would also be useful to conduct hot stage microscopy studies on these polymorphs.

The Supramolecular Materials Chemistry group is now also in possession of a pressure-DSC instrument, as well as a hot stage microscope that is connected to a DSC. This polymorphic system should be investigated with these instruments under conditions other than ambient conditions to determine whether it is possible to generate more polymorphic forms. The same type of study could also be done on the other halophenoxy cyclophosphazene derivatives, especially hexakis(4-chlorophenoxy)cyclotriphosphazene that is isostructural to **12**. No polymorphs could be generated from crystallisations from solution for these halophenoxy derivatives.

The main focus of this study was to investigate co-crystal formation with cyclotriphosphazenes. This subject was extensively explored in chapter 4 and many conclusions can be drawn from this body of work.

From the results of this study it appears that co-crystallisation with cyclotriphosphazenes does not readily occur. This could be due to the shape and size of cyclotriphosphazene molecules. Although the benzene-like ring and substituents that project almost perpendicularly from the ring are very attractive features, it has been shown that smaller more rigid molecules tend to have a higher occurrence of co-crystal formation. This is possibly due to the fact that the molecules do not have awkward shapes that need to find complementary co-crystal formers in order for co-crystallisation to take place. Therefore, the very reason for using cyclotriphosphazenes may actually be prohibiting co-crystal formation.

This could however not only be a shape and size effect as there are a small number of co-crystal structures with cyclotriphosphazenes in the CSD. The key feature in these structures appears to be a very strong interaction that guides the assembly of the different molecules. In the case of the novel hexakis(4-pyridyloxy)cyclotriphosphazene co-crystal with terephthalic acid that was isolated in this study, the structure is stabilised by hydrogen bonds between the COOH...N components of the crystal structure. This is a well-known supramolecular synthon that proves how strong these types of interactions are to overcome steric restrictions in order for heteromeric molecules to assemble in the solid state.

It is evident from this study that the aggregation of cyclotriphosphazenes into supramolecular assemblies is highly dependent on the size and shape of the *molecule itself* and that of the *co-crystal former*, as well as the reaction conditions such as the solvent system used for co-crystallisations and the temperature at which crystallisation occurs. Crystal engineering therefore makes use of a variety of interactions and reaction conditions to create the perfect set of events to design a specific molecular assembly. This study further explored the field of crystal engineering with cyclotriphosphazenes and the role these molecules play in directing the assembly of architectures in the solid state.

Appendix

Experimental techniques

1. Single crystal X-ray diffraction

Cocrystal and 5Cyano –Bruker Apex DUO

Intensity data were collected on a Bruker Apex DUO CCD diffractometer with a multilayer monochromator. Mo-K α radiation ($\lambda = 0.71073 \text{ \AA}$) was selected for the experiments. The temperature of the crystal was controlled using an Oxford Cryostream Cooler. Data reduction was done by means of a standard procedure using the Bruker software package SAINT¹ and the absorption corrections and the correction of other systematic errors were performed using SADABS.^{2,3} The structures were solved by direct methods using SHELXS-97 and refined using SHELXL-97.⁴ X-Seed⁵ was used as the graphical interface for the SHELX program suite. Hydrogen atoms were placed in calculated positions using riding models.

FluoroM, FluoroMrt, FluoroT, FluoroTrt, 273K, 253K, 13Iodo, 14Bromo, 15Chloro, 7Diamino, 3Aldehyde – Bruker-Nonius SMART Apex

X-ray intensity data were collected on a Bruker-Nonius SMART Apex diffractometer equipped with a fine-focus sealed tube and a 0.5 mm Monocap collimator (monochromated Mo-K α radiation, $\lambda = 0.71073 \text{ \AA}$). Data were captured with a CCD area-detector with the generator powered at 40 kV and 30 mA. The temperature of the crystal was controlled by constant stream of nitrogen gas produced by an Oxford Cryogenics Cryostat (700 Series Cryostream Plus). Data reduction was done by means of a standard procedure using the Bruker software package SAINT¹ and the absorption corrections and the correction of other systematic errors were performed using SADABS.^{2,3} The structures were solved by direct methods using SHELXS-97 and refined using SHELXL-97.⁴ X-Seed⁵ was used as the graphical interface for the SHELX program suite. Hydrogen atoms were placed in calculated positions using riding models.

2. Powder X-ray diffraction

Standard PXRD

Samples were ground to a fine powder with a mortar and pestle and placed on a zero-background sample holder. Experiments were carried out on a PANalytical X'Pert PRO instrument with Bragg-Brentano geometry. Intensity data were collected using an X'Celerator detector and 2θ scans in the range of $5 - 50^\circ$ were performed. During the experiment the powdered sample was exposed to Cu- K_α radiation ($\lambda = 1.5418 \text{ \AA}$).

Variable temperature PXRD

Samples were ground to a fine powder with a mortar and pestle and sealed in a 0.3 mm glass capillary. The capillary spinner configuration (with focusing mirror) of the instrument was used along with the Oxford Cryostream Cooler for accurate temperature control. The sample was allowed to equilibrate for two minutes after every temperature change. Experiments were carried out on a PANalytical X'Pert PRO instrument with Bragg-Brentano geometry. Intensity data were collected using an X'Celerator detector and 2θ scans in the range of $5 - 50^\circ$ were performed. During the experiment the sample was exposed to Cu- K_α radiation ($\lambda = 1.5418 \text{ \AA}$).

3. Differential scanning calorimetry

The samples (ranging from 1.5 to 3 mg) were placed in aluminium pans that were non-hermetically sealed with vented aluminium lids. Differential scanning calorimetry was carried out using a TA Instruments Q100 system under a N_2 gas purge, with a flow rate of 50.0 ml/min coupled to a cooling unit. Each experiment was tailored to the type of analysis that was required regarding the maximum and minimum temperatures. The ramp rate for all experiments was $10 \text{ }^\circ\text{C/minute}$ to the maximum temperature. The cooling rate was $5 \text{ }^\circ\text{C/minute}$ to the minimum temperature.

4. Hot stage microscopy

Hot stage microscopy was carried out on a Meiji EMZ-8TR microscope, fitted with an INSTEC HCS601 hot stage and an INSTEC STC200 hot stage controller. Crystalline samples were placed between two glass slips and heated in the range 25 – 140 °C at 10 °C/minute.

5. Cif files

The cif files for all structures collected in this study can be found on the enclosed CD.

Cif file	Description
Cocrystal	The co-crystal of hexakis(4-pyridyloxy)cyclotriphosphazene and terephthalic acid.
5Cyano	The crystal structure of hexakis(4-cyanophenoxy)cyclotriphosphazene.
FluoroM	The monoclinic <i>P</i> phase of hexakis(4-fluorophenoxy)cyclotriphosphazene at 100 K.
FluoroMrt	The monoclinic <i>P</i> phase of hexakis(4-fluorophenoxy)cyclotri-phosphazene at room temperature.
FluoroT	The triclinic phase of hexakis(4-fluorophenoxy)cyclotriphosphazene at 100 K.
FluoroTrt	The triclinic phase of hexakis(4-fluorophenoxy)cyclotri-phosphazene at room temperature.
273K	The monoclinic <i>C</i> phase of hexakis(4-fluorophenoxy)cyclotriphosphazene at 273 K.
253K	The monoclinic <i>C</i> phase of hexakis(4-fluorophenoxy)cyclotriphosphazene at 253 K.
13Iodo	The crystal structure of hexakis(4-iodophenoxy)cyclotriphosphazene and 100 K.
14Bromo	The crystal structure of hexakis(4-bromophenoxy)cyclotriphosphazene at 100 K.
15Chloro	The crystal structure of hexakis(4-chlorophenoxy)cyclotriphosphazene at 100 K.
7Diamino	The structure of tris(1,3-diaminoalkane)cyclotriphosphazene hydrate.
3Aldehyde	The structure of 2,2-bis(4-formylphenoxy)-4,4,6,6-bis[spiro(2',2''-dioxy-1',1''-biphenyl)]cyclotriphosphazene.

References

1. *SAINT Data Reduction Software*, Version 6.45; Bruker AXS Inc., Madison, WI, **2003**.
2. *SADABS*, Version 2.05; Bruker AXS Inc., Madison, WI, **2002**;
3. R. H. Blessing, *Acta Crystallogr., Sect. A: Found. Crystallogr.* **1995**, *51*, 33-38.
4. G. M. Sheldrick, *Acta Crystallogr., Sect. A: Found. Crystallogr.* **2008**, *64*, 112-122.
5. L. J. Barbour, *Journal of Supramolecular Chemistry* **2001**, *1*, 189-191.